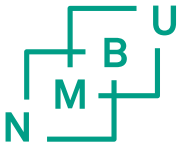
U
B
M
N

Table of Contents

Acknowledgements

I would like to thank my supervisor Professor Lars Skjeldal for all the good guidance, materials and morale support while undertaking this thesis. His enthusiasm kept inspiring me to keep going in times of difficulty.

I send my thanks to Silje Benedicte Lorentzen and Kristine Bistrup Eide from the Department of Chemistry, Biotechnology and Food Sciences (IKBM) for letting me use their instruments, providing chemicals and a fun work experience.

I greatly appreciate staff and supervisors at SKP and IPV for providing the knowledge, equipment and loan of facilities for cultivation studies.

Thanks to Professor Yngve Stenstrøm for help regarding chemistry questions and Simen Gjelseth Antonsen for operating the NMR machine and assembling the spectra.

A special thanks to my family, friends and bride to be, Emma Undrum for motivating and supporting me during writing.

Abstract

A non-destructive protocol was created for extracting, isolating and detecting cyclotides from cultivated *T. Officinale* flower heads. Optimal extraction was achieved by maceration for 15 minutes in 50% MeOH and steeping plant material at 70 °C for 3 hours. Size exclusion chromatography was applied successfully using a stationary phase with a molecular cut off at 1000-5000 Da yielding a good separation at 280nm. A molar attenuation threshold was calculated from a protein standard with purified Kalata B1 and used to validate isolated fractions. An amber colored fraction containing 0.39 mM protein was applied to a 400 MHz NMR to determine the presence of cyclotides using extraordinary chemical shifts. Kalata B1 was not confirmed but NMR showed fingerprint similarities to the standard and a signal at -0.1 ppm. This work demonstrates the viability of the protocol for future use.

Abbreviations

NMR	Nuclear Magnetic Resonance
CCK	Cyclic Cysteine Knot
NMBU	Norwegian University of Life Sciences
SEC	Size Exclusion Chromatography
FLC	Flowering Locus C
VIN3	Vernalization Insensitive 3 protein
MeOH	Methanol
EtOH	Ethanol
UV	Ultraviolet
MSE	Mean Square Error
D_2O	$[^2H]_2$-Water
ppm	parts per million
SI Units	International system of units
MS	Mass Spectrometry
HETP	Height Equivalent of a Theoretical Plate
Tris-HCl	2-Amino-2-hydroxymethyl-propane-1,3-diol
NaOH	Sodium hydroxide
HCl	Hydrochloric acid
NaH_2PO_4 x H_20	Sodium phosphate monobasic monohydrate
Na_2HPO_4 x $2H_2O$	Sodium phosphate dibasic dihydrate
k (g-forces)	Kilo (x1000)

1 Introduction

1.1 History

Cyclotides were discovered during an investigation of tribal medicine in Africa.
A Norwegian doctor named Lorents Gran traveled to The Democratic Republic of Congo in the 60s and discovered that the Zulu tribe's medicine men/women in Zaire made a special decoction from the leaves of the plant *Oldenlandia affinis* to induce labor in pregnant African women. This piqued the interest for further studies in search for the responsible compounds, and in 1973 Lorents Gran successfully isolated the protein and called it after the tribe's name for the medicine, Kalata B1 [1]. Research continued through 2 decades with the suggested three-dimensional NMR structure isolated from the medicinal plant *O. affinis* in 1995 [2]. Over 100 different cyclotides have since been isolated from the Violaceae, Rubiaceae and Cucurbitaceae families [3].

Figure 1: T. Officinale in bloom.

A Norwegian master thesis under the supervision of L. Skjeldal, NMBU, Norway suggested in 2007 that antimicrobial polypeptides of a molecular weight of around 2916 Da were easily extracted from *T. Officinale* (S. Troland, unpublished work) [4]. Nearly no published work has been done on cyclotides in relation to the *T. Officinale* flower apart from one paper by a Russian scientist who isolated cysteine-rich antifungal peptides from *T. Officinale* [5]. Because of this the thesis also includes cultivation of the plant. It is suggested that because of cyclotides' resistance to the human digestive environment that it can be utilized for drug development and act as a reliable scaffold, as water soluble drugs are easily hydrolyzed in gastric fluids [6].

1.2 Chemical Properties

Cyclotides are small proteins consisting of around 30 amino acids where the C- and N-terminus ends are connected with a peptide bond creating a circular protein. The protein has a high incidence of cysteine enough to form three intramolecular disulfide bridges. The three disulfide bridges in combination with cyclisation create the cyclic cysteine knot motif (CCK) which are characteristic for all cyclotides [7]. The structural integrity of cyclotides is very high due to conservation of the cysteines and surrounding amino acids; the CCK is structured in such a way that 6 loops are formed between the cysteine amino acids that take part.

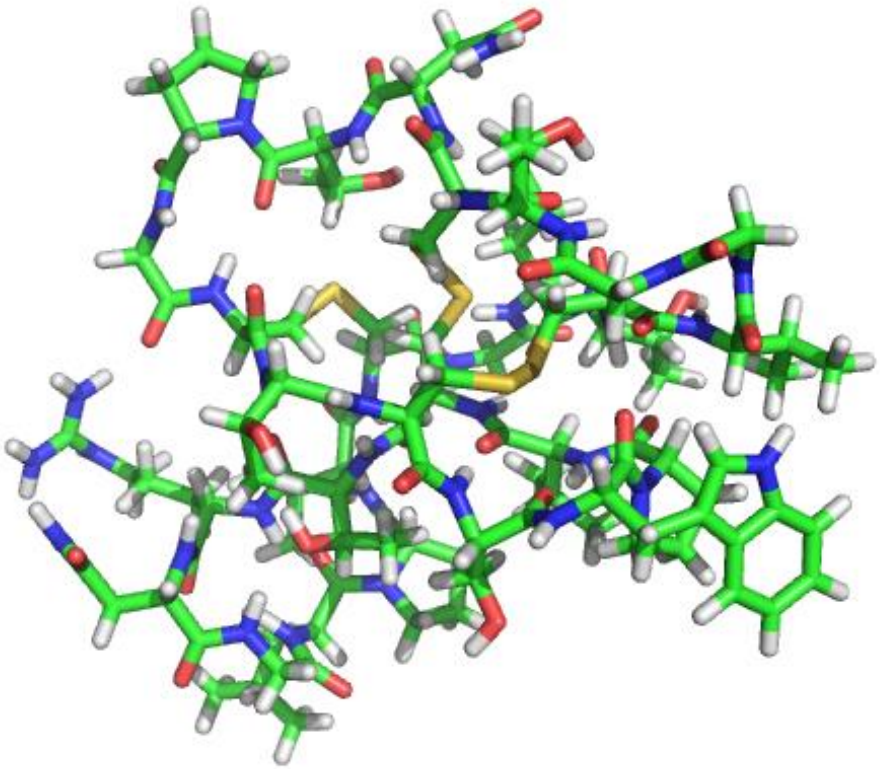

Figure 2: Sticks representation in PyMOL showing Kalata B1 with cysteine bridges in yellow (PDB ID: 1KAL) [2].

The most elucidating quality of cyclotides is their cyclic nature which has given them their name, but it has also given cyclotides an innate resistance against proteases which aids them in their enzymatic stability [7]. Kalata B1 has been reported to tolerate exposure to pH as low as 0.3, 8M urea, 6M guanidine, boiling water and both exo- and endoproteases without damaging the proteins secondary and tertiary integrity. The CCK motif is the main reason for its high thermal, chemical and enzymatic stability [8].

Cyclotides take part in a plants defense system and has shown considerable effect against insects and microorganisms. Effects like anti-microbial, anti-insecticidal, anti-HIV, anti-tumor, anti-fouling, as well as hemolytic and uterotonic effects have been reported [4] [9] [10] [11].

These properties are highly desired for their medicinal applications making work on optimization essential. Because of the cyclotides innate protein stability and diverse fields of use it has been subjected to extensive research. Production or modification of cyclotides with goal of creating a scaffold protein to transport medicine without being denatured by the digestive system is a major milestone in drug discovery [12] [13].

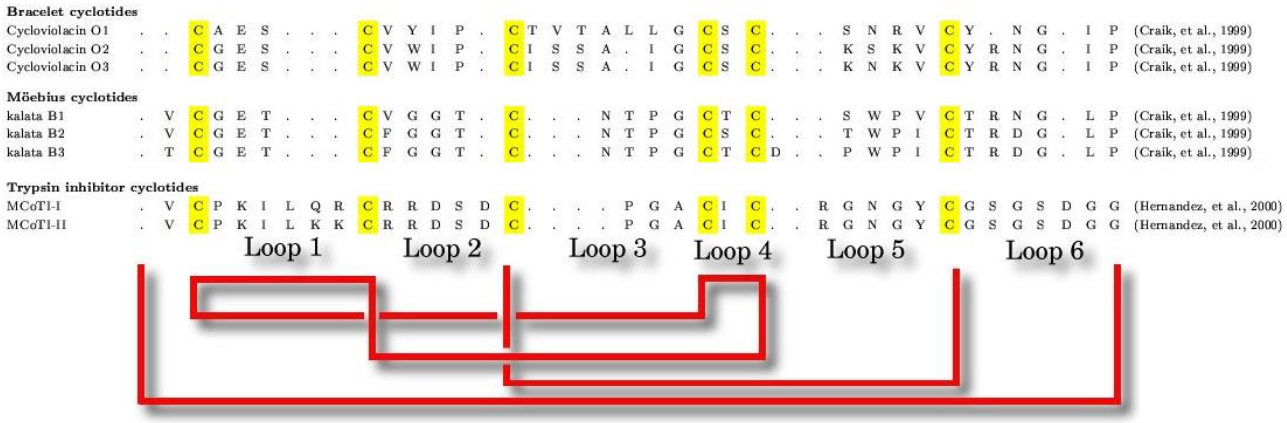

Figure 3: Excerpt showing cyclotide subfamilies, sequence, loops and cysteine bridge connectivity [14].

Cyclotides are divided into two subfamilies called Möbius and Bracelet cyclotides based on the state of the backbone. The presence of a cis-Pro peptide in loop 5 decides the subfamily that a cyclotide belongs to Möbius [7] [15]. A third cyclotide subfamily, Trypsin inhibitor cyclotides has been established but this subfamily has more sequence identity to other non-cyclic trypsin inhibitor proteins than Möbius and Bracelet cyclotides [7].

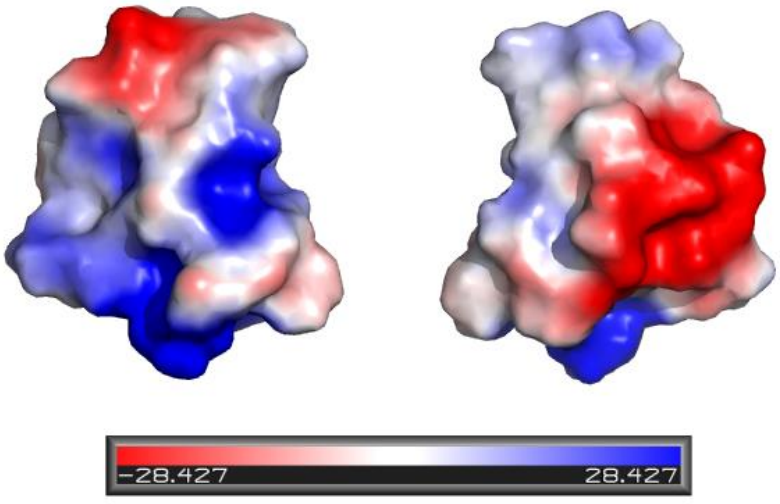

Figure 4: Surface representation showing the electrostatic potential of Kalata B1, made in PyMOL (PDB ID: 1KAL) [2].

Cyclotides are amphiphilic proteins with positive and negative charge clusters split by hydrophobic patches as shown in figure 4. Reports suggests that this polarity causes self-association in order to permeate cell membranes of microorganisms through interaction with membrane lipids or binding to chitin to facilitate the many diverse effects desired in drug development [16]. An optimization experiment on the *Viola Odarata* species suggest 50% MeOH as the optimal solvent for extraction of cyclotides, the use of a solvent with medium polarity corresponds well with the amphiphilic nature of Kalata B1 [17].

Presence of cyclotides in *T. Officinale* presents a golden opportunity to use a plant species otherwise considered an abundant weed to utilize it for mass production within medical research and drug development. Taking advantage of the high protein stability is important when developing a method for isolating proteins.

Aim

The aim of this work was to optimize the extraction and isolation of cyclotides from the *T. Officinale* flower, and experiments were designed and performed to meet this goal. The work was performed in a laboratory at the Department for Chemistry, Biotechnology and Food Science (IKBM) at the Norwegian University of Life Sciences with the supervision of Professor Lars Skjeldal.

The following aims for this master thesis have been assessed:

- Find optimal extraction and isolation conditions for cyclotides from the *T. Officinale* flower.
- Confirm specific cyclotide markers for *T. Officinale*.
- Reflect on next steps for further optimization of the process.

2 Theory

2.1 Cultivation of *T. Officinale*

The main reason for cultivating *T. Officinale* is for harvesting their flowers since it has been reported to contain cysteine rich antifungal peptides of approximate molecular size roughly around that of cyclotides [5].

T. Officinale is foremost regarded as a weed abundant in temperate regions of the world but has a very specialized lifecycle. This perennial plant germinates when the temperature in the soil reaches 10 °C and is moist, though it germinates best at 25 °C. The common dandelion is one of the early plants to bloom during spring and can be seen as soon as March. Blooming normally occurs shortly after the germination phase but requires a vernalization period of minimum 4 weeks to be able to enter the flowering phase. Vernalization is a complex genetic process including a repressor gene FLC which inhibits the vernalization pathway. When a plant is subjected to a cold period, a gene called VIN3 is expressed which changes the structure of the chromosome allowing the silencing of the FLC gene. Buds appearing is a sign that the FLC gene expression is suppressed in enough plant cells to allow the plant to enter the flowering stage. Depending on the weather conditions *T. Officinale* can bloom several times during the summer and autumn seasons and may produce up to 15 or more flowers per plant.

When cultivating plants one needs to emulate the plants most natural environment to achieve the best and quickest results. Temperature, day & night cycle, humidity, soil, water content, fertilization, light quality & quantity, biocides are all parameters that needs to be addressed in order to maximize the yield.

Cyclotides are one of the plants natural antimicrobial defense systems and fight off both virus and bacterial infections brought on by wind, insects or other contacts. Plants with different growth conditions will affect the proteome of each plant cell and thus affect the amount of cyclotides present.

2.2 Protein Stability

When performing protein extraction, it is important to ensure the stability of the protein does not get compromised before, during or after the extraction process. Protein stability is a measurement for how tolerant a protein is against denaturation, which is the process where proteins loses their bioactivity by either altering their secondary, tertiary, quaternary structure, modifying the amino acids or nucleic acid backbone. Protein stability is affected by several external and internal factors such as temperature, pH, solvent composition, glycine/proline composition, polar/hydrophobic exterior and cysteine bridges to mention some. Although the denaturation process depends on many factors, proteins may allow alterations in conformation and modifications to the amino acids without losing the proteins bioactivity, in some cases these changes may even lead to increased stability or productiveness [18] [19].

During protein folding a newly synthesized peptide chain undergoes an immediate conformational change to attain its native state. The specific conformation of this state depends on the amino acid sequence, solvent composition, pH, salt concentration, temperature and protein folding complexes called chaperones. Protein folding is a very complex process due to the specificity of different folding pathways. During a folding pathway the peptide is folded into several intermediate states in order to attain the global minima of free energy to become a fully functioning and bioactive protein. This can best be described by a folding funnel, which is a free energy diagram with the global minima at the bottom and local minimas and intermediary states along the sides. Each slope symbolizes the amount of free energy needed to transform into a different state. Protein folding pathways are illusive and difficult to predict due to the complex energy landscape for each protein and diversity of folding mechanisms. Intermediary protein conformations has molecular lifetimes of mere micro or nanoseconds and are difficult to measure accurately without costly instruments.

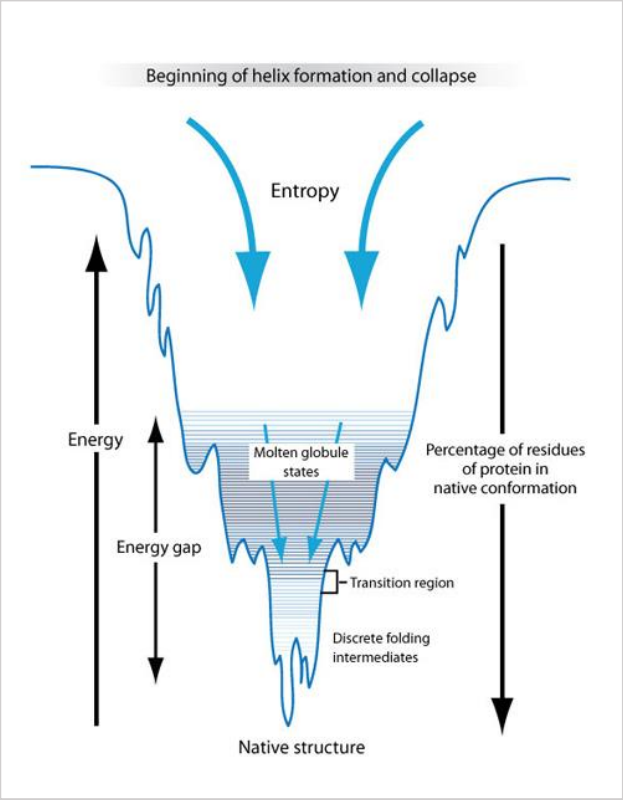

Figure 5: Protein folding tunnel.

A problem of protein folding was addressed by Cyrus Levinthal in 1969 by Levinthal's paradox; as an unfolded protein which has a seemingly unlimited amount of conformational states between amino acids, it would take the protein longer than the age of the universe to fold sequentially. And even so proteins facilitates the folding in mere microseconds [20]. Even if protein folding is well documented today a lot of the intermediary stages are still unknown. Cyclotides are renowned for their high protein stability due to the cyclic cysteine knot motif (CCK). The cysteine knot is comprised by three entwined and intramolecular cysteine bridges which makes it highly resistant to conformational changes. The cysteine bridges force the hydrophobic amino acid residues outwards creating a hydrophilic center making it resistant to high concentrations of hydrogen donors.

Since several cyclotides with varying hydrophobicity have been found in a single plant [21], identifying the extraction method wielding the solvent causing minimal interference to the protein stability is important.

2.3 Extraction Method

Decoction is an old brewing method dating back before the 1350s, where the word is derived from Latin [22]. In modern time decoction is used for drug extraction from plants for pharmaceuticals, brewing and making food. This extraction method is simply about boiling mashed plant material in water, the water permeates and dissolves the plant cells allowing compounds to diffuse into the solvent. Water is highly polar and favors polar to medium polar compounds best.

Infusion is an old extraction method used to brew tea since the early 1400s, the method replaced decoction as the primary way of brewing tea by using a bag in which the herbs could be steeped in boiled water [23]. This extraction method presents a different approach due to its instantaneous introduction of heat, upkeep of high temperature under the solvents boiling point in addition to having the plant material in a filter. All these factors will affect the compound composition of the extract but especially the temperature. Compared to the gradual increase in temperature seen with decoction a set temperature at 70 °C is carefully monitored while the plant material is steeped.

Percolation is the third method for extraction utilized and has been used since the 1700s for pharmaceutical purposes [24]. The principle behind it is that the plant material is sparged with boiled water through a filter. Today percolation remain the primary extraction mechanism for making coffee. To simulate percolation a soxhlet extractor is used, as the solvent gets boiled it condenses into the soxhlet chamber extracting compounds from the plant material through a filter, the amount of extract builds up pressure enough for it to escape the soxhlet chamber by a secondary exit into the primary flask. This results in a constant concentrating extract over time without losing solvent in the process.

2.4 Solvent Composition

Solvent and buffer composition is paramount when performing protein extraction because in order to ensure the chemical and conformational stability of the protein of interest a stable and versatile system/media is needed. This can be achieved by having a buffer with a pH range which does not cause denaturation of the protein due to change in overall charge and aggregation due to a pH close to the isoelectric point. Mimicking the native system where the protein comes from i.e. inside the cell may prove useful as well as choosing a solvent with the same hydrophobicity and/or polarity.
A solvent assay is an easy way to find out which combination produces the highest or most favorable yield by varying the composition of solvent and buffer. This is a common chemical application when dealing with uncharted proteins and easily provides sufficient data for statistical analyses. Previous reports suggest that 50% methanol is the optimal solvent for extracting cyclotides from *Viola Odarata* and is the starting point chosen for this thesis [17].

2.5 Maceration

Maceration is a necessary step in plant protein extraction not only for disrupting plant cells in order to release proteins into the solvent, but also to homogenize the sample to allow for representative results. This is done by using a suitable inert container and a mixer with sharp blades not unfamiliar to a blender or a food processor and a suitable solvent composition. The more time the plant material is macerated the more plant cells are disrupted and the more protein escapes into the solvent. The rate of protein released from disrupted plant cells decreases as the maceration time goes on until the maximum possible cyclotide concentration is reached. For a successful homogenization step a combination of the correct solvent composition and homogenization technique is required.

2.6 Filtration

Filtration is an important purification step to separate compounds above a certain size or with unwanted qualities from the sample, this is achieved by letting a liquid sample pass through a filter in the form of paper or pad to produce a purer sample and decrease turbidity. Depending on the aim different pore dimensions and materials are utilized such as cellulose, aluminum, sand and polyethylene terephthalate. These materials also have different adsorption effects which may or may not contribute to the purification step. The quality of pore dimensions are created by several different types of stranded matrixes where some are more refined than others and can with higher certainty separate molecules of a specific hydrodynamic diameter.

There are different ways to introduce the liquid sample when filtrating, such as cross-flow filtration and dead-end filtration.

Cross-flow filtration is intuitively enough a filtration method where the liquid sample is applied in a horizontal manner or across the filter rather than upon which is where the name originates from. This filtration method is highly preferred in industrial applications due to the increased output from having a higher area of permeability which makes it much more cost effective.

Dead-end filtration is a filtration method where the liquid sample passes through a filter and ends up in a container hence the name dead-end. This filtration method is normally used for research purposes as high quality filters is more important than high throughput capacity and high quality cross-flow filters are often expensive.

For the purpose of filtrating crude protein extractions a simple coffee filter and extraction thimble are used to separate solid matter from the crude extract. Coffee filter is also cheap and simple to find at the local store.

2.7 Centrifugation

Centrifugation is a heavily used purification method that separates based on sedimentation created by a centrifugal force. Compounds with a high molecular weight, that has an easy time precipitating or aggregate are affected most from centrifugal forces due to their high mass. Upon successful centrifugation a pellet is created while the remaining aqueous sample is called supernatant and depending on the compound of interest either the supernatant or pellet is discarded.

Although centrifugation is commonly used alone as minor purification and sample preparation steps in between treatments the technique is thoroughly combined with several others to create new robust methods to treat samples such as centrifugal evaporators, centrifuge columns, UV detection and ultracentrifuges.

2.8 Centrifugal Evaporation

A centrifugal evaporator is an instrument designed to remove volatile solvents from liquid and aqueous samples by taking advantage of the boiling point of liquids under vacuum, this can be compared to freeze drying as it increases the concentration of protein while reducing the sample volume. The most known centrifugal evaporator is called a Speedvac™ and is used throughout this thesis. While a rotary evaporator is commonly used for single samples a centrifugal evaporator can be used to concentrate several small volume samples in a reasonable amount of time depending on the solvent. This makes a centrifugal evaporator prime for optimization assays.

The complexity of some biological samples may result in bumping due to the lowering of boiling points, this can be suppressed when using centrifugation making it an advantage compared to freeze drying and rotary evaporation. When performing protein purification using a centrifugal evaporator ensures that protein stability isn't thermally compromised by reducing the boiling point while holding the temperature constant.

A centrifugal evaporator consists of a sample chamber with a rotor to drive the centrifuge, vacuum secured tubing from which vapor can travel through, a vacuum system that maintains vacuum throughout the device and a cold trap in liquid nitrogen which condenses the vapor into a flask.

To minimize the interference caused by solvents such as 50% MeOH during qualitative measurements, centrifugal evaporation is used to remove as much MeOH as possible before analysis. Evaporation can cause stress to the protein structure when removing intramolecular water though cyclotides have their hydrophilic core stabilized by the CCK and therefore shouldn't be a problem. As cyclotides have shown an optimal extraction in 50% MeOH they may precipitate in 100% MeOH and reports show that cyclotides can be separated by using an acetonitrile and ethanol gradient [25] [17].

2.9 Protein Determination

Many methods exist for determining protein concentration, three examples that were considered were the Lowry Protein Assay, Ninhydrin dying and Bradford Assay. The Lowrey Protein Assay is one of the most cited and used methods for protein determination [26], but this method operates under alkaline conditions and depends on the oxidation of aromatic amino acids for detection. Since cyclotides are prone to aggregation when the proteins exterior charge is altered and the goal with this thesis is to produce a non-destructive method for isolation this method was not deemed suitable [27]. The Bio-Rad protein assay is a kit based on the Bradford Assay which is also one of the most cited methods for protein determination. The Bradford method uses a protein binding agent called “Coomassie Brilliant Blue G-250” which irreversibly binds to proteins [28]. For this reason any protein determination approximations of the Bradford method are not suitable for quantification of cyclotides. Ninhydrin is yet another dye-binding compound used a lot in organic chemistry and for coloring proteins and has a protein determining method invented by H. Rosen and improved by R. McGrath [29] [30]. This method alters the amino acid by binding to primary amines and causes denaturation of certain amino acids. Because of this the method is not suitable for determining cyclotides.

In protein science UV spectroscopy is the easiest and most reliable way to determine the quality and concentration of a protein extract retaining the proteins biological activity. This is most commonly done by use of the protein standard curve which can be derived by either a previously purified protein or a ladder compromised by several proteins with a set of molecular weights to provide a significant fit to the plotted data. When using a ladder the protein standard should bear close resemblance in stability, thermal and chemical traits as the target protein to support reproducibility.

2.10 UV Spectroscopy

UV spectrophotometry is used to detect chromophores on compounds in a sample as a method to detect the presence of your target molecule(s) and the conformation in real time. This is done by emitting light at a specific wavelength that is directed through a cuvette containing the sample. The chromophore will absorb light accordingly depending on solvent composition and conformation, the light that passes through is detected by a photo diode. A computer transforms the data by measuring the transmittance (A) on a sample, comparing the amount of light at a given wavelength that passes through the sample (I) and the light emitted at that wavelength (I_0).

$$A = -\log\left(\frac{I}{I_0}\right) \quad (1)$$

By using a standard curve and Beer-Lambert's law you can find the concentration of a compound by comparing it to a sample with known concentration over a linear area.

$$A = \log_{10}\left(\frac{I_0}{I}\right) = \varepsilon cL \quad (2)$$

A is for absorbance, I_0 is for light intensity of the light source, I is for light intensity detected on photo diode, ε is for molar attenuation coefficient with the SI unit ($M^{-1}cm^{-1}$), c is for the molar concentration of chromophore with SI unit (mol/L) and L is for the length the light passes through the sample in cm. The path length of a cuvette is normally 1 cm.

Four requirements need to be met to produce a spectrophotometer, a source of light with sufficient wavelengths, a way to select a single wavelength and direct it to the sample, a stable compartment for the sample and a detector that measures the intensity of light. The light source is usually comprised of a deuterium and tungsten lamp which covers the wavelengths 190-380nm and 350-2500nm respectively, though wavelengths above 900nm are considered non-relative. The lightbeam is directed through a monochromator in which a concave mirror spreads the wavelengths so that only one wavelength may proceed. The selected wavelength passes through the sample and hits a photo diode which captures the intensity of light and delivers the data to a computer where the absorbance is calculated. On older machines you need to zero out with a blank sample before using the sample compartment for analyzing samples, this can be done simultaneously by adding a beam splitter and a secondary photo diode after the monochromator.

Proteins in general will give absorbance for the peptide bond between 180-230nm, interpretation of the absorbance in this area however is difficulty as many chromophores overlaps in this range. Most cyclotides contain the amino acid tryptophan, this amino acid has an aromatic moiety with an absorbance maximum at 280nm. This wavelength is commonly used to detect and quantify the concentration of proteins. When a tryptophan residue is beside a cysteine bridge or in the vicinity a reduction of the disulphide bond may be facilitated by the aromatic moiety through excitation in the presence of light. This phenomena is called photoexcitation and quenching where photons are absorbed by tryptophan and transferred to a cysteine bridge which quenches the light transferred [31] [32] [33]. Photoexcitation reduces protein stability and may cause tryptophan to oxidize, therefore it is important that all samples produced are kept dark [34]. A red shift of a fluorescence specter has been reported when quenching is facilitated, with a shift of up to 10nm [35].

Oxidized Trp represent the degradation products of cyclotides and has been determined by MS-MS studies [36]. The most interesting degradation products are derived from tryptophan, oxindolylalanine has a reported upshifted absorbance maximum at 285nm and kynurenine which is derived from oxindolylalanine

has an absorbance maximum of 360nm. This data proves valuable in determining the degradation of your sample by simple UV measurements and may indicate presence of cyclotide when radiated by light.

The Beer-Lambert's law is often used when determining protein concentration in a sample with unknown protein concentration, but since a sample may contain several chromophores and especially other proteins containing tryptophan the molar attenuation coefficient may be used to determine the purity of your sample. The molar attenuation coefficient measures how strong a chromophore absorbs light at a certain wavelength [37]. If the molar attenuation coefficient is known the protein concentration can be estimated.

In 1967 Harold Edelhoch published a paper postulating the connection between the molar attenuation coefficient of tryptophan and tyrosine in a protein sample. The experimental work resulted in an equation which easily predicted the molar attenuation coefficient from protein sequence [38]. This equation was later improved upon to include disulphide bridges by C. N. Pace et al. [39] and is shown below:

$$\hat{\varepsilon}_{280} = \left(5500 \times n_{Trp}\right) + \left(1490 \times n_{Tyr}\right) + \left(125 \times n_{S-S}\right) \quad (3)$$

To determine the presence of cyclotides in *T. Officinale* with more certainty, the molar attenuation coefficient (ε) was used. To calculate the molar attenuation for a sample with known protein concentration and a measured absorbance at 280nm, the molar weight of the protein is first divided by the concentration to find the molarity of the protein in the sample which is lastly divided by the absorbance. If several chromophores from different species absorbs light at the same wavelength, the molar attenuation coefficient is larger than a standard containing only one protein. A higher molar attenuation than predicted symbolizes an impure sample.

2.11 Protein Purification

Purification is a common scientific process for biochemists in which the goal is to increase the relative amount (%) of a target molecule in the sample. This is done through several steps where interfering molecules and other impurities are removed without removing or altering the target molecule(s). Purification steps are specifically designed to exploit the physical and chemical properties of the target molecule(s). Filtration, pH precipitation and chromatography are some methods that all lead to a more purified sample but requires a certain degree of purity prior to application. It's important that purification steps be applied in a correct order as their degree of purity would drastically decrease if the sample contains compounds which interfere with the purification process. Filtration is a useful step to begin with because it removes any raw extraction material as well as absorbing any big molecules. The filtration paper though may be too rough for small samples and may give negative yields if any. The same reason applies to

precipitation by change in pH and chromatographic separation, as raw extracts may clog the chromatographic column and pure protein may be altered with slight changes in pH. To increase the chance of finding the optimal conditions for protein purification any resource containing information about matrix interactions and treatments should be used to help understand the different systems and limitations the target protein(s) has.

Cyclotides are highly resistant to heat, low pH ranges as well as proteolytic treatments due to their CCK motif. Such an innate protein stability allows them to survive boiling water and nonspecific proteases unscathed and makes it an effective purification step. Reports suggest that cyclotides have high tolerance for extremely low pH ranges, but may precipitate when subject to pH 6 or higher. This may vary with the exterior of amino acid residues, but chances are the variations are minimal due to their hydrophobic nature.

A commonly group of compounds known to brewers which can interfere with protein extraction are tannins. Tannins are polyphenols and have been found to interfere with protein extraction due to their high hydrophilic activity, this causes proteins which are susceptible to precipitate [40]. A widely used thumb of rule in brewing is to not exceed a steeping temperature of 77°C using water and a pH over 5.8 to avoid high concentrations of tannins. This means however that tannins are still extracted in a smaller degree if extraction conditions are controlled carefully. Water is a medium/high polar solvent suitable providing good solubility conditions for tannins. The use of 50% MeOH as extraction solvent in room temperature was reported to extract tannins from leaves [41]. Factors such as extraction time, presence of light and solvent composition are also found to affect the yield of tannins [42].

2.12 Column Chromatography

Chromatography is a technique that separates molecules in a sample based on adsorption effects with the goal of increasing the concentration of analyte while purifying it from interfering compounds in the sample. Adsorption effects are weak reversible interactions between two compounds and includes hydrophobic, hydrophilic, polarity, charge and van der Waals' forces which the stationary phase uses to retain the analyte in order to separate. Chromatography was first established by the Russian scientist Mikhail Tsvet and published in 1905 as a biochemical analysis based on adsorption [43]. Since then chromatography has developed into a massively integrated separation technique in industry and research disciplines with a diverse collection of chromatographic methods. Column chromatography is one of these methods and uses a column to hold the stationary phase. Numerous different stationary phases separate by taking advantage of different chemical aspects for example, normal/reverse phase, cation/anion exchange or size exclusion.

A normal or reverse phase separates compounds based on polarity or hydrophobicity respectively using either hydroxyls or long carbon chains as the most common retaining groups.

Cation/anion exchange separates based on positive or negative charges and polarity using either positively or negatively charged ligands bound to silica to facilitate reversible ionic interactions.

Size exclusion separates based on molecular size and used in this thesis, therefore it is explained in more detail in the next section.

A common rule about adsorption in chromatography is that the stronger affinity for the stationary phase, the longer a compound will be retained.

A chromatographic separation consists of a perpendicular and prepared column, a conditioned stationary phase with the desired separation qualities and a mobile phase with good solubility for the target analyte as well as providing minimal upkeep. Column packing is essential when performing column chromatography because it highly affects the quality of the separation. To ensure a high quality separation, the column needs to be of uniform length, diameter and density, and also the stationary phase needs to be packed uniformly without air bubbles. If the stationary phase is loaded unevenly, has air bubbles, too little sand, or diluted sample this will result in the separation being distorted.

The column packing method used for this thesis is the slurry method, this is done by measuring the amount of dry gel material needed and suspending it in a degassed conditioning buffer to allow the stationary phase to properly swell. Specifics regarding swelling of stationary phase is covered in the next chapter about size exclusion chromatography.

Collection of fractions eluted from the column may be done manually but is commonly done automatically by immediately feeding the effluent into a detector. UV is the most commonly used detector for liquid chromatography and produces a chromatogram showing the absorption of the eluate at a set wavelength on the Y-axis and retention time on the X-axis. When fractionating manually a fraction volume is chosen, the less fraction volume used the more data points may be created for making a more accurate plot. If too few data points are created the peaks cannot be used to calculate the resolution of the chromatogram. Another important thing to remember when fractionating manually is the possibility for human error, since you can't control the drop size calculating the fraction volume is inaccurate at best and adds to the overall variance. When managing many fractions while the flowrate is high, manually switching tubes and maintaining a constant fraction volume may prove difficult.

When interpreting a chromatogram the peaks may vary in size, width and shape. This information helps uncover any flaws that might be causing a column to produce a poor separation. An example of poor separation is when two peaks are partially melded together creating an overlapping region. If this region becomes too big one cannot distinguish or deduce the peaks from each other because there is a chance

they are the same compound, there may also be underlying compounds within the overlapping region. The resolution is calculated to determine if two peaks have been successfully separated and the represented compounds differentiated. Resolution (R_s) is defined as two times the difference in retention time (t_R) between two separated compounds in proportion to the Gaussian curve width (W) of their peaks.

$$R_s = \frac{2(t_{RB} - t_{RA})}{(W_B + W_A)} \quad (3)$$

The retention time is the difference in time between solvent and compound from injection to detector and is unique for each substance as there are small adsorptive variations. The equation above shows us that even though the retention times are just slightly different, if the peak widths are thin enough the resolution will be good enough to differentiate peaks from each other. A resolution above 1.5 is considered baseline separation where two compounds are completely separated from each other, while a resolution of 1 is deemed acceptable, a resolution below 1 is not as peaks would contain a big overlap area in between. A separation factor (α) can also be used to indicate a separation but this factor only takes into account the retention time, a separation factor value of above 1.1 is usually good. The separation factor is defined as the proportion between capacity factor (k') of solute A and solute B. The capacity factor is defined as the proportion between the difference in retention time and void time (t_M).

$$\alpha = \frac{k'_2}{k'_1} \quad (4) \qquad k' = \frac{(t_R - t_M)}{t_M} \quad (5)$$

Even though resolution takes point in a gaussian shaped peak, in reality this is nearly never the case as tailing occurs as well as band broadening effects. Tailing is caused by having more than one retention factor present in the column [44]. This presents a problem as the curve width cannot be accurately measured and thus the compound cannot be differentiated. Besides tailing and adsorption effects there are kinetic factors that affect the band broadening of a peak, these effects depend on the diffusion rate of solvent and solute and interactions with the stationary phase. An equation postulated by J. J Van Deemter in 1956 [45] accounts for these effects in the Van Deemter law as they increase the variance of the separation process.

$$HETP = A + \frac{B}{u} + (C_s + C_m) \times u \quad (6)$$

Resolving power is also called the height equivalent of a theoretical plate (HETP) and is defined as the column length needed for the solute to achieve one equilibrium within the stationary phase. The Van Deemter law is used to find the optimal linear velocity with the smallest theoretical plate height as possible.

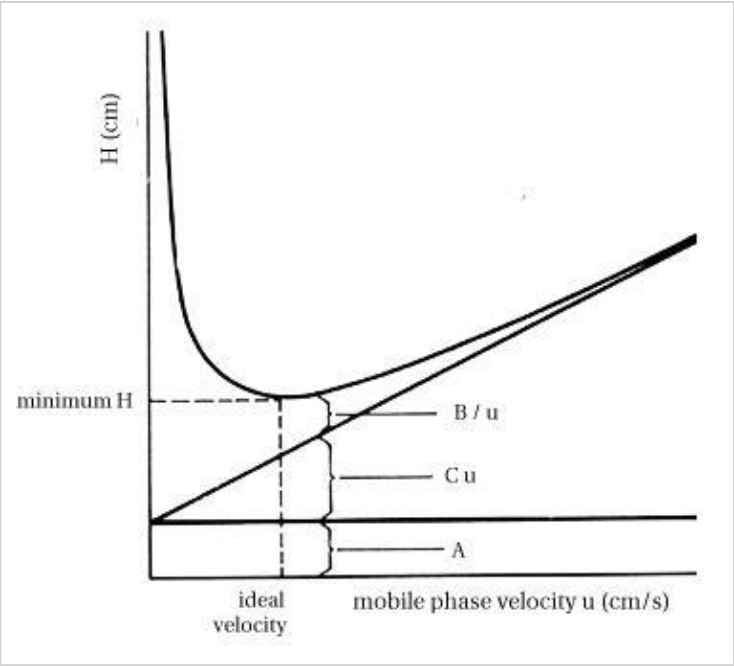

Figure 6: Demonstration of Van Deemter law plotting the plate height (H) against flowrate (u).

A low HETP symbolizes a good separation efficiency by having minimal variance due to kinetic factors, the amount of stationary phase needed to separate the solute from the sample efficiently is then small. In contrast a high HETP means that a factor within the column is causing band broadening thus increasing the theoretical plate height needed to separate the solute from the sample, which is indicative to a bad separation. Factors that affects the resolving power in a column are described as such:

Eddy diffusion (A): Diffusion along the stationary phase, the analyte takes different routes some longer than others, which leads to band broadening.

Mobile phase mass transfer (A): Diffusion from a high concentration to an area with lower concentration, a high concentration of analyte will seek equilibrium by diffusing further down the column where the concentration of analyte is low which leads to band broadening.

Eddy diffusion and mobile phase mass transfer are dependent of particle size and the diffusion rate of the analyte.

Longitudinal diffusion (B): Diffusion along the column causing band broadening due to flowrate fluctuations. Analyte close to the stationary phase has a slower flowrate than analyte in the middle of the flow, this leads to band broadening due to the fact that solute with minimal contact with the stationary phase will elute first. Longitudinal diffusion is dependent on flowrate and the diffusion rate of the analyte.

Stationary phase mass transfer (C_s): Compounds which are adsorbed into the stationary phase spend different times bound to it. Because of this the difference between bound analyte and stagnant analyte within the pores of the stationary phase create band broadening.

Stagnant mobile phase mass transfer (C_m): Analyte solved in stagnant mobile phase spends more time in

the column than analyte solved in the flowing mobile phase thus causing band broadening. The reason behind this is because the diffusion rate of the analyte outside the pores is different than the diffusion rate inside the pores.

Linear Velocity / flowrate (u): The speed in ms^{-1} at which the mobile phase is flowing in a linear fashion.

The height equivalent to a theoretical plate is also referred to as the theoretical plate height (H) and is the proportion between the column length (L) and the number of theoretical plates (N).

$$H = \frac{L}{N} \qquad (7)$$

In order to improve the separation one needs to know how much separation is done for every theoretical plate over time. There are two ways to improve the separation process, either improve the separation efficiency of each theoretical plate or increase the number of theoretical plates by increasing the column length. Mass transfer between analyte and stationary phase, a percentage of the sample will bind irreversible to the stationary phase reducing the resolving power due to having less stationary phase available for retaining the analyte. If the stationary phase's affinity for the analyte proves too strong, the analyte will take a long time to elute expending huge amounts of mobile phase. Switching to a secondary mobile phase with higher polarity will help elute.

2.13 Size Exclusion Chromatography / Gel Filtration chromatography

Size exclusion chromatography (SEC) also called gel filtration chromatography is a chromatographic method separating molecules based on their hydrodynamic diameter or molecular size. The technique was first created by Grant Henry Lathe and Colin R Ruthven in 1955 where they demonstrated a separation based on molecular weight using starch as the filtration medium and water as the mobile phase [46]. SEC is dependent on the analyte not interacting with the stationary phase on the molecular level but rather be retained solely based on the space available within each grain of filtration medium. For the purpose of separating cyclotides which has a molecular weight between 2800-3200 Da, a gel filtration medium trademarked Sephadex G-25 medium is used due to its specific weight range of 1000-5000 Da. Due to the CCK motif, cyclotides' hydrodynamic diameter is assumed to be smaller than normal proteins which does not contain this motif. The Sephadex medium is made up of a series of dextran networks making up a cavernous matrix fitting only molecules within a certain size range. Molecules which are too big to fit into the pores will remain in the mobile phase and be eluted first while smaller molecules under the molecular cut off will have such a high diffusion rate from stagnant mobile phase into flowing mobile phase that it provides close to no retention. A representation of size exclusion is found in figure 7.

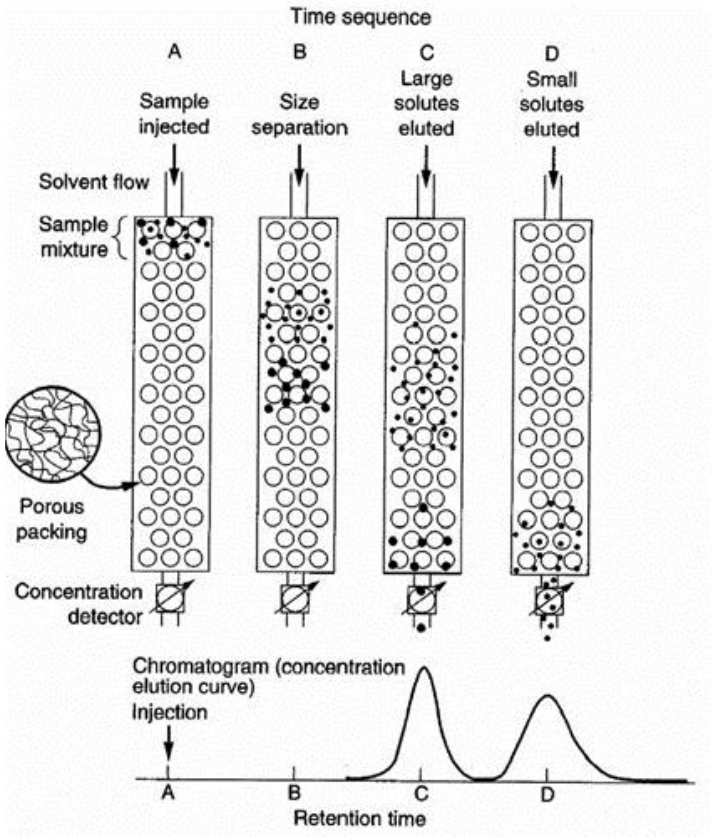

Figure 7: Representation of SEC.

A big advantage with size exclusion chromatography is that it is a non-destructive method and uses small amounts of mobile phase. This allows for a good separation without denaturizing any proteins or enzymes. The challenge with this technique is that it may not purify the protein enough as it only separates based on molecular size, so proteins or substances of near equal size behave similarly to cyclotides and will elute at the same time. Even though size exclusion separates exclusively on molecular size other retention factors may be present. A more polar mobile phase or addition of NaCl is commonly employed, though this may increase interference in later detection steps [47].

2.14 Nuclear Magnetic Resonance

Nuclear Magnetic Resonance (NMR) and has been used for structural elucidation since the late 1940s and early 1950s. The technique was first discovered by I. I. Rabi et. al. in 1938 [48] and has since expanded to include liquids and solids greatly contributing to the field of spectroscopics as well as diagnostic medicine. One dimensional (1D) NMR such as H^1 and C^{13} NMR is commonly used today to gain structural information based on signals produced from hydrogen and carbon isotopes.

NMR is based on the principle of nucleus spin. Only nuclei that has a spin not equal to zero are visible in NMR. As a nuclei has charge and spins in a direction they produce a magnetic moment and when an external magnetic field is applied to it the nucleus' magnetic moment will either align with or against the external field.

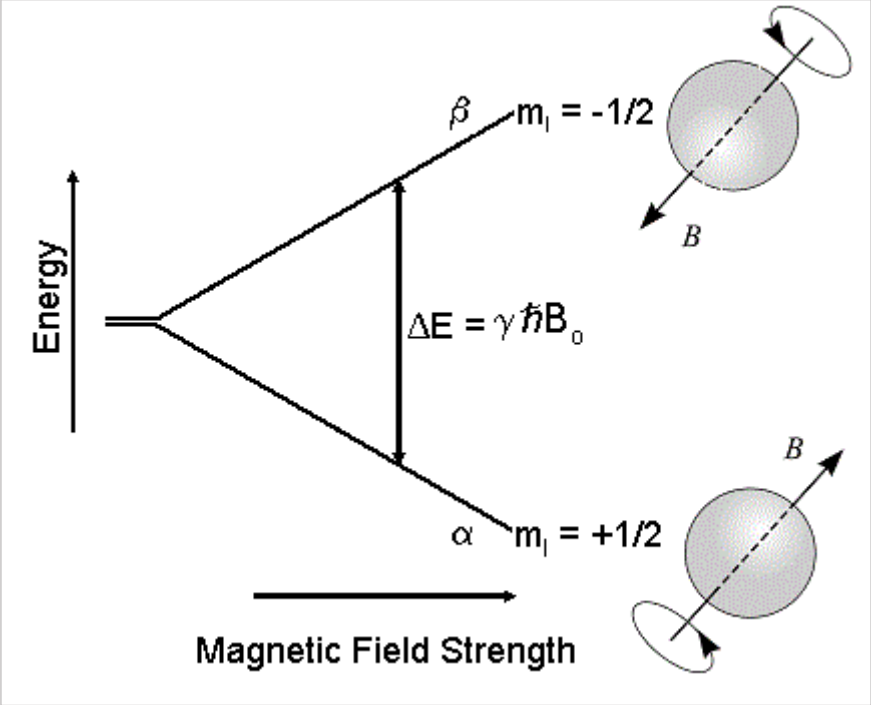

Figure 8: Energy level representation of nuclei and magnetic moment orientation in an increasing applied magnetic field.

Aligning against the external magnetic field requires more energy just like you would need to use force to hold a compass needle away from north. What ends up happening to the two energy states is that they split up and the stronger the magnetic field the larger the energy difference becomes. The energy difference is illustrated in figure 8 and calculated by the following formula below:

$$\Delta E = \gamma \hbar B_0 \quad (8)$$

After an equilibrium is met where all nuclei are either aligned with or against the external magnetic field a spin flip is facilitated by radiating the nuclei with a low radiofrequency pulse. As nucleus' can absorb and reemit energy, some nuclei will absorb this radiation and switch from the α-state to the β-state. Upon switching to another state the atom is said to be in resonance and the energy absorbed corresponds to a specific frequency given by the following formula:

$$E = h\nu \qquad (9)$$

Nuclear magnetic resonance is only produced when the frequency matching the absorbed energy and it is this resonance that is measured in NMR.

Even though similar atoms are tested they will not create signals at the same frequency unless the molecule is mirrored. Just as charged nuclei produces their own magnetic moment as do the electrons orbiting around them. The electrons magnetic moment counteracts the magnetic moment of the nuclei reducing the frequency in which resonance is achieved, it is said that the electrons shield the nuclei. This shielding affects the overall magnetic field of the atom depending on what interactions the electrons of that specific atom has with other atoms. The result will be slightly different chemical shifts due to different angles and distances between protons. Only atoms with a spin will have their energy levels split and makes it possible to measure in a detector.

Methods based on interactions between similar atoms are categorized as homonuclear through-bond correlation methods showing the J_3-couplings between two identical neighboring atoms, while interactions between different atoms are categorized under heteronuclear through-bond correlation methods. A J-coupling signifies how two spinning nuclei interacts with each other through electrons and the atoms magnetic field. The J-coupling provides structural information through something called spin-spin splitting which is seen in an NMR spectra from which atomic distance in angstrom and angles may be derived.

Kalata B1 has been structurally determined in H^1-NMR and has two adjacent amino acids with two distinct proton signals which are unique that can be used as markers for identifying cyclotides in NMR. A tryptophan and proline adjacently placed are conserved amino acids in Kalata B1 which affect each other giving extreme chemical shifts outside the "crowded" area for peptide signals. An upfield shifted H^{β} from proline gives a chemical shift of -0.25 ppm and a downfield shifted 2° amine proton from tryptophan gives chemical shift of approximately 11.5 ppm [15].

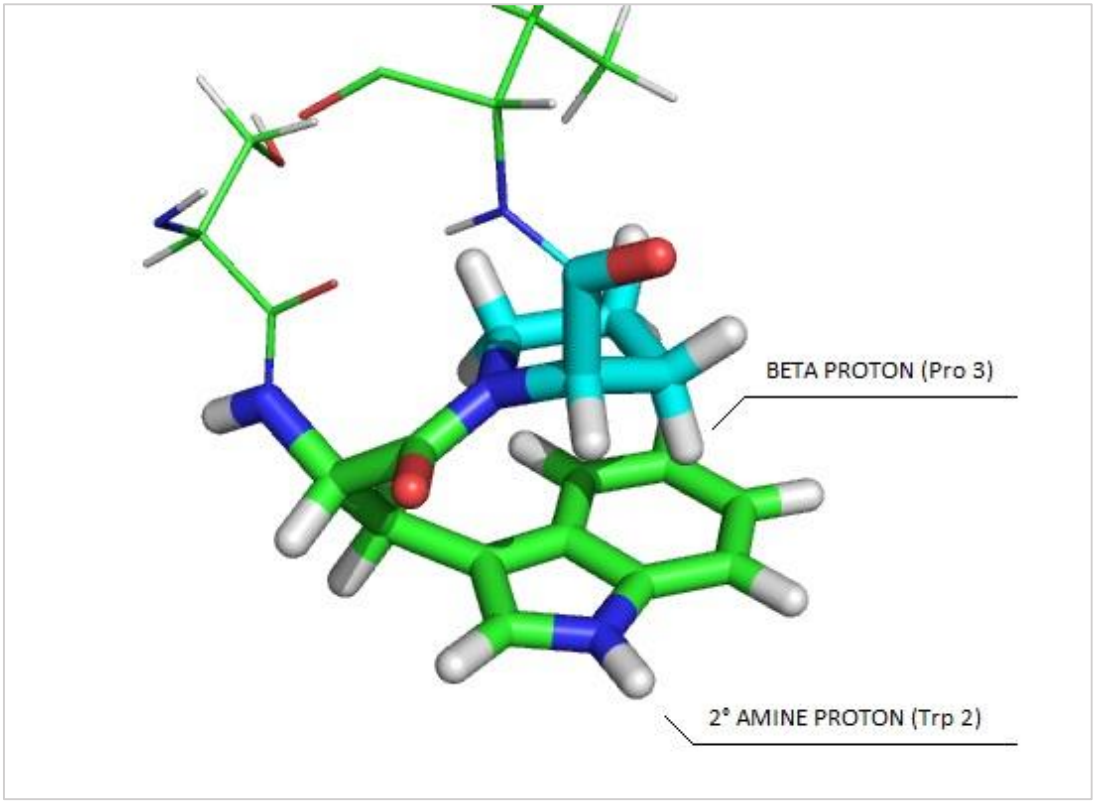

Figure 9: Sticks representation of tryptophan (Trp 2) in green and proline (Pro 3) in light blue showing the spatial orientation of the beta proton and secondary amine proton made in PyMOL (PDB ID: 1KAL) [2].

The unusual chemical shift from proline can be explained by the H^{β} being in close vicinity to the aromatic moiety of Trp 2 as seen in figure 9 where the proton is shielded by anisotropic effects created by the ring. The amine proton in tryptophan is also affected by the ring, but has instead a downfield shift due to the benzene ring drawing electrons away from the amine deshielding the proton [15]. These two chemical shifts make it easy to elucidate cyclotides from NMR which is a less sensitive even when operating with low concentrations.

Two-dimensional (2D) spectroscopic methods introduced combining two one-dimensional (1D) NMR methods together to produce even more structural insight. Correlation spectroscopy (COSY) was first suggested in 1971 by Jean Jeener and tested by Walter P. Aue et. al. in 1976 as the first two-dimensional (2D) NMR method [49]. The connectivity of these couplings are depicted in a 1D H^1NMR spectra plotted against itself with a diagonal line drawn across the middle, human perception quickly reveals that boxes may be illustrated in a COSY plot to elucidate connectivity between different signals. NMR methods with higher dimensions help provide more detailed structural information where 1D NMR proves insufficient and is required with larger and more complex molecules. Although higher dimensional NMR methods seem to decrease the complexity of NMR interpretation they are all based on the same principles which is the atomic spin system. The most common 2D NMR methods used for undocumented cyclotides are H^1-H^1 NOESY, H^1-H^1 COSY, H^1-H^1 TOCSY and H^1-N^{15} HSQC [15].

2.15 Analysis of Variance (ANOVA)

An assay is a great tool for measuring the quantity of a target analyte by altering the parameters in order to find which combination of parameters give the optimal yield. Parameters such as solvent type, temperature, filters, maceration time, extraction time, centrifugation strength etc. may all affect the quality and quantity of cyclotide yield, but may also have a negative impact by reducing yield by altering the product in an unwanted way. By systemizing data from an assay into a stacked table one can easily extract relevant information and plot graphs to illustrate important differences. Statistical analyses such as ANOVA provide valuable information by testing which treatments make a significant difference and which do not. Treatments or parameters which do not produce a significant positive difference in yield may be further excluded to shorten and make the extraction process more effective. To find which parameters are significant, analysis of variance (ANOVA) may be used to find what combination of treatments yield the most cyclotides compared to dryweight.

3 Methods

3.1 Cultivation of *T. Officinale*

For this master thesis 56/60 seeds of *T. Officinale* were successfully germinated by using a moist chamber which comprised of a pressed moist cotton layer inside a zip bag. The zip bag was closed with a small amount of air and incubated in 25 °C on the windowsill with July light time. As sprouts emerged, they were transferred with pincers to planting trays with cell dimensions of approximately 8 x 8 x 6 cm (width x length x depth) containing perlite soil. The growth conditions were 25 °C, 70% humidity, 150 µmol light and watering every morning. Fertilized water was used occasionally. When the plants outgrew their current pots they were transplanted into 13 x 10cm (height x diameter), 1 liter pots. Prior to transplantation the pots were prepared by pressing fertilized soil to create a concave surface allowing enough space for the plant. The plant, roots and entwined soil were drawn up from the planting tray and soaked properly before planting it in the middle of the pot. The plants were watered every day with regular tap water the first two weeks before introducing fertilized water with a concentration of 1.5 g fertilizer per liter three to four times a week. After two months of growth, the plants were vernalized in a refrigerated room with 4-5 °C for six weeks or until buds appear. During this time, the plants were watered with regular water once every two days. After vernalization, the plants were put back into a growth room with a temperature of 10 °C to allow a smooth acclimatization from the cold temperatures. The temperature was increased to 15 °C and watering with fertilized water once every morning.

3.2 Collection of Samples

400 *T. Officinale* flower heads were collected during two days of summer from a field on campus which is not sprayed with pesticides ensuring that pesticides do not reside in the soil or plants. Flowers were gathered into plastic bags, marked and put in a freezer.

From the cultivated plants, flowers were picked as they matured and put in a plastic bag container and transferred to plastic bags in a freezer, a total of approximately 500 flower heads were collected over a month.

For preliminary experiments sundried flowers of T. Officinale were provided, these flowers have been dried for over 1 year and contained in a plastic beaker.

3.3 Crude Sample Extraction

For this thesis sundried flower are provided and used for the extraction assay, but both sundried and frozen cultivated flowers are used in SEC separation. Frozen flowers are thawed to room temperature before the extraction process by placing the flowers on sheets of paper.

- Two sundried flower heads are macerated for 5, 10 or 15 minutes in a food processor with approximately 100 mL of the methods respective solvent.
- The macerated sample is transferred to a container depending on the extraction method.
- Three protein extraction methods are utilized in finding the optimal extraction conditions:

Table 1: Extraction treatments and parameters tested.

Method 1: Decoction	Plant material is boiled in MilliQ water for 0.5, 1, 2 or 3 hours.
Method 2: Infusion	Plant material is warmed in 50% methanol at 70 °C for 0.5, 1, 2 or 3 hours.
Method 3: Percolation	Plant material is packed in an extraction thimble where condensed vapor from either MilliQ water or 50% methanol is applied by Soxhlet extraction for 0.5, 1, 2 or 3 hours.

- Additional MilliQ or 50% MeOH is added to replace lost solvent due to evaporation in method 1 and 2, while method 3 and 4 operates with a closed solvent system without the need of extra solvent.
- Nearing the end of extraction treatment, the crude sample is topped off with solvent to a total volume of 50 mL. If for some reason less or more is produced, the total amount of dryweight is multiplied with the dilution factor.
- A coffee filter is used after extraction to separate plant material from the crude extract. The coffee filter is tested with a sample of purified cyclotide prior to the extraction to ensure that the cyclotide did not absorb into the filter.
- Crude samples from method 1 and 2 are filtrated by coffee filter, the filter is squeezed to ensure all sample is filtrated.
- Three tubes are filled with 1 mL from each method and marked for centrifugation.
- Samples are centrifuged at 10.000, 12.000 or 14.000 g-forces in room temperature for 10 minutes. The supernatant is transferred to a weighed and marked tube.
- Samples are evaporated by Speedvac for 2 to 3 hours, or until fully dried. When using 50% MeOH as solvent, tubes need to be washed with MilliQ water minimum three times to remove traces of methanol in order to reliably measure UV absorbance.

- Dryweight is calculated from a 1 mL aliquot from a batch of 50mL crude extract. 1 batch of crude extract contains 2 sundried flowers of approximately 0.18g.
- Dryweight is calculated by subtracting the weight of lyophilized samples with the weight of the same tubes when they were empty earlier.
- Precipitate/pellets created from solving samples (from methods with 50% MeOH as solvent) in water was neither weighed nor checked for UV.
- The evaporated samples are stored dark at 4 °C until further use.
- The extraction method that yields the most dryweight in conjunction with the highest UV measurements at 280nm is used for fractionation throughout this thesis.
- Three new 50 mL batches with 0.18 g sundried flower heads in each are produced with the optimal extraction method, divided into tubes and evaporated in a speedvac.
- Samples are stored dark at 4 °C and used for purification, SEC separation and NMR.

  A batch with thawed flower heads was produced with the optimal extraction method for SEC separation only.

- 195.8 g frozen flower heads were thawed and solved in 600 mL 50% MeOH.
- Crude sample is created using the optimal extraction method yielding 400 mL of crude extract.
- The crude extract is transferred to a secure and marked flask and kept dark in room temperature until further use.
- All aliquots from this batch are centrifuged, using the supernatant for application onto the SEC column.

3.4 Centrifugal Evaporation

- Evaporation was performed by a Thermo Scientific SpeedVac SPD121P centrifugal evaporator.
- Crude extracts, UV measured samples, SEC fractions and protein standards are evaporated and stored in the dark at 4 °C.
- The cooltrap is turned on and allowed to warm up for 30 minutes before starting.
- Eppendorf tubes with 1 mL samples are opened and placed with the cap turning outwards into the centrifuge chamber and the lid closed.
- The vacuum pump for aqueous solutions is turned on along with the centrifuge.
- Samples are centrifuge evaporated at 35 °C, without light until dried completely. When over 20 mL of sample is loaded the cool trap is switched halfway with a secondary bottle to ensure a fast and optimal evaporation.
- The speedvac, centrifuge and cooltrap is turned off after use.

3.5 UV Spectroscopy

- 3 mg purified Kalata sample determined by NMR is provided for quantification of crude extract and purified samples by standard curve.
- The protein standard is made by diluting the purified sample with MilliQ up to 1mL and dividing into eppendorf tubes with the concentrations 0.2, 0.4, 0.6, 0.8, 1 mg/mL the samples are diluted up to 1 mL with MilliQ.

Crude extracts and purified samples are tested by UV spectroscopy. Samples that have been treated with MeOH are evaporated by speedvac at least three times prior to taking measurements, this is done to remove interference from solvent interactions.

- All samples are diluted to 1mL with MilliQ as the last step of sample preparation and mixed by vortex prior to measurements. pH is measured before moving to the next step.
- In case of precipitation, samples are centrifuged at 13.000 g-forces for 10 minutes and supernatant transferred to a new marked tube. The tube containing the pellet is diluted to 1 mL with MilliQ and tested for protein at 280nm, 285nm and 410nm.
- If the absorbance is over 0.8, the sample is diluted 1:1 with MilliQ before a new measurement. Samples are diluted until absorbance is between 0.2 and 0.8.
- The wavelengths 280nm, 285nm, 360nm, 450nm, 550nm are measured after extraction while only 280nm, 285nm and 410nm are measured after SEC. Samples are put back into their designated tubes and stored in the dark at 4 °C.

3.6 Purification of Crude Extract by Proteolysis

Pepsin, an endopeptidase from porcine gastric fluids is tested as a preliminary purification step to increase the concentration of cyclotides and prepared as follows:

- A standard of 10 mM HCl is made in advance by adding 0.8 mL 37% HCl to a 1 L volumetric flask and filling it with MilliQ water, the solution is transferred to a secured flask and marked. The pH is measured and corrected to 2 by adding HCl.
- The pepsin standard is made by adding 1 mg pepsinogen in 1 mL 10 mM HCl and vortexing, the solution is stored at 4 °C.

To disable the enzyme activity, the pH needs to be increased to 6. To do this a sodium phosphate buffer is used. This buffer is made as follows:

- Sodium phosphate buffer is made by creating two 100 mL solutions, one with sodium phosphate dibasic dihydrate and another with sodium phosphate monobasic monohydrate.
- 2.7598 g NaH_2PO_4 x H_20 and 3.56 g Na_2HPO_4 x $2H_2O$ are each solved in 100 mL volumetric flasks with MilliQ water and transferred to secured and marked bottles.
- These two standards are then mixed 2.65 mL / 47.35 mL accordingly into a volumetric flask and filled to 100 mL.
- The buffer is corrected by adding additional sodium phosphate dibasic dihydrate until the pH reaches 8. The buffer is transferred to a secured bottle and marked.
- 10 µL pepsin is added to samples solved in 0.323 mL solvent and stored dark in room temperature overnight.
- The pH is increased to approximately 5 by adding 0.667 mL sodium phosphate buffer. The sample is centrifuged, transferred to a new tube which is used for separation.
- The sample is stored dark at 4 °C until separation by exclusion chromatography (due to the added acid, samples cannot be dried by using a centrifugal evaporator).

3.7 Separation by Size Exclusion Chromatography

Two Econa columns were utilized (2.5 x 10 & 1.5 x 10) for the separation of crude extract samples and purified samples.

- 7 g or 3.2 g of Sephadex G-25 medium is swelled in degassed 10 mM Tris-HCl pH 8 buffer twice the amount of gel. The use of 7 g or 3.2 g gel filtration medium is based on packing a 2.5 x 10 or 1.5 x 10 column respectively.
- The medium is put on a mixing board at 45 °C overnight.
- After completely swelled the gel is cooled off and as much solvent decanted without losing too much stationary phase.
- The slurry is carefully applied to the perpendicular column as the buffer is collected from opening the stopcock.
- The excess buffer is added to the slurry to ensure that most of the stationary phase is transferred to the column. The column cannot run dry as this introduces air bubbles and decreases the resolution of separations made by the column.
- When most of the stationary phase is transferred to the column, the stopcock is closed to allow the gel to settle in the column. If the gel surface is uneven or crooked the column is nudged until the gel becomes perpendicular.
- The buffer is brought down to just under the meniscus and 1-2% sample is applied carefully by circling the inner wall of the column without interrupting the bed.
- 3 cm of Tris-HCl is pipetted on top without interrupting the bed leaving 5 cm of the column left.

- 3 cm mobile phase is carefully pipetted on top of the buffer creating a water film between the two solvents.
- After the column has been equilibrated, mobile phase is connected to the column by a hose to a bottle of degassed 50% MeOH, utilizing the siphon principle.
- The separation is now ready to run and eppendorf tubes are marked and prepared for fractionation.
- A stopwatch is used to note the retention time once the stopcock is opened. Since the sample has a yellow/brown color it's easy to follow as the band progresses down the column.
- 1 mL fractions are collected manually when the band nears elution and until the band has completely escaped the column.
- The column is regenerated by washing with 2 column volumes of 0.2 M NaOH, rinsing with water and re-equilibrating with 2 to 3 column volumes buffer.
- Fractions are kept in room temperature and evaporated by speedvac 3 times before measured with a UV spectrophotometer at 280nm, 285nm and 410nm. Samples are put back into their respective tubes, measured for pH and evaporated by speedvac and stored at 4 °C.

3.8 Determination of Cyclotides by NMR

- Samples which are separated by SEC and eligible for NMR studies are eluted with 50% MeOH and are evaporated by speedvac before sample preparation.
- Sample preparation involves solving in either 100% d_4-MeOH or 50% d_4-methanol, 45% MilliQ water and 5% D_2O to a total volume of 500 µL.
- A sample of 1 mg/mL protein standard is used twice by solving separately in 500 µL 100% d_4-MeOH and 50% d_4-methanol, 45% MilliQ water, 5% D_2O by evaporating with speedvac between NMR runs.
- All fractions is solved in 50% d_4-MeOH, 45% MilliQ water and 5% D_2O apart from fraction 7 from SEC run 4 which is solved in 100% d_4-MeOH.
- All samples are vortexed until solved and their pH measured before transferring the sample to an NMR tube.
- In case of particle matter when solved in 100% d_4-MeOH, the sample is centrifuged and the supernatant used for testing in NMR.
- The NMR tubes are properly loaded to a Bruker Ascend™ 400(MHz) NMR machine with the help of a professional by an automated sampler.
- H^1-NMR scans from -10-20 ppm are performed with solvent settings set to 90% H_2O, 10% D_2O with water suppression to minimize the water absorption.
- Measured fractions are put back into their respective tubes and evaporated by speedvac.
- NMR spectra of fractions are edited in Topspin to overlay the NMR spectrum of the protein standard solved in the same solvent.

4 Results

4.1 Cultivation Studies

Cultivation of *T. Officinale* was performed with the goal of optimizing cyclotide yield by affecting early growth conditions. The cultivation was performed using growth parameters given in page 27.
Even as *T. Officinale* has been considered an abundant weed, no other studies have taken upon themselves combining cultivation, extraction and isolation studies making the results in this thesis unique.

Figure 10: Cultivated T. Officinale in bloom.

56 of 60 seeds were successfully germinated and cultivated until repotted. The flowers grew until a secondary rosette was formed signaling that they were ready for vernalization. With some difficulty regarding fertilizer dosage plants were successfully vernalized. Buds were formed signaling that the plants had entered the flowering phase. Blooming cultivated plants are seen in figure 10. Each plant produced 7-10 flowers, and though more buds were present when the cultivation was stopped this yielded a total of approximately 500 flowers. The amount of flowers produced with optimal growth conditions showed that cultivation was very easy using *T. Officinale* as a model plant. The difficulty with cultivation was the amount of time spent and the knowledge needed in order to cultivate.

4.2 Extraction Assay

In this section the results for dryweight yield is given chronological as an overview of the extraction protocols used in page 28-29 with subsections of the factors tested.

The extraction assay was performed first with 144 different combinations of extraction parameters using the factors extraction time, maceration time, extraction method and centrifugation intensity. For each factor there were different levels, for example 0.5, 1, 2 or 3 hours extraction time. Data produced from the crude sample extraction was stacked and organized into table 9 on page 69 in the appendix. Mean values were calculated for each level within each factor and were represented by the bar charts in figures 11-14. Dryweight measured in mg was considered the response variable and was represented by the Y-axis. A highest possible dryweight was important in the quest for optimal cyclotide concentration. Crude extract samples used in the extraction assay originated from a single batch with a concentration of 3.6 mg/mL.

4.2.1 Extraction Time

Different extraction times were used to see if this factor had a significant effect on dryweight yield. Levels tested for this factor were 0.5, 1, 2 and 3 hours where the data produced in the extraction assay was ordered in an increasing fashion depending on extraction time. The results were shown in figure 11.

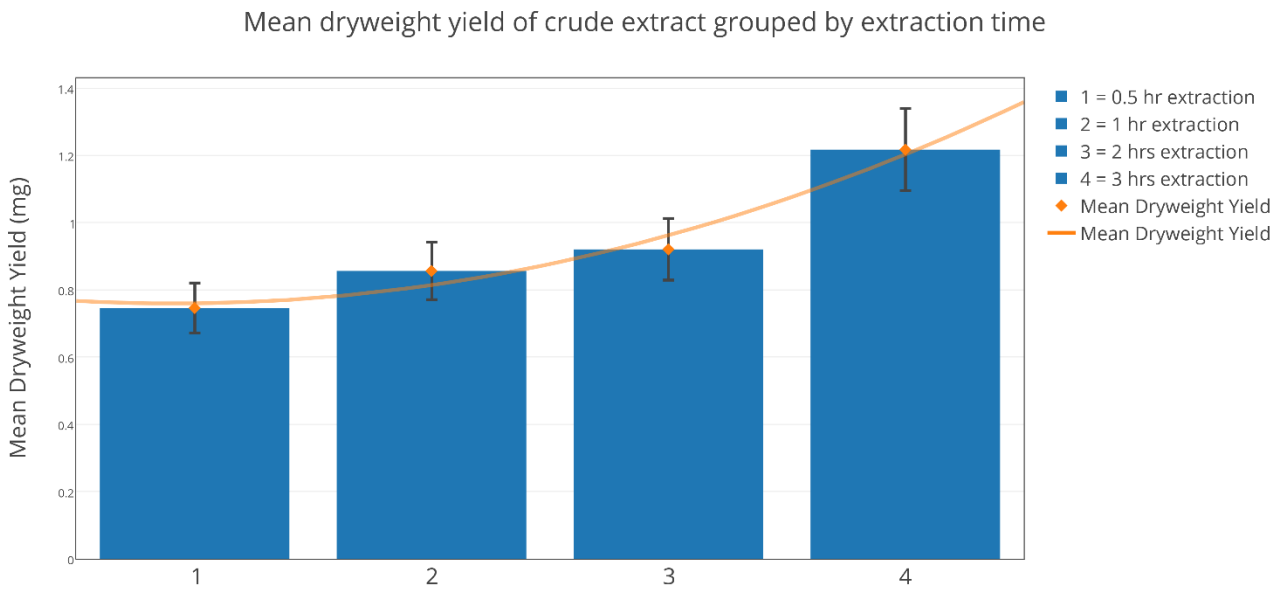

Figure 11: Plot showing trend of mean dryweight yield (Y-axis) for crude extract samples extracted by 0.5 hr. (1), 1 hr. (2), 2 hrs. (3) or 3 hrs. (4) (X-axis).

Figure 11 showed a positive trend of mean dryweight yield with an estimated maximum at 3 hours where the yield increased proportionate to increasing extraction time. The estimated maximum was not the optimal duration of extraction time as the curve continued to increase after 3 hours. The positive trend was consistent with another assay which had an optimal extraction time of 6 hours using 50% MeOH in room temperature [17]. Error bars marked the uncertainty of the mean value and increased in proportion to increasing extraction time, this was probably due to different methods being used.

4.2.2 Maceration Time

Three levels of maceration time (5, 10 and 15 minutes) were tested in order to determine the one that gave the optimal yield. Maceration was used as an important extraction step to increase the solvent contact with the protein contents of the cell. The rate of protein release was reflected by the dryweight yield. The data produced were shown in figure 12 and ordered by increasing maceration time.

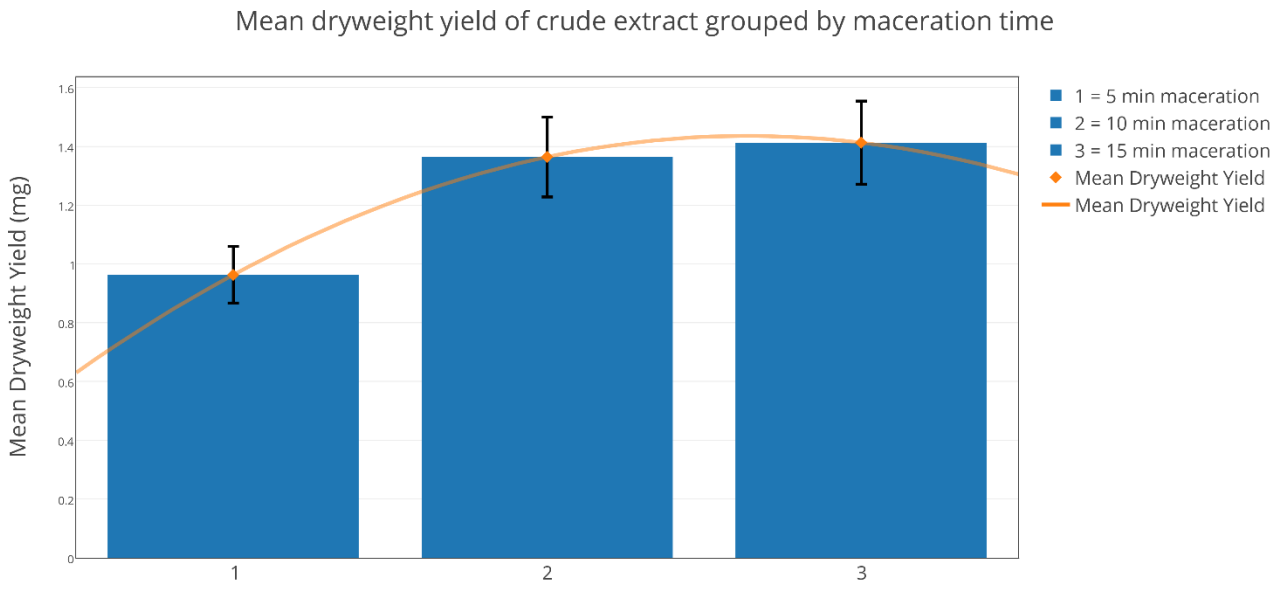

Figure 12: Plot showing trend of mean dryweight yield (Y-axis) for crude extract samples extracted by 5 (1), 10 (2) or 15 (3) minutes maceration time (X-axis).

The bar chart in figure 12 showed the mean dryweight yield for samples macerated at increasing durations. The trend line declined after the estimated maximum which meant that the yield would stabilize if maceration time stretched on. The reason for this was because the approximated total amount of protein had been successfully diffused into the solvent. As the solute contained all the protein, prolonging maceration time would not have increased the yield. Data showed that 15 minutes maceration gave the highest estimated dryweight yield.

4.2.3 Extraction Method

Four extraction methods were assessed: decoction with MilliQ water, infusion with 50% MeOH and soxhlet with both solvents. Crude extract samples were produced using one of the extraction methods with the goal of finding the one yielding the most. Two different solvents were utilized as well as different temperatures which greatly influenced the dryweight yield. The results were shown in figure 13 below.

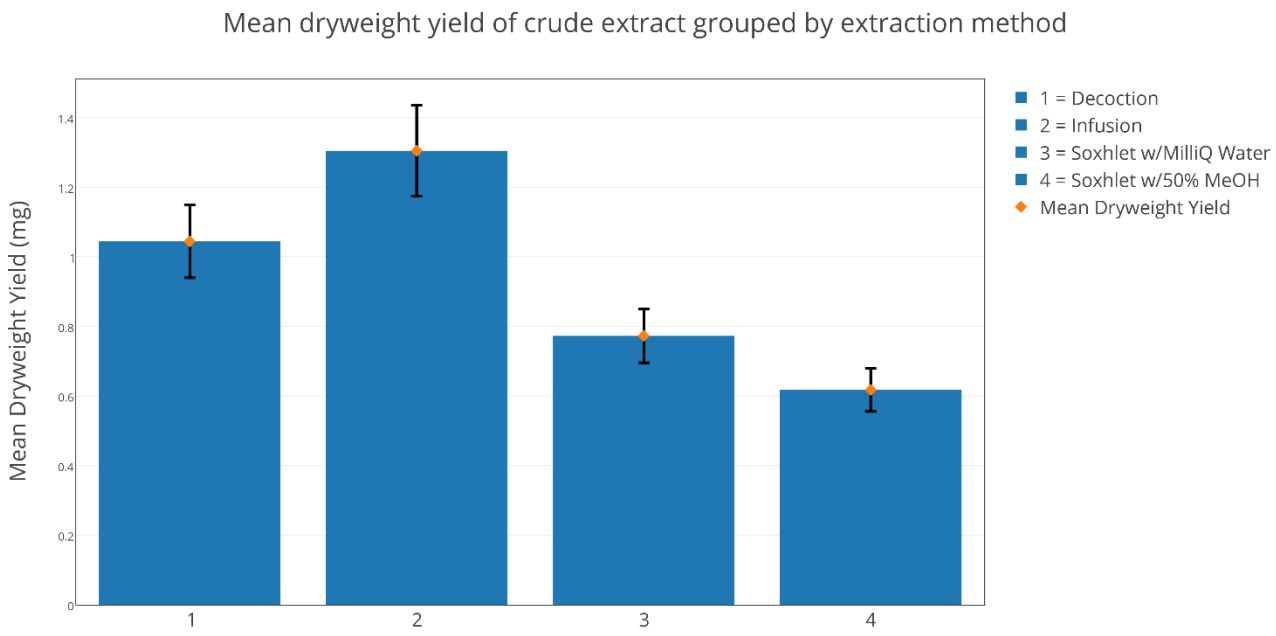

Figure 13: Plot showing trend of mean dryweight yield (Y-axis) for crude extract samples extracted using the extraction methods Decoction (1), Infusion (2), Soxhlet w/MilliQ water (3) and Soxhlet w/50% MeOH (4) (X-axis).

Figure 13 illustrated that the mean dryweight yield varied depending on which extraction method was used. An estimated maximum yield was attained using infusion with 50% MeOH as solvent and a temperature of 70 °C. Decoction also yielded good results which corresponded well with the practices of the Zulu tribe [16]. Compared to decoction and infusion, method 3 and 4 had the lowest yield due to using an extraction thimble.

4.2.4 Centrifugation Intensity

The crude extracts were centrifuged prior to dryweight measuring to remove particle matter. This was done in order to find out if the intensity of centrifugation had an effect on dryweight yield, this factor was tested for 3 levels: 10k, 12k and 14k g-forces. Figure 14 below showed the results ordered by increasing intensity.

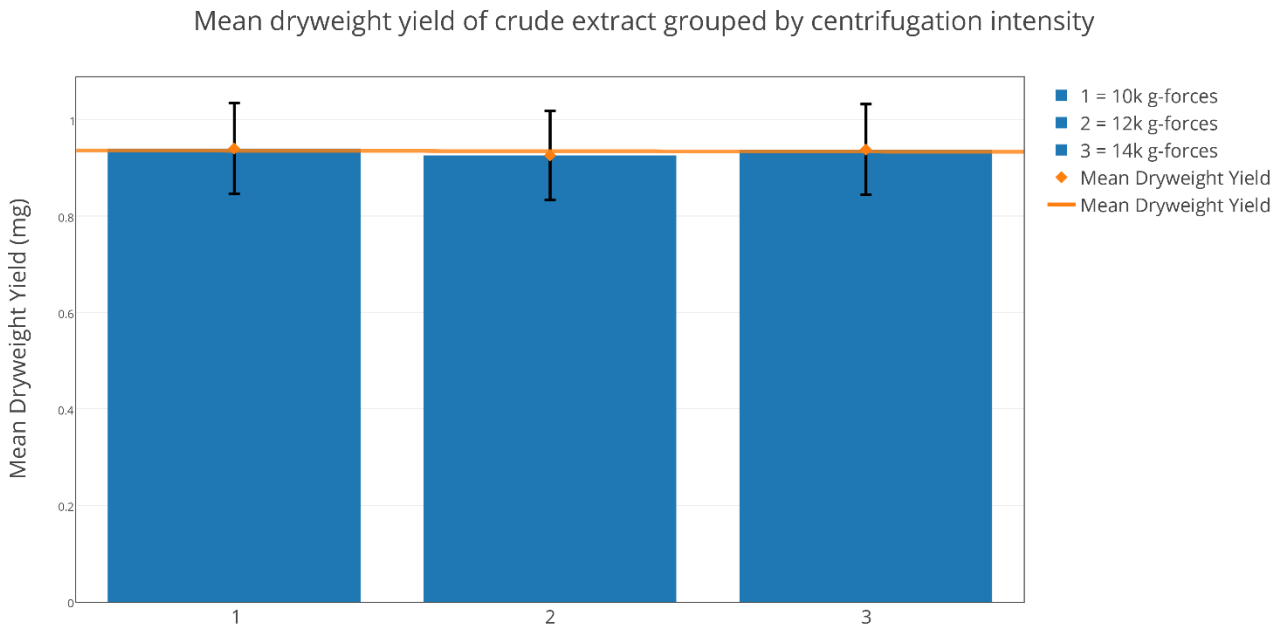

Figure 14: Plot showing trend of mean dryweight yield (Y-axis) for crude extract samples extracted with different centrifugation intensities (X-axis).

The results in figure 14 showed that all levels were equal which meant that centrifugation intensity did not influence dryweight yield. Centrifugation was therefore only used to remove particle matter for UV detection. As centrifugation was applied after adding MilliQ water for inspection with UV cyclotides may have been precipitated. Therefore the pellets were solved in 50% MeOH and checked in NMR.

4.2.5 ANOVA for Extraction Assay

Data from table 9 in the appendix was properly stacked and used to produce regression and ANOVA statistics. Dryweight yield was assigned as the response variable and compared to the designated factors ‘Boiltime’ (extraction time), ‘Centrifugation’ (centrifugation intensity), ‘Homogenization’ (maceration time) and ‘Method’ (extraction method). P-values in figure 15 were given for each factor showing the chance that the same results would be reproduced in an extraction assay where there was no real effect on dryweight. A significance level of 5% was established. In the regression analysis the slope (x) was represented for the different factors as ‘Estimate’.

```
Call:
lm(formula = Dry_weight_mg_50mL ~ Boiltime_hours + Centrifugation +
    Homogenization_min + Method, data = Dryweight)

Residuals:
     Min       1Q   Median       3Q      Max
-0.86021 -0.27273 -0.05858  0.27620  1.26590

Coefficients:
                       Estimate Std. Error t value Pr(>|t|)
(Intercept)            0.934861   0.036838  25.378  < 2e-16 ***
Boiltime_hours(0.5)   -0.189028   0.063805  -2.963  0.00361 **
Boiltime_hours(1)     -0.078750   0.063805  -1.234  0.21929
Boiltime_hours(2)     -0.014306   0.063805  -0.224  0.82294
Centrifugation(10k)    0.005347   0.052096   0.103  0.91840
Centrifugation(12k)   -0.008819   0.052096  -0.169  0.86582
Homogenization_min(5) -0.212778   0.052096  -4.084 7.59e-05 ***
Homogenization_min(10) 0.088056   0.052096   1.690  0.09332 .
Method(1)              0.109583   0.063805   1.717  0.08822 .
Method(2)              0.369861   0.063805   5.797 4.67e-08 ***
Method(3)             -0.162083   0.063805  -2.540  0.01222 *
---
Signif. codes:  0 '***' 0.001 '**' 0.01 '*' 0.05 '.' 0.1 ' ' 1

Residual standard error: 0.4421 on 133 degrees of freedom
Multiple R-squared:  0.4039, Adjusted R-squared:  0.3591
F-statistic: 9.011 on 10 and 133 DF,  p-value: 3.152e-11


> Anova(LinearModel.1, type="II")
Anova Table (Type II tests)

Response: Dry.weight..mg.50mL.
               Sum Sq  Df F value    Pr(>F)
Boiltime       4.3815   3  7.4741 0.0001160 ***
Centrifugation 0.0057   2  0.0145 0.9855611
Homogenization 3.2920   2  8.4234 0.0003594 ***
Method         9.9286   3 16.9365 2.244e-09 ***
Residuals     25.9894 133
---
Signif. codes:  0 '***' 0.001 '**' 0.01 '*' 0.05 '.' 0.1 ' ' 1
```

Figure 15: Excerpt from R Commander with linear regression (top half) and ANOVA analysis (bottom half) of dryweight yield in the extraction assay.

The P-values found in the ANOVA table in figure 15 agreed with the results described for figure 11-14 and are well within the designated significance level. Centrifugation intensity had no significant effect on yield, while maceration time, extraction method and time increased dryweight yield. The adjusted R^2 from the regression analysis showed that only 35% of the variance was explained by the given model. This meant that a lot of the variance in the extraction assay were still caused by unknown factors and should be assessed in future experiments. Some estimates in the regression analysis showed a negative slope meaning that some combinations would decrease the yield.

4.3 Estimation of Protein Concentration by UV Spectroscopy

As Lowry, Ninhydrin and Bio-Rad were deemed unfit for determining cyclotides, UV spectroscopy was utilized for its non-destructive and simplistic nature without sacrificing robustness.

4.3.1 Standard Curve

A standard curve using pure cyclotide was produced using data from table 10 on page 69 in the appendix. The standard curve was made to serve as a tool for quantification of cyclotides following the protocol written on page 30. The regression lines for absorbance at 280nm, 285nm and 410nm were calculated for protein concentrations 0.2, 0.4, 0.6, 0.8 and 1 mg/mL. The standard curve and associated lines were shown in figure 16 and represented as equation 10, 11 and 12 in table 3 below. The determination coefficient (R^2) and mean square error (MSE) were also included in table 3.

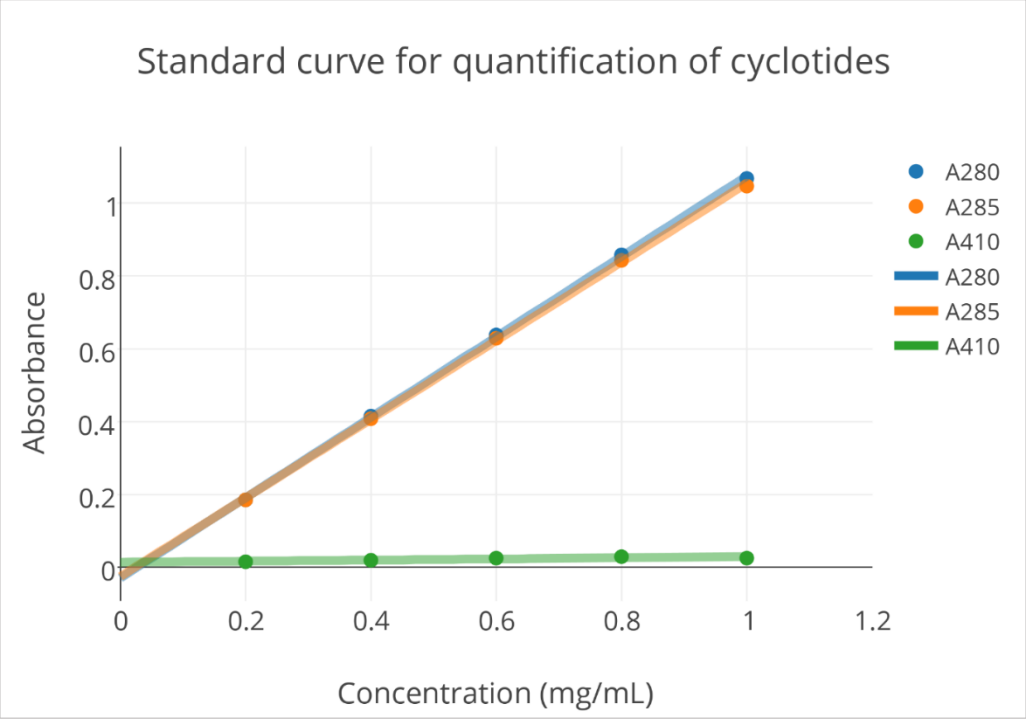

Figure 16: Standard curve showing the linear range between cyclotide concentration (X-axis) and UV absorbance (Y-axis).

Table 3: Overview of standard curve functions with their corresponding R^2 and mean square errors.

Line of best fit for A_{280}	Line of best fit for A_{285}	Line of best fit for A_{410}
$R^2 = 0.9997$ $f(x) = -0.0299 + 1.1x$ (10) $MSE = 0.0067$	$R^2 = 0.9997$ $f(x) = -0.0253 + 1.08x$ (11) $MSE = 0.0071$	$R^2 = 0.07305$ $f(x) = 0.0136 + 0.015x$ (12) $MSE = 0.0033$

4.3.2 Protein Concentration Estimation

Lyophilized crude samples precipitated when solved in MilliQ water, the samples were centrifuged and the supernatant used further. A report observed different cyclotides from the same plant with specific retention times using MeOH and EtOH gradients [17].

An acceptable R^2 value of over 0.999 was achieved for the regression lines of 280nm and 285nm, but not 410nm. Absorbance data between 0.2 and 1 mg/mL for 410nm yielded a slope of 0.015x shown in equation 12. The corresponding R^2 showed poor correlation between the data and curve for 410nm and therefore no calculations for this wavelength were done. Absorbance of 410nm was still included in the methods due to the amber color of the samples.

Absorbance was measured for the lyophilized crude extract samples from the extraction assay according to the protocol on page 30. The data produced was organized into table 11-14 on page 70-73 and used to calculate the estimated protein concentration for crude extracts. This was done by multiplying the dilution factor with the absorbance and using equation 10 and 11 to calculate the estimated protein concentration. Only protein concentrations for 280nm and 285nm were calculated due to insufficient standard curve. The calculated protein concentration was organized into table 4.

Table 4: UV detection assay of the extraction assay partially stacked by extraction time (E), maceration time (M) and centrifugation intensity (C).

E	M	C	Estimated cyclotide concentration in crude sample (mg/mL)							
			Method 1		Method 2		Method 3		Method 4	
			A_{280}	A_{285}	A_{280}	A_{285}	A_{280}	A_{285}	A_{280}	A_{285}
0.5t	5min	10k	5.34692	5.2308	4.29284	4.18224	0.50096	0.47046	0.90272	0.87948
		12k	5.1266	5.0064	4.53476	4.4352	0.49016	0.46128	0.76556	0.75096
		14k	5.0618	4.9452	4.41812	4.30464	0.46856	0.44496	0.87896	0.86112
	10min	10k	3.58436	3.50496	3.34676	3.34176	0.7418	0.69588	1.42328	1.3752
		12k	3.7442	3.65184	3.26468	3.26016	0.8606	0.80094	1.43084	1.38438
		14k	3.60596	3.52536	3.80468	3.77832	0.82172	0.77034	1.68572	1.64448
	15min	10k	4.31444	4.02312	5.06612	5.08392	0.77096	0.71934	1.82072	1.671
		12k	3.74852	3.4968	4.42676	4.45152	0.8876	0.82542	1.892	1.73832
		14k	4.46996	4.17	4.90196	4.92888	0.81956	0.76014	1.66736	1.51698
1t	5min	10k	4.30148	4.2312	3.54116	3.52536	1.0064	0.94374	1.18784	1.15386
		12k	5.105	5.0064	4.12436	4.09656	1.15544	1.08552	1.43516	1.46088
		14k	5.0186	4.9248	3.86084	3.83136	0.73964	0.71424	1.44056	1.467
	10min	10k	3.07892	2.99904	3.3338	3.30504	0.7526	0.71832	1.8704	1.85052
		12k	3.7226	3.59472	2.74628	2.7624	0.88328	0.84072	1.6814	1.65774
		14k	3.58004	3.48048	3.29924	3.36624	0.81632	0.77952	1.80128	1.7781
	15min	10k	4.23668	4.14552	2.56052	2.5788	0.85304	0.81726	1.3142	1.34154

		12k	4.241	4.14552	3.92132	3.87624	0.81524	0.77952	1.26452	1.2324
		14k	4.97108	4.84728	3.89108	3.85176	1.136	1.06716	1.3358	1.3038
2t	5min	10k	3.39428	3.30912	5.24756	5.35728	0.96536	0.89274	0.74396	0.72648
		12k	4.00772	3.85176	6.5954	6.75672	0.99452	0.91926	0.87896	0.855
		14k	3.8522	3.69672	5.74436	5.8632	0.94268	0.87234	1.18892	1.10082
	10min	10k	4.07684	3.99048	4.43108	4.3944	1.22888	1.12326	1.0496	0.97638
		12k	4.33172	4.26384	5.37284	5.33688	1.11548	1.02636	1.37684	1.32216
		14k	4.42244	4.30464	4.72484	4.69224	1.55072	1.49352	1.3628	1.3089
	15min	10k	3.0098	2.844	7.85684	8.17656	1.19324	1.1661	1.06148	0.98658
		12k	3.05732	3.0072	5.85236	5.81424	1.3142	1.29054	1.14032	1.05696
		14k	2.99684	2.95824	7.77044	8.0664	1.23644	1.22016	0.79796	0.77748
3t	5min	10k	4.6298	4.35768	5.213	5.18592	1.0172	0.94884	1.1036	1.11816
		12k	4.31444	4.05576	4.4354	4.52496	1.03016	0.95802	0.83252	0.81318
		14k	4.9322	4.63104	4.72484	4.83504	1.16084	1.07736	0.8768	0.86214
	10min	10k	3.87812	3.70488	6.65156	6.49968	0.94376	0.88254	0.73424	0.73056
		12k	3.77444	3.60288	6.97988	6.822	0.98696	0.92334	0.68132	0.67854
		14k	3.41156	3.24384	6.77684	6.60168	1.10252	1.04676	0.62624	0.62652
	15min	10k	4.04228	3.94152	8.38388	8.7192	1.18244	1.11714	0.6716	0.65814
		12k	4.07684	3.99048	8.59124	8.91504	1.1522	1.0845	1.23536	1.25994
		14k	3.86516	3.75384	7.39892	7.69104	1.09604	1.02636	1.028	1.05594

The results from table 4 corresponds well with the extraction assay where the method combining Infusion, a maceration time of 15 minutes and an extraction time of 3 hours gave the most absorbance at 280nm and 285nm. A protein concentration of 8.59 mg/mL was estimated. The absorbance at 285nm was higher than 280nm in several methods.

4.4 Purification of Crude Extract with Pepsin

Purification of lyophilized crude extract samples was accomplished by following the protocol established on page 30-31. Samples used for the two first SEC runs were treated by a nonspecific endopeptidase, pepsin prior to separation. The estimated protein concentration in separated fractions treated by pepsin was insufficient and treatment using pepsin was ceased. Subsequent samples followed the same methods as before but skipping purification by proteolysis.

4.5 Separation of Cyclotides from Crude Extract Samples

4.5.1 Separation by Size Exclusion Chromatography

New batches of crude extract with different flower concentrations were produced using the optimal extraction parameters with the purpose of purification. Four purification runs were attempted using different separation parameters to improve the efficiency of the separation. Size exclusion chromatography was performed according to the protocol written on page 31-32 using the parameters organized in table 5.

Table 5: Overview of size exclusion chromatography parameters and statistics.

SEC run	#1	#2	#3	#4	#5
Column Dimension (height x diameter)	10 x 2.5	-	10 x 2.5	10 x 1.5	10 x 1.5
Mobile Phase	50% MeOH	-	50% MeOH	50% MeOH	50% MeOH
Conditioning buffer	10 mM Tris-HCl pH 8	-	10 mM Tris-HCl pH 8	10 mM Tris-HCl pH 8	10 mM Tris-HCl pH 8
Stationary Phase (Sephadex G-25 medium)	new	-	reused	new	new
Volume Stationary Phase	35 mL	-	36.82 mL	15.9 mL	15.72 mL
Flowers used	Sundried	-	Sundried	Sundried	Cultivated
Flower concentration	0.0036 g/mL	-	0.0036 g/mL	0.0036 g/mL	0.4895 g/mL
Treated by Pepsin	Yes		Yes	No	No
Sample (1 mL)	1x crude extract in 10 mM HCl pH 2	-	10x crude extract in 10 mM HCl pH 2	10x crude extract in 10 mM HCl pH 2	1x crude extract in 50% MeOH pH 6
Injection Volume	700 µL (2%)	-	700 µL (1.9%)	159 µL (1%)	314 µL (2%)

SEC run #2 was excluded due to column contamination where the sample was absorbed onto the stationary phase and would not elute with mobile phase. A treatment with pepsin was performed on samples prior to separation in SEC run #1 and #3 described in further detail on page 30-31. Sample used in SEC run #5 was produced from an entirely new batch with a flower concentration 135 times greater than the samples used for the previous SEC runs. A fast and slow flowrate were tested in the two first SEC runs. For small proteins a fast flowrate of 5 mL/min was recommended when using Sephadex G-25 medium as stationary phase [50]. Due to limited time and many test parameters, statistical application of the separation was not accomplished. As the sample had a distinct amber color it was easy to determine when the fractionation should start.

4.5.2 Constructing Chromatograms from UV Detection

UV at 280nm, 285nm and 410nm was measured for the fractions in the four SEC runs, the results were organized into table 15-18 on page 74-79 in the appendix. Absorbance at 280nm represented cyclotide concentration, the absorbance at 285nm represented the concentration of oxindolylalanine and the absorbance at 410nm represented the complimentary wavelength to the color yellow. Fractions from SEC run #1, #3 and #4 were lyophilized three times prior to UV measurements where MilliQ water was used as solvent and blank sample. Samples were centrifuged to remove particle matter before measuring UV. Due to the possibility of precipitation and loss of cyclotides when using another solvent, UV of SEC run #5 was measured directly using 50% MeOH as both solvent and blank sample. The absorbance varied by lower than 0.0005 points. The raw absorbance was multiplied by the dilution factor and ordered sequentially by fraction number to create the chromatograms shown in figure 17-20. The chromatograms were used to determine if cyclotides were successfully separated.

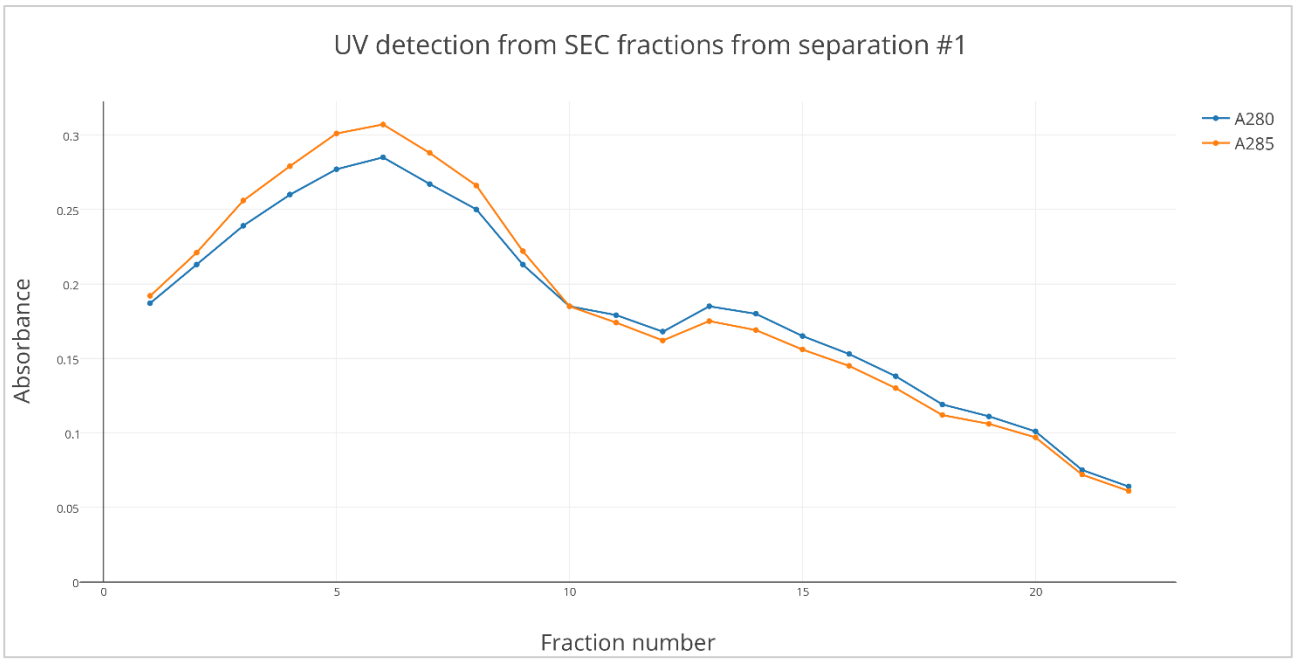

Figure 17: Chromatogram created by UV measurements from eluted fractions from SEC run #1.

A separation was observed for the peaks found at fraction 6 and 13 illustrated in the chromatogram in figure 17, but they were too melded together to distinguish a successful separation. The absorbance at 285nm was higher than 280nm at fraction 6 and lower than 280nm at fraction 13. Due to poor separation and absorbance the chromatogram was deemed inconclusive.

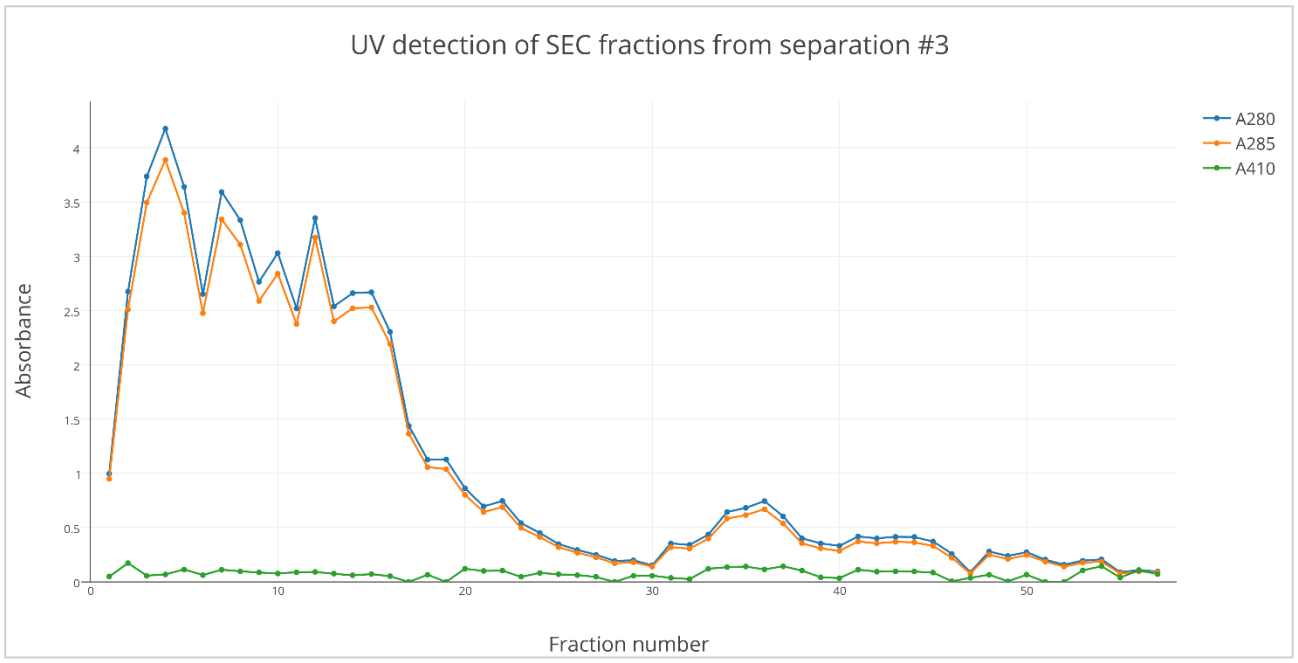

Figure 18: Chromatogram produced by fractions eluted in SEC run #3.

The chromatogram in figure 18 was created using fractions from SEC run #3. Unretained compounds eluted in fractions 1-20 were observed. Peaks in this region lacked baseline separation and were not distinguishable. The peak observed in fraction 33-38 had been retained by the column with some absorbance at 410nm observed.

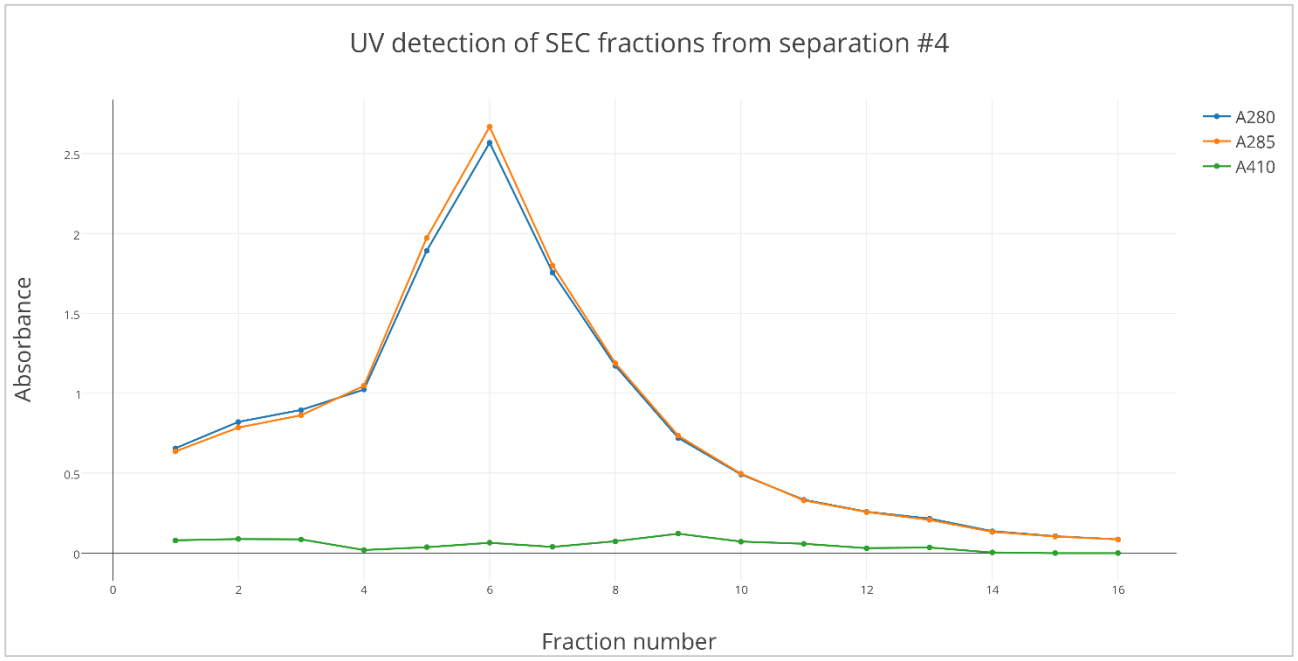

Figure 19: Chromatogram produced by fractions eluted in SEC run #4.

Only one peak was observed for SEC run #4 in figure 19. The peak was eluted since it was easy to distinguish where the retained sample would elute due to the amber color. Since there were no other peaks eluted no separation could have been determined. The peaks absorbance at 285nm was higher than 280nm.

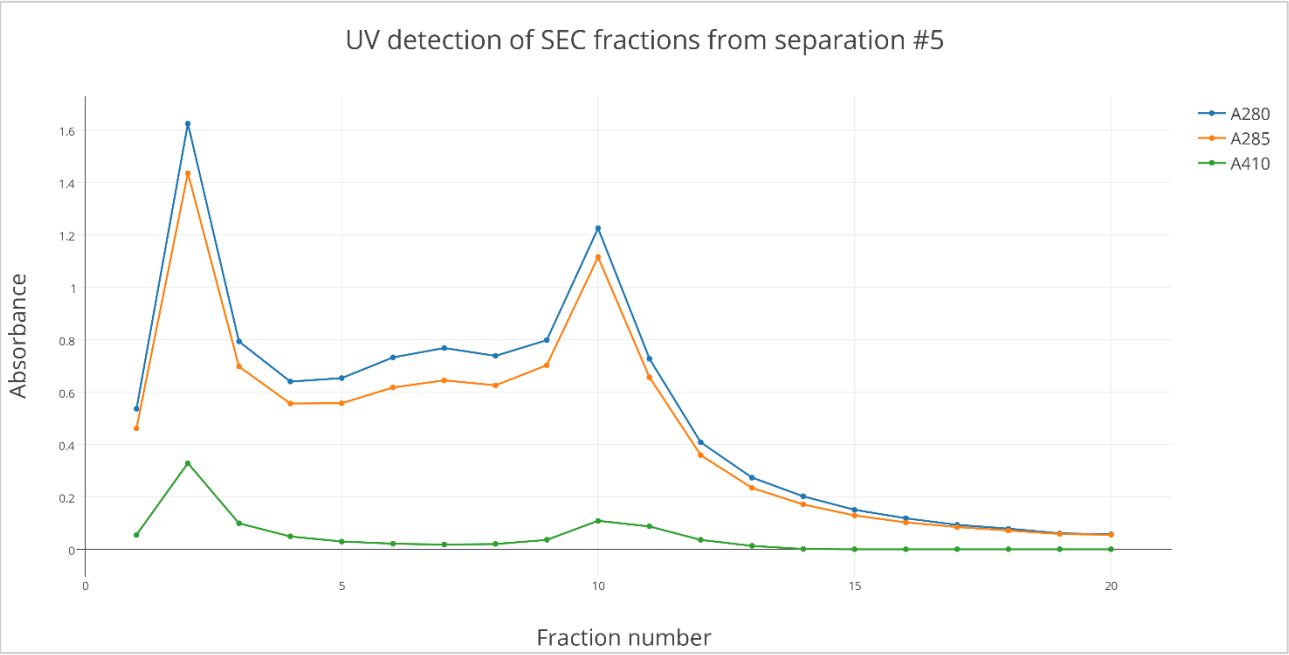

Figure 20: Chromatogram produced by fractions eluted in SEC run #5.

The chromatogram for SEC run #5 was illustrated in figure 20. Two distinct peaks at fractions 1-3 and 9-12 were observed. Absorption at 280nm and 285nm from fraction 4-8 was observed between the peaks, but none at 410nm. Tailing for the peak at fraction 9-12 was observed. Absorption at 410nm was observed for fraction 2 and 10-11. The estimated concentration of separated protein was 1.14 mg/mL.

4.5.3 SEC statistics

Flowrate, number of fractions, elution time and dead time were noted for each SEC separation and organized into table 6 below. The flowrate was measured by filling a 10mL volumetric flask with mobile phase and taking the time. The elution time was measured from when the mobile phase started until it was stopped. Dead time was the time the mobile phase started running until the start of fractionation.

Table 6: Overview of analytical information from samples separated by size exclusion chromatography.

SEC run	#1	#2	#3	#4	#5
Flowrate	1.28 mL/min	-	5.28 mL/min	1.66 mL/min	1.25 mL/min
Fractions	24 à 24 mL	-	57 à 54.55 mL	16 à 16 mL	25 à 25 mL
Elution Time	1785s +/- 5s	-	680s +/- 10s	831s +/- 5s	1265s +/- 5s
Dead Time	644s	-	70s	252s	65s

The elution times in table 6 had an uncertainty designated to them since fractionation was done manually. SEC run #3 operated with a higher flowrate making manual fractionation difficult which resulted in a higher uncertainty and inconsistent fraction volumes.

4.5.4 Molar Attenuation Assay

4.5.4.1 Prediction of a Molar Attenuation Threshold

The molar attenuation coefficient (ε) was calculated from the absorbance data used for constructing the chromatograms and by using Beer Lambert's law in equation 2. This unit was used qualitatively as a measurement which determined the purity of SEC fractions. The molar attenuation coefficient for Kalata B1 was predicted using the protein sequence of Kalata B1 found in figure 2 and was calculated by using equation 3 on page 16.

Kalata B1: $n_{Trp} = 1$, $n_{Tyr} = 0$, $n_{S\text{-}S} = 3$

$$\hat{\varepsilon}_{280} = (5500 \times 1) + (1490 \times 0) + (125 \times 3) = 5875\ M^{-1}cm^{-1}$$

Kalata B1 had a calculated molar attenuation coefficient of 5875 $M^{-1}cm^{-1}$. The molarity was calculated using the estimated concentration of the sample and a predicted molecular weight of 2916 Da suggested on page 6 in the introduction. The molar attenuation coefficient was calculated for the protein standard using the data from table 10 in the appendix and displayed in table 7 on the next page.

Table 7: Overview of the calculated molarity and molar attenuation coefficient for the protein standard.

Molarity (mol/L)	Molar attenuation coefficient ($M^{-1}cm^{-1}$)
6.85772E-05	2697.689
0.000137154	3025.786
0.000205732	3101.127
0.000274309	3127.86
0.000342886	3114.737

A molar attenuation plot of the protein standard was produced using the data calculated in table 7 and table 10 in the appendix. The plot was displayed in figure 21.

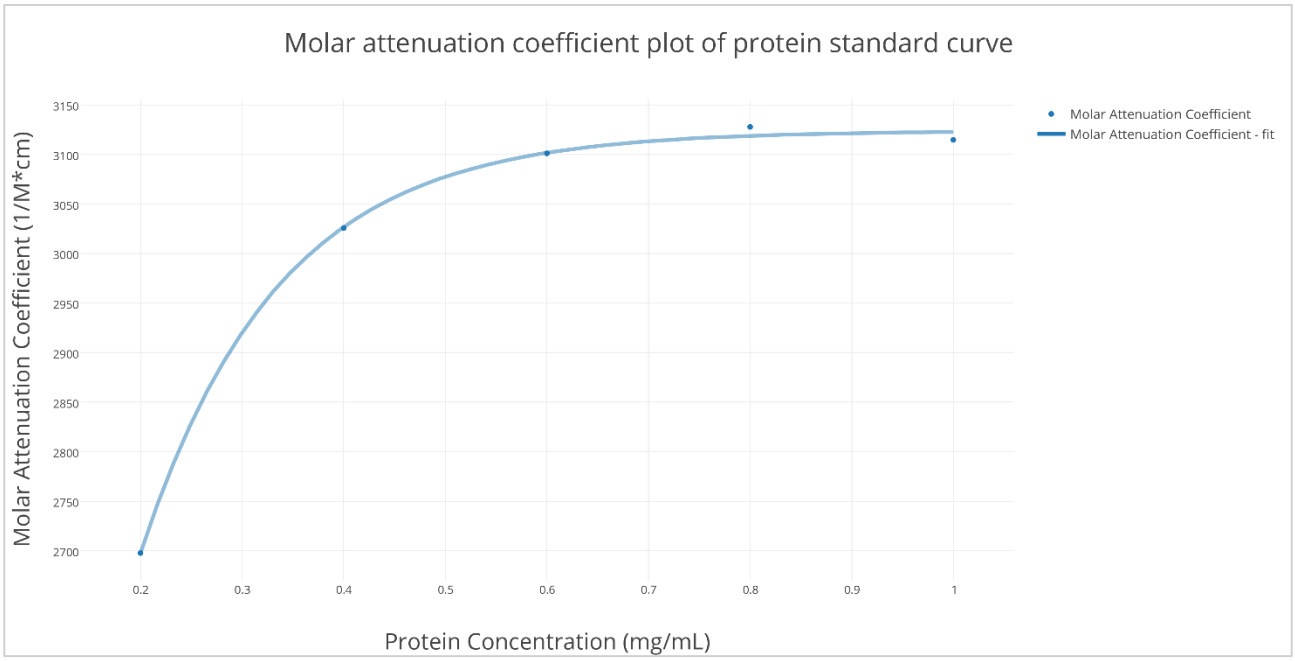

Figure 21: A logarithmic plot of the molar attenuation coefficients for the protein standard (blue line).

Table 8: Overview of molar attenuation plot statistics.

$R^2 = 0.9989$

$$f(x) = 3124 - 1869^{-7.39x} \quad (13)$$

MSE = 8.561

The plot showed in figure 21 resulted in a logarithmic curve showing the relation between protein concentration and molar attenuation. As the protein concentration increased to 1 mg/mL, the molar attenuation for the protein standard closed in to a maximum of approximately 3125 $M^{-1}cm^{-1}$. The molar attenuation of the protein standard diverged from the predicted molar attenuation of Kalata B1.

The function, correlation coefficient and mean square error for figure 21 was organized into table 8. An intercept value of 3124 was observed in equation 13 which agreed with the predicted maximum molar attenuation coefficient for the protein standard. The estimated molar attenuation coefficient of 3125 $M^{-1}cm^{-1}$ was used as a threshold for determining the purity of fractions separated by SEC.

4.5.4.2 Selection of Qualified SEC Fractions

Chromatograms of the previous SEC separations were transformed into molar attenuation plots with data from table 15-18 in the appendix. The same procedure used for the protein standard was used for the molar attenuation plots. The plots were displayed in figure 22-25 with a threshold at 3125 $M^{-1}cm^{-1}$ symbolized as an orange line.

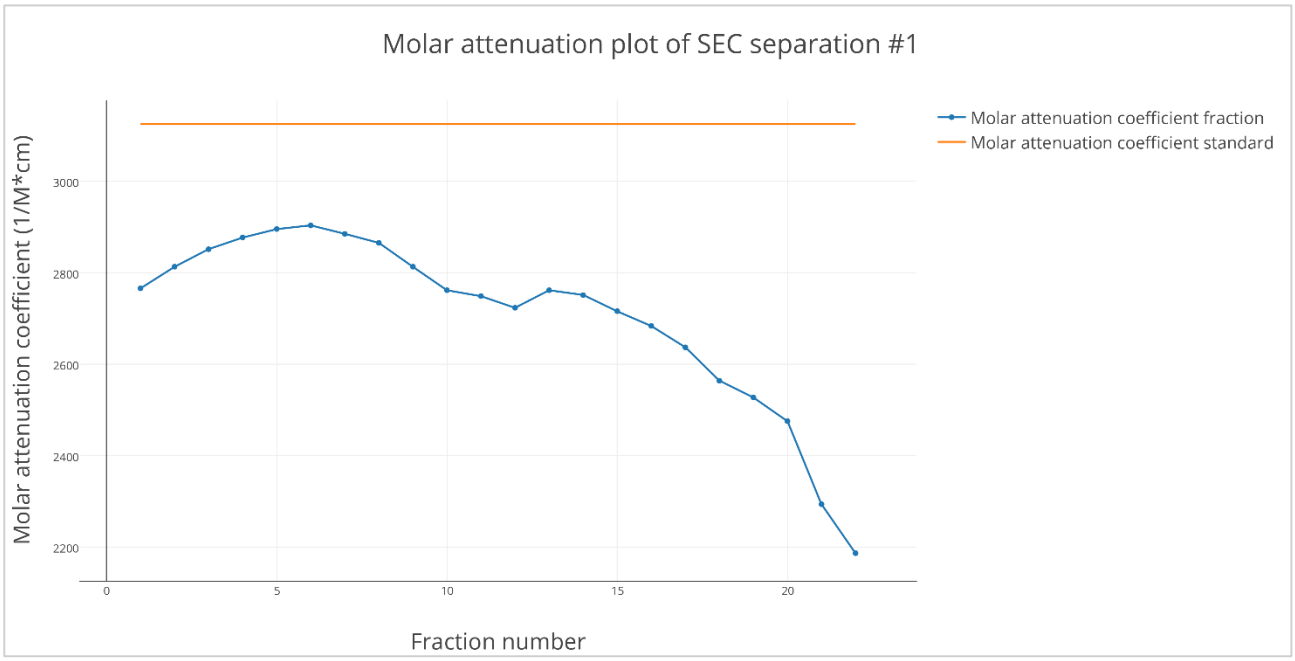

Figure 22: Molar attenuation plot created from chromatogram for SEC run #1 (in blue) compared against the molar attenuation threshold (in orange).

The molar attenuation levels for the chromatogram from SEC run #1 observed in figure 22 were lower than the threshold. Fractions from SEC run #1 were therefore not used further in NMR studies.

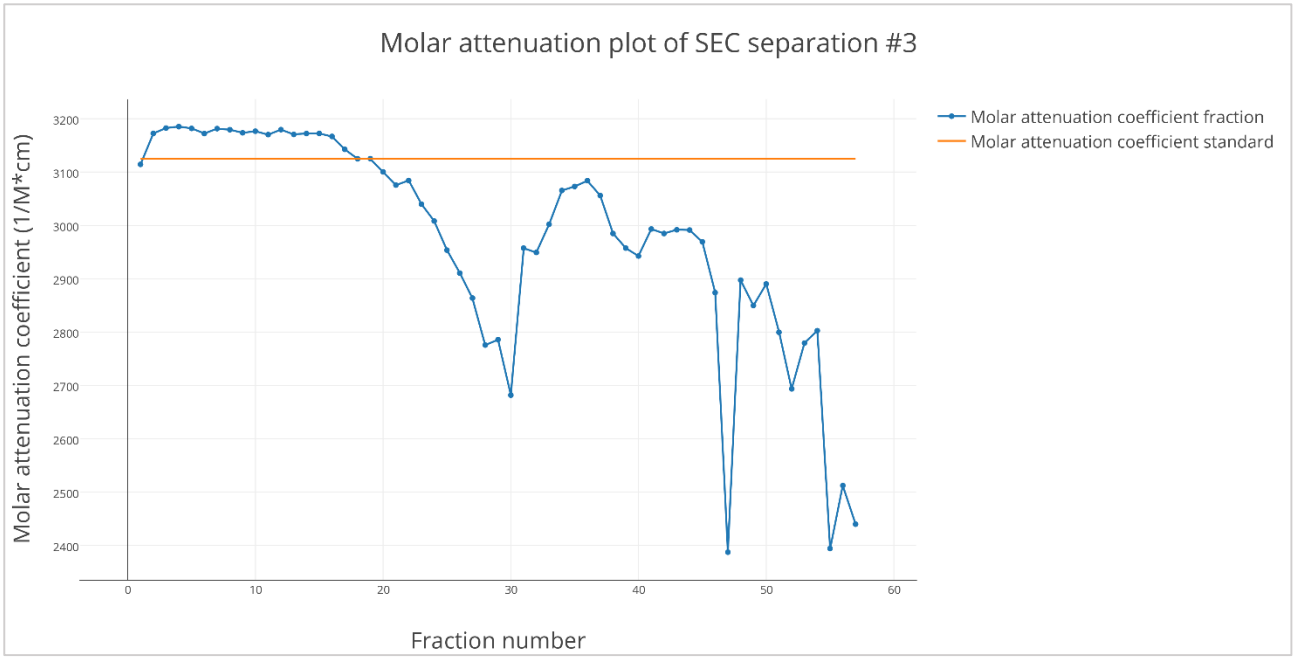

Figure 23: Molar attenuation plot created from chromatogram for SEC run #3 (in blue) compared against the molar attenuation threshold (in orange).

Figure 23 displayed the molar attenuation levels of the chromatograms for SEC run #3. The molar attenuation for fractions 2-17 were higher than the threshold. Fraction 1 and 18-19 were observed having molar attenuation close to 3125 $M^{-1}cm^{-1}$ but had no observed peak in figure 18 making the fractions illegible for NMR. Fraction 34-37 showed promise but did not fulfill the minimum requirements for further studies.

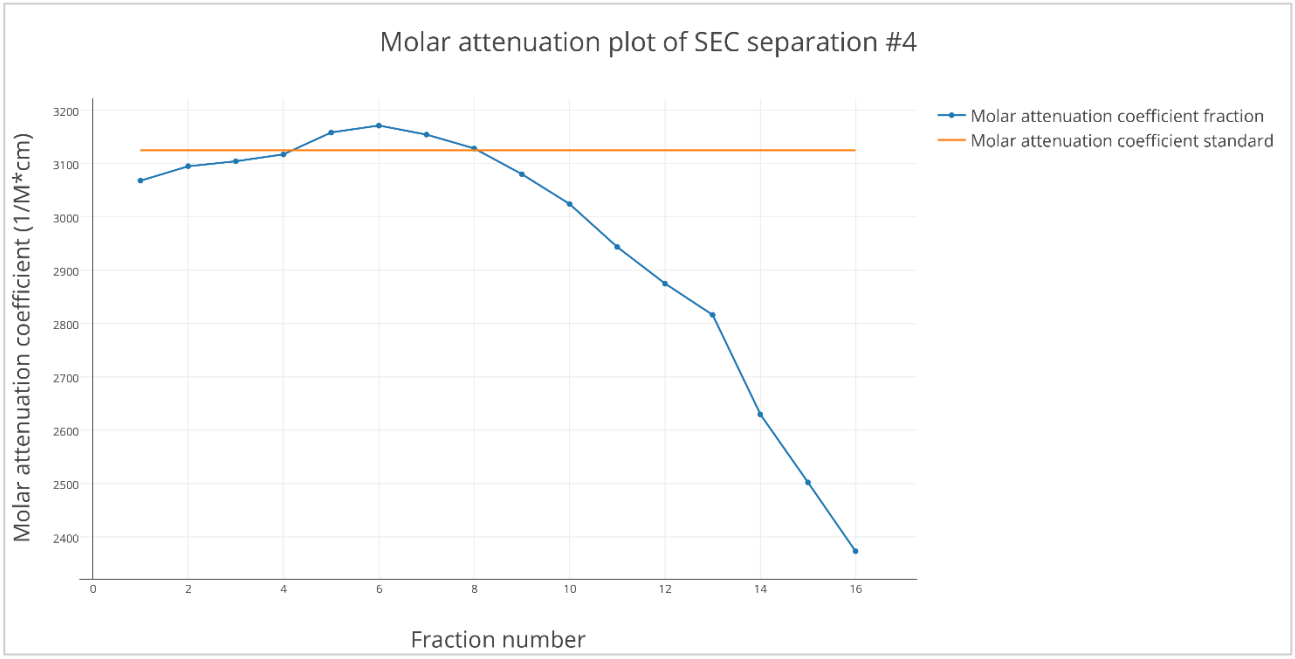

Figure 24: Molar attenuation plot created from chromatogram for SEC run #4 (in blue) compared against the molar attenuation threshold (in orange).

The molar attenuation coefficients for fractions eluted in SEC run #4 were displayed in figure 24 on the previous page. Fractions 4 and 8 were both observed close to the threshold and could have been used for NMR studies. Fraction 5-7 formed a peak and had a higher molar attenuation than the protein standard, which are probably caused by impurities. As only one peak was present presence of cyclotides cannot be concluded. Nevertheless fraction 7 was selected for further NMR studies.

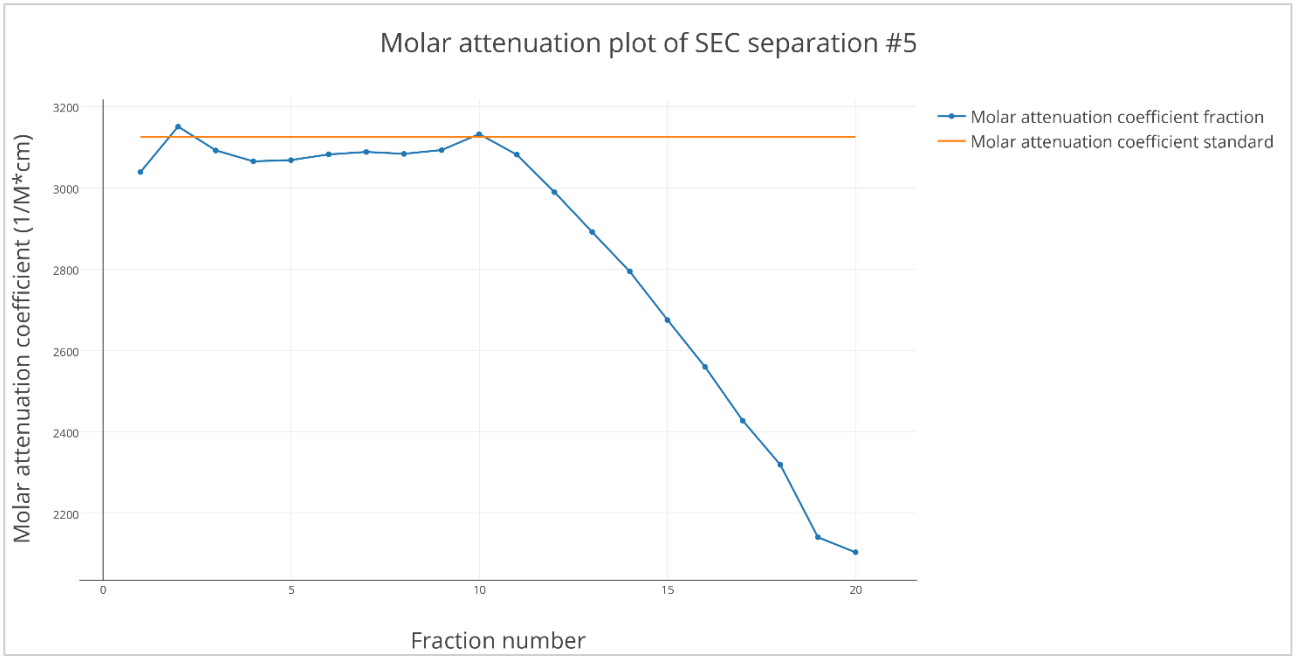

Figure 25: Molar attenuation plot created from chromatogram for SEC run #5 (in blue) compared against the molar attenuation threshold (in orange).

The molar attenuation levels for fractions eluted from SEC run #5 were displayed in figure 25. The levels for fraction 2 and 10 were observed close to the molar attenuation threshold and have been selected for NMR studies. Fraction 3-9 had an observed molar attenuation below the threshold and contained no cyclotides.

Cyclotides have been successfully separated by SEC with an estimated molarity of 0.39 mM yielding a purification strength of 7.5 times.

4.6 Determination of Cyclotides by H^1-NMR

Due to the big size of the NMR spectra, the body text in this section was written chronological but prior to all the figures.

Fractions that showed a molar attenuation level close to 3125 $M^{-1}cm^{-1}$ and a separable peak in the SEC chromatogram were selected for structural elucidation by 1D H^1-NMR. An NMR template spectrum was produced using the protein standard in 50% deuterated methanol and 100% deuterated methanol. Fraction 7 from SEC run #4, fraction 2 and 10 from SEC run #5 as well as a 10x crude extract were analyzed with the protocols written on page 32. Comparisons were done between the selected samples and the protein standard in the same solvent. All fractions were analyzed in 50% deuterated methanol and with water suppression except the 10x crude extract which was analyzed in 100% deuterated methanol without water suppression. A proline proton at -0.25 ppm and a secondary amine proton from tryptophan at 11.50 ppm were used as markers for determining the presence of cyclotides in tested samples.

Figure 26-27 showed the NMR spectrum comparison of protein standard analyzed in different solvents. Both marker signals were found in the spectrum using 50% deuterated methanol. Only the proline proton marker was found in the spectrum using 100% deuterated methanol at the reported chemical shift.

The NMR spectrum in figure 28 showed the comparison between fraction 7 from SEC run #4 and the protein standard. Precipitation of the entire sample was observed with 100% deuterated methanol. The fraction was saved by removing half the solvent and replacing it with MilliQ water completely solving the sample. Aromatic protons were observed at 6-8 ppm as well as an amide proton at 8.5 ppm. A proton signal at -0.1 ppm was observed. The signal found at -0.1 ppm did not match the marker for proline but may have been a deshielded proline. As no signal was observed at 11.50 ppm and the signal to noise ratio for the rest of the spectrum was too low cyclotides, cyclotides were not observed.

The crude extract was tested in NMR because of the absence of cyclotide markers found in the previous spectrum of fraction 7 from SEC run #4. Figure 29 showed the NMR spectrum of the crude extract compared to the protein standard. High salt concentrations caused heavy baseline distortions and an NMR spectrum was barely extracted from the NMR software Topspin. Therefore the spectra were not properly aligned.

NMR spectrum comparisons for fraction 2 and 10 from SEC run #5 were made and presented in figure 30 and 31. Figure 30 showed no proline signal at -0.25 ppm though showed aromatic protons between 6-8 ppm. Amide and amine protons are easily exchanged with the solvent.

Fraction 10 in figure 31 showed no signal for proline at -0.25 ppm but had more and stronger signals than fraction 2 at 5-8.5 ppm. The three evenly spaced multiplets at just over 8 ppm in red resembled that found in the protein standard at 9.4-10 ppm. No secondary amine protons were observed between 10-12 ppm. Even though fraction 2 and 10 originated from a new batch with a higher flower concentration the signal strength for both NMR comparisons showed that the concentration of protein was too small for the presence of cyclotides to be determined.

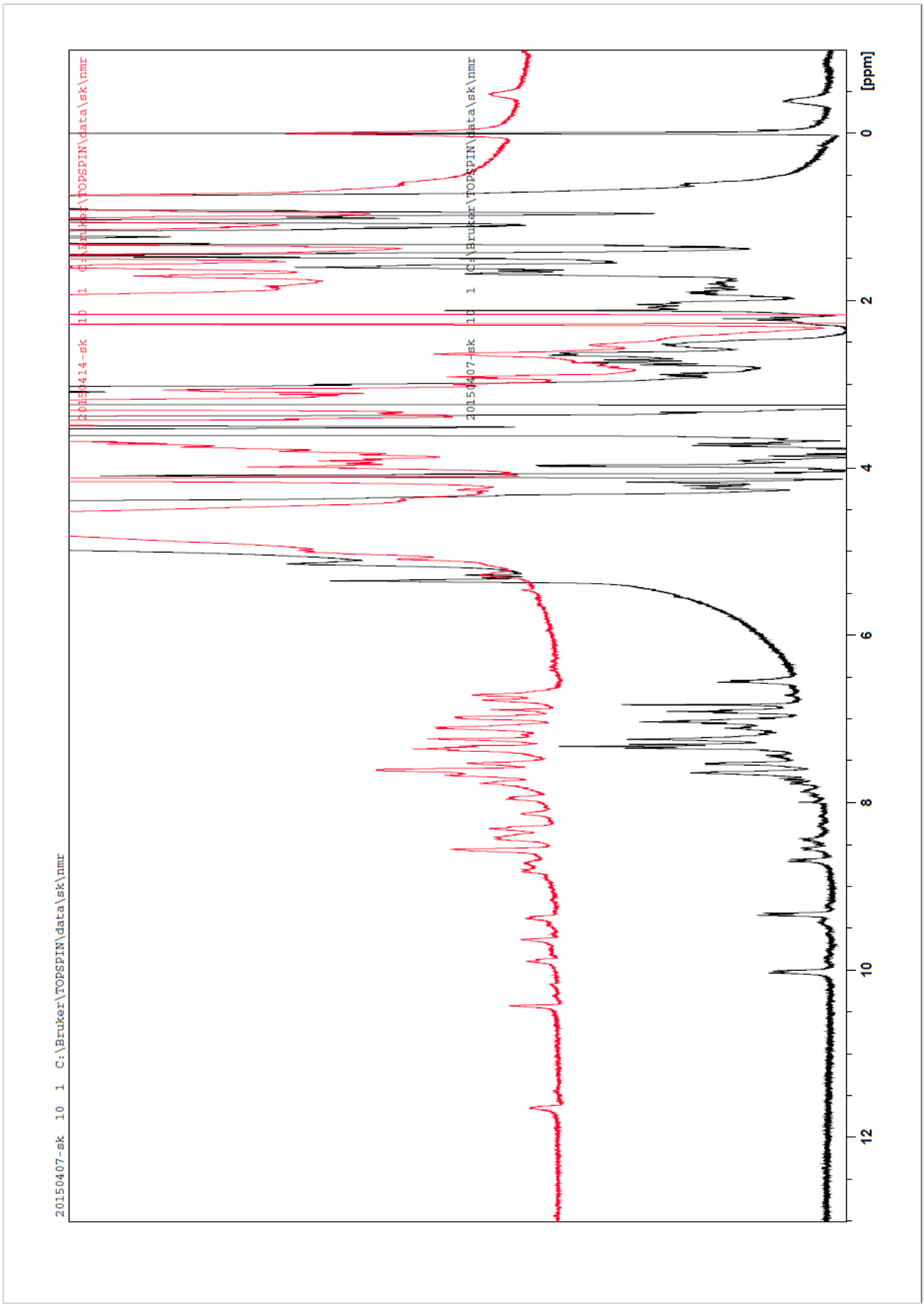

Figure 26: NMR spectrum comparison between the protein standard in 50% d_4-MeOH (in red) and 100% d_4-MeOH (in black).

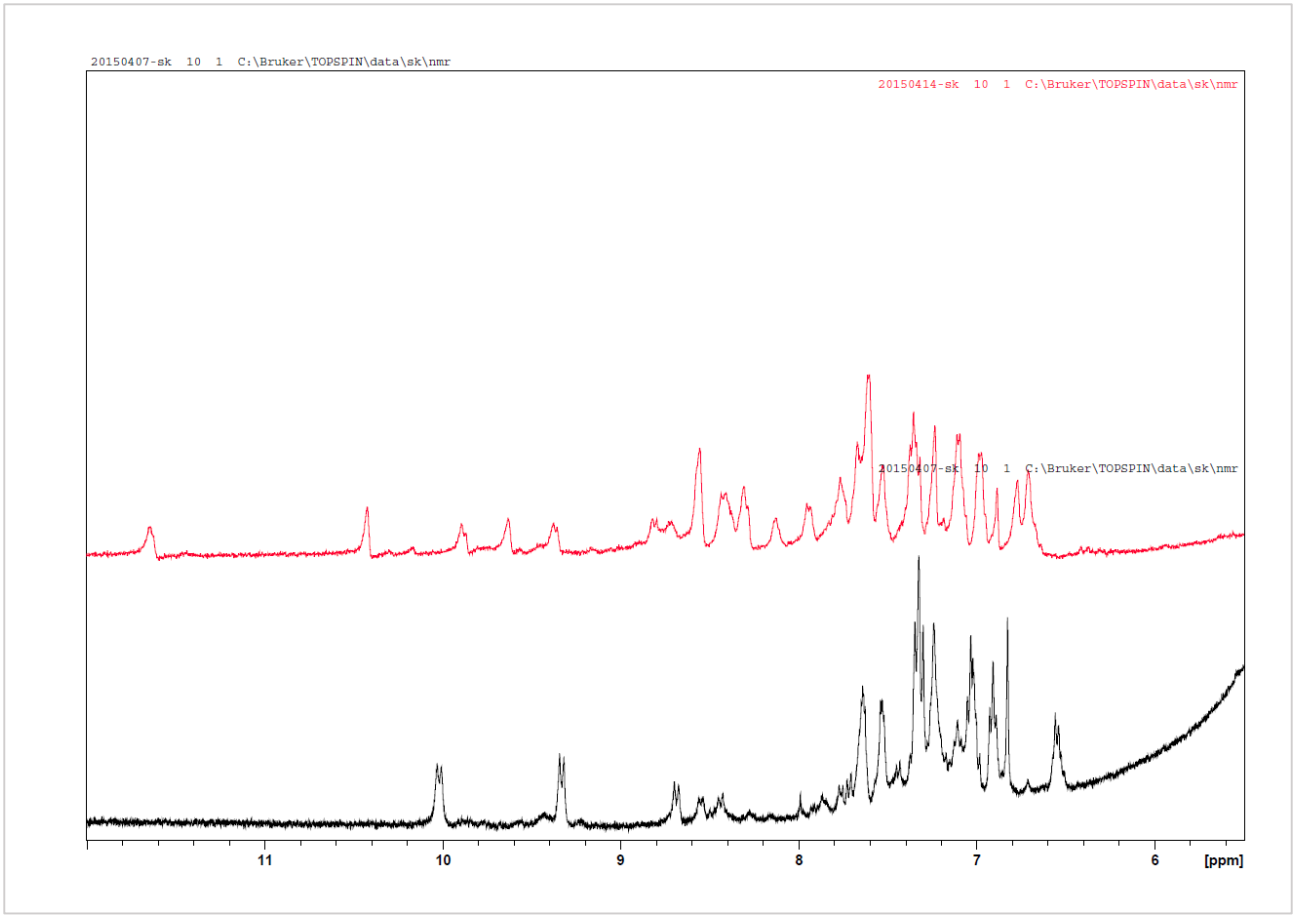

Figure 27: Excerpt of figure 19 showing amide chemical shifts (5.5 ppm to 12 ppm).

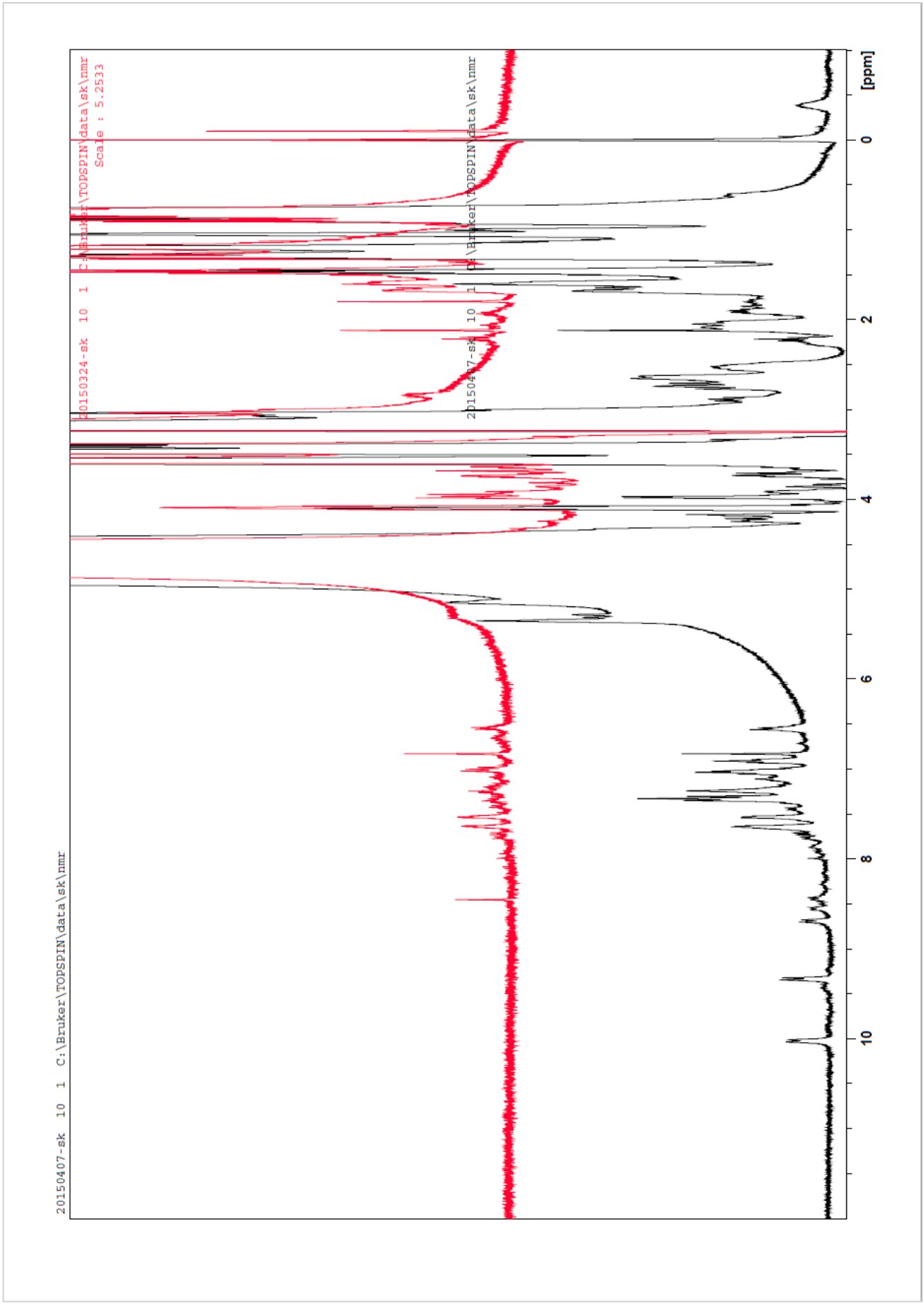

Figure 28: NMR spectrum comparison between fraction 7 from SEC separation 4 (in red) and the protein standard (in black).

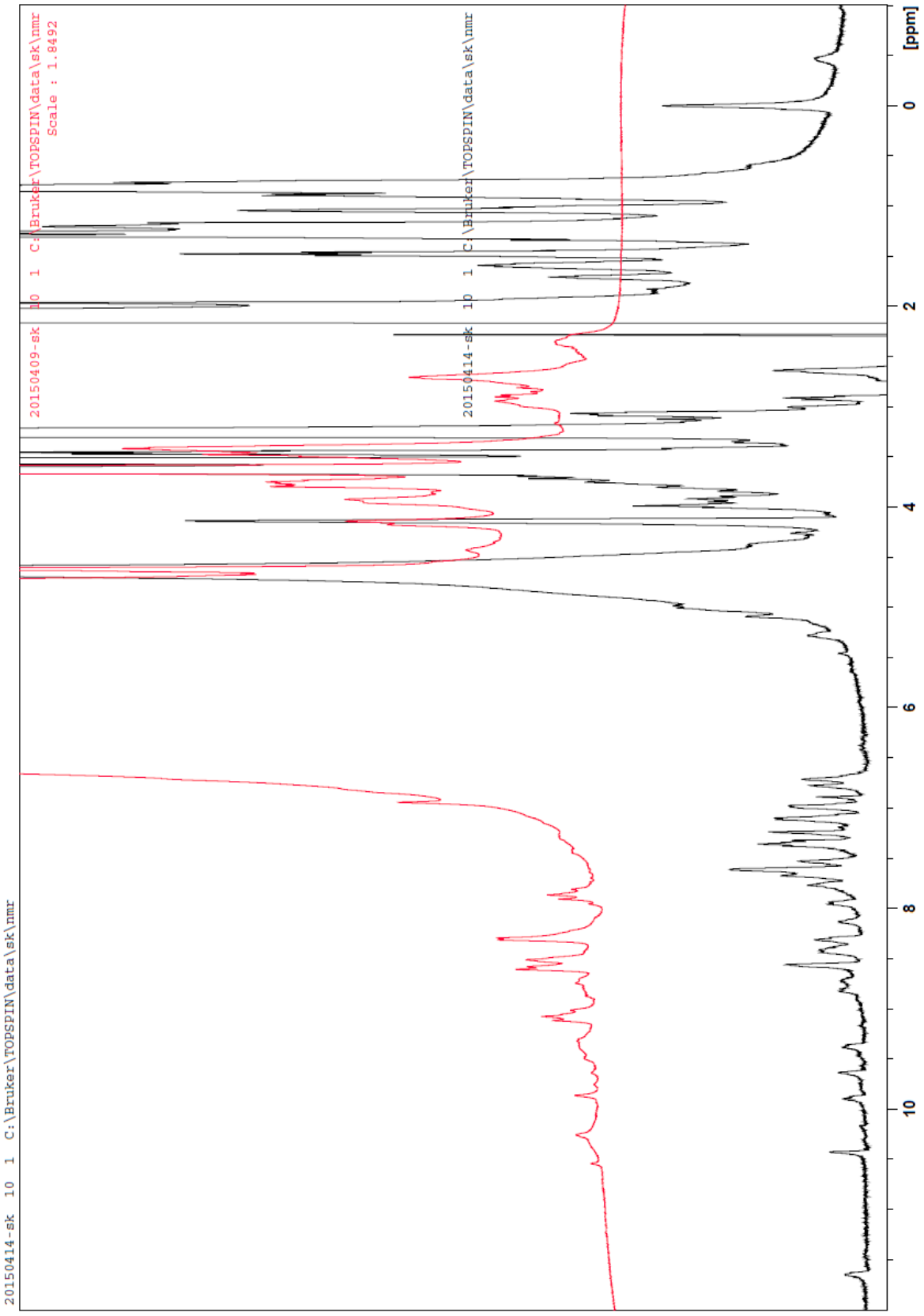

Figure 29: NMR spectrum comparison between 10x crude extract (in red) and the protein standard (in black).

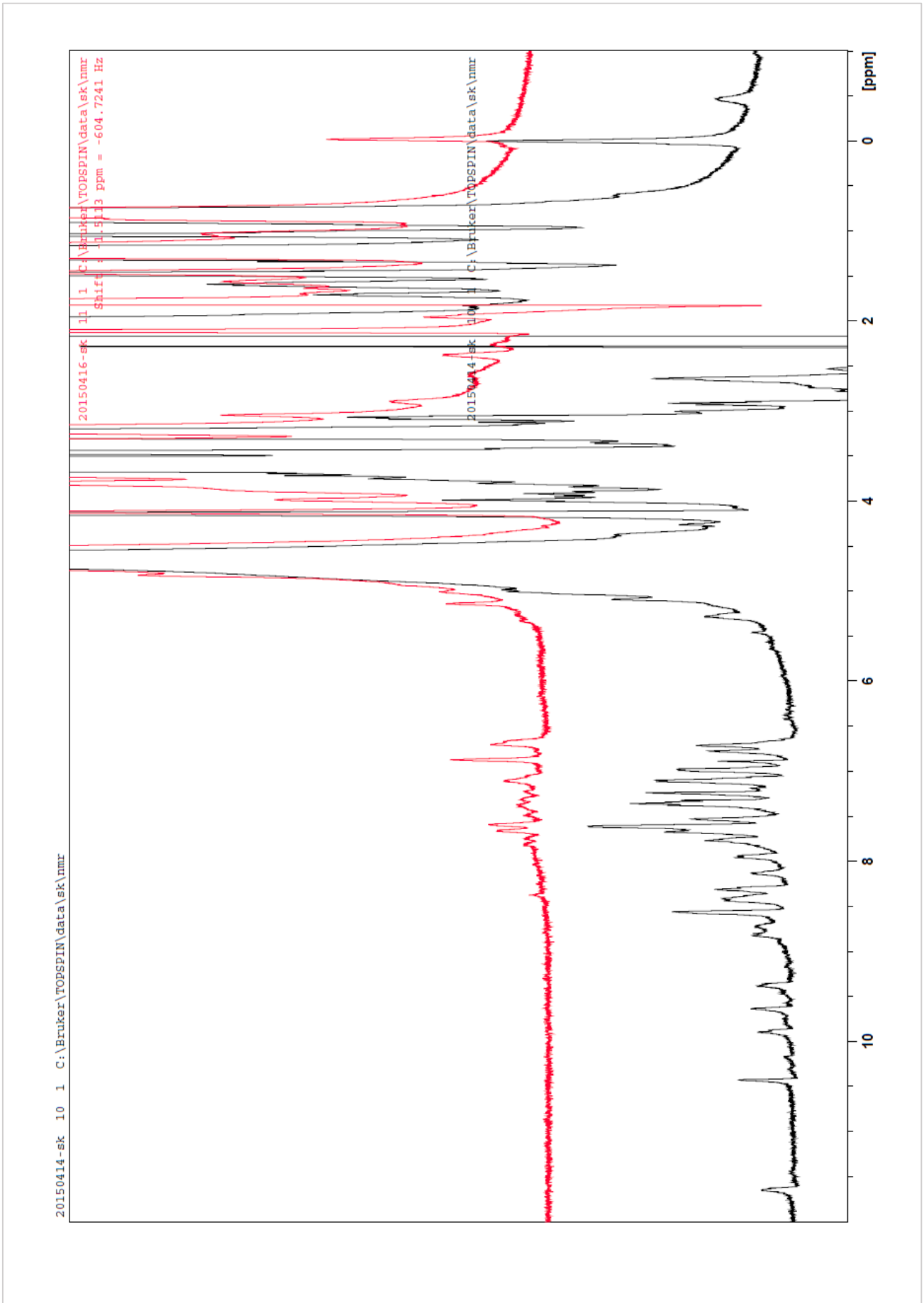

Figure 30: NMR spectrum comparison between fraction 2 from SEC separation 5 (in red) and the protein standard (in black).

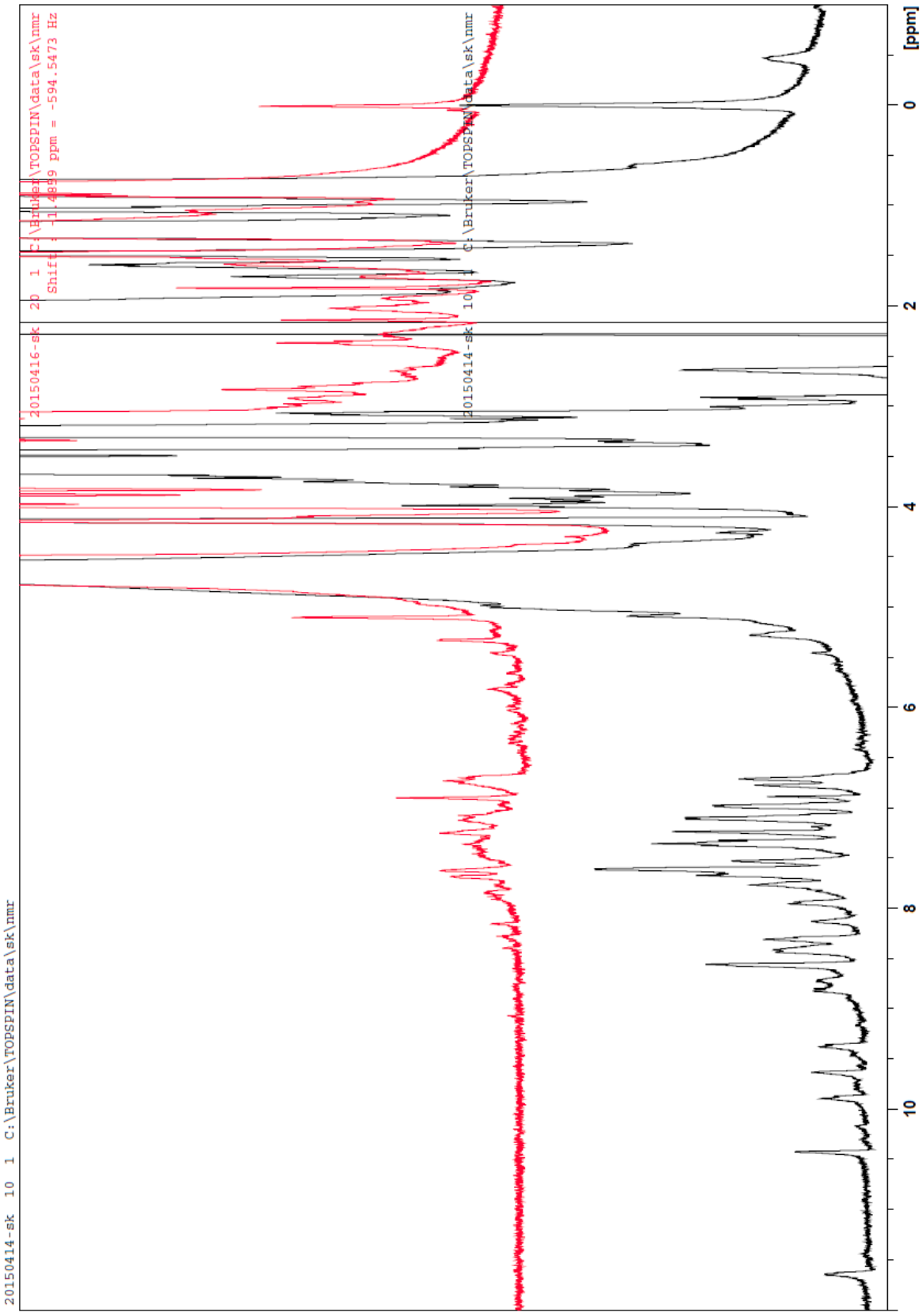

Figure 31: NMR spectrum comparison between fraction 10 from SEC separation 5 (in red) and the protein standard (in black).

5 Discussion

Results in this section are presented chronologically by summarizing the goal of the thesis followed by a quick assessment of the key findings. Secondly a more elaborate discussion explains the meaning behind each key finding in relation to literature and what implications this has for the entire method. Lastly, a conclusion is given reflecting on parts of the method which could be worked more on.

5.1 Summary

To identify the optimal conditions for cyclotide extraction and isolation from *T. Officinale*, yield depending factors are tested in an extraction assay with 144 different combinations and purified by SEC. An estimated minimum purity was experimentally established and then used to validate samples for NMR in order to observe any cyclotide markers.

5.1.1 Key Observations

93% of *T. Officinale* seeds were successfully germinated creating around 500 flowers which were used in the extraction of cyclotide. Cultivation of flowers for the purpose of extracting cyclotides has never been reported and make this thesis unique as it presents results based on cultivated flowers. Time invested and knowledge on cultivation were limiting factors and would require training or a trained professional in case of reproduction or statistical assay.

The extraction assay, ANOVA and UV analysis revealed “Infusion” as the best extraction method with the factor levels: 15 minutes maceration time, 3 hours extraction time yielding the highest dryweight and protein concentration. The extraction time coincides well with reports from M. Y. Yeshak et. al. [17] where an extraction time of 6 hours and maceration was used. Though a comprehensive assay combining more than 4 parameters have never been reported for the extraction of cyclotides. Due to the lack of time and budget, more parameters were not introduced as the amount of samples needed for statistical significance would increase exponentially.

A molar attenuation threshold of 3124 $M^{-1}cm^{-1}$ was found experimentally using a standard containing purified cyclotides to provide a more conclusive method for the assessment of SEC fractions. A cyclotide concentration of 0.39 mM was estimated using a protein standard curve after a successful separation with SEC. Both molar attenuation plot and chromatogram were used to determine the quality and quantity of the separated compound. As there is only one previously reported paper isolating cysteine rich peptides from *T. Officinale* [5] there is a possibility that the cyclotides present may be different from Kalata B1 found in other plant species. This means that a predicted molar attenuation coefficient from Kalata B1 amino acid sequence cannot be used.

NMR results for SEC separation 5 show more amide signals at 6-8.5 ppm for the retained fraction 10 than for fraction 2 from the same separation and also a pattern of three evenly spaced multiplets emerge at 8.5 ppm matching the protein standard. An amide signal at 8.5 ppm is shown in acidic conditions in fraction 7 from SEC separation 4 but not for fraction 2 from SEC separation 5 which had a pH of 6 although all the other signals were identical. A proton signal at -0.1 ppm was observed for fraction 7 in SEC run #4.

5.1.2 Elaboration

Cultivation. Because of the current focus on cyclotide synthesis and drug development, emphasis on discovering a model plant for promoting cultivation and extraction has been neglected. As *T. Officinale* provides a good yield of flowers and isolation of only two flowers yields a detectable amount of cyclotides, it qualifies to be used as a model plant. Using *T. Officinale* as a model plant for isolating cyclotides solves the issue of limited plant material in case of increasing production and the guidelines provided in this thesis can be used as a template. Knowledge of cultivation and growth conditions was the limiting factor as well as the amount of time needed, therefore a trained professional taking the responsibility for cultivation or supplementary supervisor with the necessary knowledge is needed in case of reproduction. Because of the limited knowledge cultivation took 2-3 months longer than expected. Appropriate facilities were provided for by a collaboration between SKP and NMBU which was necessary for cultivation assay studies. The access to red and blue high quality lighting armatures, fertilized water, humidity and temperature controlling systems are important for such studies to be conducted. More studies on optimizing the extraction and isolation process of cyclotides is needed to justify the use of expensive facilities. Indoor cultivation proved valuable and though arduous provides a useful platform for further understanding into optimizing cyclotide yield. The success of the cultivation was dependent on many factors described on page 9 under the theory section and can be used further for statistical analysis in case of reproduction.

Extraction Assay, ANOVA and UV detection. The yield of dryweight was found dependent on the factors extraction time, maceration time and extraction method, while ANOVA results (figure 14) shows that centrifugation intensity receives a p-value of 0.98 meaning it has no effect on dryweight. The extraction and maceration time determines the output of cyclotide dryweight where prolonged treatment results in a higher yield. While extraction method shows differences in yield this parameter is a combination of solvent, temperature and filter meaning that the method itself might not be the determining factor for the output. No other studies were observed utilizing different temperatures and solvents to achieve optimization though a solvent assay using different n% MeOH/EtOH at room temperature had reported good yield for 50% MeOH and cited in several papers [17]. As seen in the regression analysis some of the parameters had a negative impact on yield. If all the factors within extraction method were accounted for it would change the results and increase the adjusted correlation coefficient (R^2) as more variation will be accounted for. A high purification degree of 7.5x is found for the separation after using the optimal

parameters, showing that the crude samples contains a lot of impurities. This means that soxhlet w/ 50% MeOH might contain just as much cyclotide and that the use of a filter under this extraction process may have been a purification process in itself. 50% MeOH was used as the extracting solvent for infusion and corresponded well with previous reports about optimal solvent composition for cyclotides [17]. The extracted proteins were observed soluble in 50% MeOH but not in 100% MilliQ water or 100% MeOH confirming the amphiphilic nature of cyclotides. As most samples from the extraction assay precipitated when solved in water, this was centrifuged away prior to UV detection. Later it was discovered due to the lack of NMR signals that changing the solvent composition may have caused some of the cyclotides to precipitate washing them away leaving only free tryptophans in the supernatant. This was discovered in the chromatograms as the absorbance at 285nm was observed higher than at 280nm. A review through all the steps involving a switch of solvent was done to find out where the sample was split up. The centrifugation step prior to UV detection was the reason for the lack of NMR signals where the solvent changed from 50% MeOH to 100% MilliQ water. Oxindolylalanine with its absorbance maximum at 285nm provides useful information about both presence of free tryptophans and degree of denaturation of proteins containing tryptophan after purification. This information can be used in a quality assessment of crude and purified samples. Absorbance at 410nm was detected in undiluted fractions with an estimated cyclotide concentration over 1 mg/mL, indicating a correlation between cyclotide concentration and the amber color though this was not explored further. The pH was measured but only controlled prior to purification by protease and separation. Purification of cyclotides using pepsin was attempted but did not give a big enough degree of purification to justify the use and it was thus excluded from the method. In case of reproduction on a bigger scale, purification using proteases may be justified but pH and solvent effects need to be taken into account. Reports show that the cysteine rich peptides isolated from *T. Officinale* has a positive exterior charge meaning the use of acid precipitation may be possible as a purification step in further studies [8] [51]. Few research papers take point in optimizing the extraction process making the results achieved beneficial for further assessment. The work in this thesis provides a stepping stone for producing more comprehensive assays for isolation, cultivation and extraction in the future.

Size exclusion, chromatograms and molar attenuation plots. The separation process was perfected after the fourth attempt changing parameters such as flowrate, column dimension, the use of pepsin, pH, solvent, different flowers, % injection volume and flower concentration. No statistics were applied as the number of separations needed to try every combination if each parameter had 2 levels would be 2^8 or 256, and even then variability is high due to the lack of replicates. The main goal of improving the outcome of the chromatographic separation was based on trial and error. The separability in the stationary phase was improved by increasing the flow rate as reported by GE Healthcare [50] but made fractionation too difficult to handle manually. The separability was therefore improved by changing to a smaller column. The column was equilibrated with a 10 mM Tris-HCl buffer with pH 8, but changed with a mobile phase of 50% MeOH

with pH 6 during elution. The sample was loaded in such a way that it was associated in buffer both over and under while a layer of mobile phase was placed on top filling the column creating a water front between the two phases. As the buffer and mobile phase proceeded through the column, the sample would first be associated in Tris-HCl before switching to 50% MeOH. This created a secondary purification step as the change in pH may have aggregated thus removing the retention of unwanted species. The chromatograms were the only results that could show the efficacy of the separations as fractionation was done manually. Qualitative information about the separation i.e. resolving power and resolution, was impossible to calculate due to tailing and too few data points. The tailing indicated that more than one retaining factor was present in the column, but no work was done to ascertain the reason for this. A protein quantification curve was produced by dividing up 3 mg purified Kalata B1 provided by L. Skjeldal. The function associated by the standard curve was used to determine the amount of protein present in SEC fractions within the linear range of quantification. But as the chromatograms showed a varying degree of separation nothing could really be properly determined by UV since the first peak could as well contain cyclotides but of a different size. This was solved discretely by calculating the molar attenuation coefficients for each chromatogram including the quantification curve giving molar attenuation plots. The molar attenuation is unique for each species containing a chromophore and shows how strongly it absorbs light. The resulting molar attenuation standard curve showed a logarithmic relationship between the protein concentration and the molar attenuation where a maximum molar attenuation of 3124 $M^{-1}cm^{-1}$ was determined between 0.2 and 1 mg/mL. It remains unclear whether the graph resembles a common (log) or naturally (ln) based logarithmic relation. The maximum molar attenuation was used as a threshold which separated fractions need to surpass in order to contain cyclotides for certain. A molar attenuation coefficient of 3131 $M^{-1}cm^{-1}$ was found for fraction 10 in SEC run #5 indicating that all the absorbance found for this fraction in the chromatogram may represent cyclotides. A protein concentration of 0.39 mM was calculated for fraction 10. In protein NMR a concentration within 1-2 mg/mL is required for detection using todays NMR technology, meaning that the protein concentration would need to be doubled to guarantee peaks in NMR with a sufficient signal to noise ratio. The last separation used 1 mL crude extract from a batch with a flower concentration of 0.4895 mg/mL. To satisfy the minimum detection range 2 mL crude extract or more would need to be combined by lyophilization. A predicted molar attenuation coefficient may also be determined by protein sequence through the Edelhoch method further explained on page 16 in the theory section. The predicted value of 5875 $M^{-1}cm^{-1}$ did not match the value found experimentally for the protein standard which gives reason to believe that prediction based solely on protein sequence may be based on assumptions which does not apply to cyclotides such as cysteine quenching [52]. By using both UV and molar attenuation plots the presence and concentration of proteins could be determined with certainty.

Elucidation of cyclotides by NMR. The markers used for determining cyclotides are based on reports made by L. Skjeldal where Kalata B1 showed unique NMR signals for the 2° amine proton for Trp 2 and the β-proton for Pro 3 [15]. The protons chemical shifts were reported to have chemical shifts of around 11.5 ppm and -0.25 ppm respectively, which is outside the "crowded" area where peptide signals are usually detected. Figure 9 on page 25 shows that the β-proton from proline is in the vicinity of the magnetic anisotropic field created by the benzene ring in the adjacent tryptophan which is the reason for its unusual chemical shift. The cis-Pro isomer also causes steric stress further contributing to the chemical shift of the beta-proton [15]. The unusual shift from the 2° amine proton of tryptophan can also be explained derived from the same figure where the proton is deshielded by the ring drawing away electrons due to differences in electronegativity. As these two amino acids are highly conserved they can be used as markers for determining cyclotides. The chemical shifts of these markers may vary depending on ambient and non-conserved amino acids in addition to conformational changes to the magnetic anisotropic fields. As the 2° amine and amide protons are easily exchanged, some NMR signals are dependent on pH to become visible in NMR and prolonged exposure to deuterated solvents will significantly reduce the amount of peptide signals [15]. The unusual hydrophilic core of cyclotides can be used to investigate the exchange rate of protons in NMR. The pH is important for proteins as it decides the net charge for the protein exterior. In a paper studying the mechanisms for cyclotide membrane association, cyclotide monomers are reported to associate in polymers by amphiphilic interactions in Kalata B2 [53]. The pH is best controlled to prevent unnecessary polymerization as NMR signals will appear weaker than anticipated due to an established equilibrium from monomers to tetramers and octamers. The pH was not assessed in this thesis due to the lack of time but statistical assays using different pH, i.e. titration in size exclusion and NMR would produce interesting results. As NMR was only used to find indications, no interpretations of chemical shifts were done. Even after a few simple purification steps cyclotides may be indicated in 400 MHz NMR using proline and tryptophan markers from a purified protein standard [15]. Fractions 2 and 10 separated in SEC run #5 showed different NMR patterns in figure 31 in the amide area meaning more or different peptides are present in fraction 10. Since fraction 10 was retained by the size exclusion medium this further supports the indication that peptides between 1000-5000 Da are present and that the peptide signals in NMR are from cyclotides. Proline and tryptophan proton markers were not found in fraction 10 but this may be caused by prolonged exposure to deuterated solvent as the NMR machine was occupied. Lack of these extreme markers may also indicate bracelet cyclotides in *T. Officinale*. The NMR spectra for fraction 7 in SEC run #4 and fraction 2 in SEC run #5 are nearly identical but from one peak at 8.5 ppm which is present in fraction 7 and not fraction 2. The difference between the two spectra is that fraction 7 had an observed pH 2 while fraction 2 had a pH of 6 prior to NMR testing. This may indicate that the peptides are dependent on pH but may also have been caused by prolonged exposure to deuterated solvent. A proton signal found at -0.1 ppm for fraction 7 from SEC run #4 may indicate a proline with a different conformation than found in Kalata B1.

5.2 Conclusion

The protocol described in this study shows how peptides of approximate weight of 2916 Da can be optimally extracted and purified by size exclusion yielding detectable amounts by NMR using conserved amino acids with unique chemical shifts. NMR shifts and molar attenuation coefficients observed indicate a different configuration of cyclotide present in the *T. Officinale* flower than found for Kalata B1. Additional studies around increasing substrate concentration with statistical assays and pH titration in NMR might help elucidate the exact conditions to increase detectability of cyclotides for spectrum interpretation.

Literature

[1] L. Gran, F. Sandberg, K. Sletten (2000) "*Oldenlandia affinis* (R&S) DC: A Plant Containing Uteroactive Peptides Used in African Traditional Medicine" *Journal of Ethnopharmacology*, volume 70 (3), p. 197-203

[2] O. Saether, D. J. Craik, I. D. Campbell, K. Sletten, J. Juul, D. G. Norman (1995) "Elucidation of the Primary and Three-Dimensional Structure of the Uterotonic Polypeptide Kalata B1" *Biochemistry*, volume 34, p. 4147-4158

[3] D. J. Craik, N. L. Daly, T. Bond, C. Waine (1999) "Plant Cyclotides: A Unique Family of Cyclic and Knotted Proteins that Defines the Cyclic Cystine Knot Structural Motif" *Journal of Molecular Biology*, volume 294 (5), p. 1327-1336

[4] S. Troland (2007) "A fractionation protocol for separation and isolation of polypeptides from the plant *Taraxacum Officinale* Methanol used as an extraction solvent" NMBU, Master Thesis (unpublished work)

[5] A. A. Astafieva, E. A. Rogozhin, Y. A. Andreev, T. I. Odintsova, S. A. Kozlov, E. V. Grishin, T. A. Egorov (2013) "A Novel Cysteine-rich Antifungal Peptide ToAMP4 from *Taraxacum officinale* Wigg. Flowers" *Plant Physiology and Biochemistry*, volume 70, p. 93-99

[6] D. J. Craik, M. Cemazar, N. L. Daly (2006) "The Cyclotides and Related Macrocyclic Peptides as Scaffold in Drug Design" *Current opinion in drug discovery & development*, volume 9 (2), p. 251-260

[7] L. Chiche, A. Heitz, J.-C. Gelly, J. Gracy, P. T. T. Chau, P. T. Ha, J.-F. Hernandez, D. Le-Nguyen (2004) "Squash Inhibitors: From Structural Motifs to Macrocyclic Knottins" *Current Protein and Peptide Science*, volume 5 (5), p. 341-349

[8] M. L. Colgrave, D. J. Craik (2004) "Thermal, Chemical and Enzymatic Stability of the Cyclotide Kalata B1: The Importance of the Cyclic Cystine Knot" *Biochemistry*, volume 43, p. 5965-5975

[9] U. Göransson, M. Sjögren, E. Svangård, P. Claeson, L. Bohlin (2004) "Reversible Antifouling Effect of the Cyclotide Cycloviolacin O2 against Barnacles" *Journal of Natural Products*, volume 67 (8), p. 1287-1290

[10] K. R. Gustafson, T. C. McKee, H. R. Bokesch (2004) "Anti-HIV Cyclotides" *Current Protein and Peptide Science*, volume 5 (5), p. 331-340

[11] S. Prabhu, S. R. Dennison, B. Lea, T. J. Snape, I. D. Nicholl, I. Radecka, F. Harris (2013) "Anionic Antimicrobial and Anticancer Peptides from Plants" *Critical Reviews in Plant Sciences*, volume 32, p. 303-320

[12] A. Gould, Y. Ji, T. L. Aboye, J. A. Camarero (2011) "Cyclotides, a Novel Ultrastable Polypeptide Scaffold for Drug Discovery" *Current Pharmaceutical Design*, volume 17 (38), p. 4294-4307

[13] N. L. Daly, K. J. Rosengren, D. J. Craik (2009) "Discovery, Structure and Biological Activities of Cyclotides" *Advanced Drug Delivery Reviews*, volume 61 (11), p. 918-930

[14] D. J. Craik, N. L. Daly, T. Bond, C. Waine (1999) "Plant Cyclotides: A Unique Family of Cyclic and Knotted Proteins that Defines the Cyclic Cystine Knot Structural Motif" *Journal of Molecular Biology*, volume 294 (5), p. 1327-1336

[15] L. Skjeldal, L. Gran, K. Sletten, B. F. Volkman (2002) "Refined Structure and Metal Binding site of the Kalata B1 Peptide" *Archives of Biochemistry and Biophysics*, volume 399 (2), p. 142-148

[16] W. Nawae, S. Hannongbua, M. Ruengjitchatchawalya (2014) "Defining the Membrane Disruption Mechanism of Kalata B1 via Coarse-Grained Molecular Dynamics Simulations" *Scientific Reports*, volume 4, p. 1-9

[17] M. Y. Yeshak, R. Burman, C. Eriksson, U. Göransson (2012) "Optimization of Cyclotide Extraction Parameters" *Phytochemistry Letters*, volume 5 (4), p. 776-781

[18] B. W. Matthews (1995) "Studies on Protein Stability with T4 Lysozymes" *Advances in Protein Chemistry*, volume 46, p. 249-278

[19] L. Giver, A. Gershenson, P.O. Freskgard, F. H. Arnold (1998) “Directed Evolution of a Thermostable Esterase” *Proceedings of the National Academy of Sciences of the United States of America*, volume 95 (22), p. 12809-12813

[20] M. M. Lin, O. F. Mohammed, G. S. Jas, A. H. Zewail (2011) “Speed Limit of Protein Folding Evidenced in Secondary Structure Dynamics” *Proceedings of the National Academy of Sciences of the United States of America*, volume 108 (40), p. 16622-16627

[21] U. Göransson, T. Luijendijk, S. Johansson, L. Bohlin, P. Claeson (1999) “Seven Novel Macrocyclic Polypeptides from *Viola arvensis*” *Journal of Natural Products*, volume 62 (2), p. 283-286

[22] Decoctions. (n.d.). *Collins English Dictionary - Complete & Unabridged 10th Edition*. Retrieved November 14, 2014, from Dictionary.com website: http://dictionary.reference.com/browse/decoctions

[23] Infusion. (n.d.). *Collins English Dictionary - Complete & Unabridged 10th Edition*. Retrieved November 20, 2014, from Dictionary.com website: http://dictionary.reference.com/browse/infusion

[24] Percolation. (n.d.). *Dictionary.com Unabridged*. Retrieved November 20, 2014, from Dictionary.com website: http://dictionary.reference.com/browse/percolation

[25] H. Hashempour, A. Ghassempour, N. L. Daly, B. Spengler, A. Römpp (2011) “Analysis of Cyclotides in *Viola ignobilis* by Nano Liquid Chromatography Fourier Transform Mass Spectrometry” *Protein & Peptide Letters*, volume 18 (7), p. 747-752

[26] E. Garfield (1990) “The Most-Cited Papers of All Time, SCZ 1945-1988. Part 1A. The SCZ Top 100---Wti the Lowry Method Ever Be Obliterated?” *Current Comments*, volume 13 (7), p. 45-56

[27] A. Nourse, M. Trabi, N. L. Dali, D. J. Craik (2004) “A Comparison of the Self-association Behavior of the Plant Cyclotides Kalata B1 and Kalata B2 via Analytical Ultracentrifugation” *The Journal of Biological Chemistry*, volume 279, p. 562-570

[28] M. M. Bradford (1976) “A Rapid and Sensitive Method for the Quantitation of Microgram Quantities of Protein Utilizing the Principle of Protein-Dye Binding” *Analytical Biochemistry*, volume 72, p. 248-254

[29] H. Rosen (1957) “A Modified Ninhydrin Colorimetric Analysis for Amino Acids” *Archives of Biochemistry and Biophysics*, volume 67 (1), p. 10-15

[30] R. McGrath (1972) “Protein Measurement by Ninhydrin Determination of Amino Acid Released by Alkaline Hydrolysis” *Analytical Biochemistry*, volume 49, p. 95-102

[31] A. Holmgren (1971) “Tryptophan Fluorescence Study of Conformational Transitions of the Oxidized and Reduced Form of Thioredoxin” *The Journal of Biological Chemistry*, volume 247 (7), p. 1992-1998

[32] J. J. Prompers, C. W. Hilbers, H. A.M. Pepermans (1999) “Tryptophan Mediated Photoreduction of Disulphide Bond Causes Unusual Fluorescence Behaviour of *Fusarium solani pisi* Cutinase” *Federation of European Biochemical Societies Letters*, volume 456 (3), p. 409-416

[33] E. A. Permyakov, S. E. Permyakov, G. Y. Deikus, L. A. Morozova-Roche, V. M. Grishchenko, L. P. Kalinichenko, V. N. Uversky (2003) “Ultraviolet Illumination-induced Reduction of α-Lactalbumin Disulphide Bridges” *Proteins: Structure, Function and Genetics*, volume 51, p. 498-503

[34] M. R. R. Plan, U. Göransson, R. J. Clark, N. L. Daly, M. L. Colgrave, D. J. Craik (2007) “The Cyclotide Fingerprint in Oldenlandia affinis: Elucidation of Chemically Modified, Linear and Novel Macrocyclic Peptides” *ChemBioChem*, volume 8 (9), p. 1001-1011

[35] L.Z. Wu, Y.B. Sheng, J.B. Xie, W. Wang (2008) “Photoexcitation of Tryptophan Groups Induced Reduction of Disulphide Bonds in Hen Egg White Lysozyme” *Journal of Molecular Structure*, volume 882 (1-3), p. 101-106

[36] T. Nakai, T. Ohta (1976) “β-3-Oxindolylalanine: The Main Intermediate in Tryptophan Degradation Occurring in Acid Hydrolysis of Protein” *Biochemica et Biophysica Acta (BBA) - Protein Structure*, volume 420 (2), p. 258-264

[37] A. D. McNaught, A. Wilkinson (1997) IUPAC. Compendium of Chemical Terminology, 2nd ed. (the “Gold Book”) *Blackwell Scientific Publications, Oxford*

[38] H. Edelhoch (1967) “Spectroscopic Determination of Tryptophan and Tyrosine in Proteins” *Biochemistry*, volume 6 (7), p. 1948-1954

[39] C. N. Pace, F. Vajdos, L. Fee, G. Grimsley, T. Gray (1995) “How to measure and predict the molar absorption coefficient of a protein” *Protein Science*, volume 4, p. 2411-2423

[40] T. N. Asquith, L. G. Butler (1985) “Use of Dye-Labeled Protein as Spectrophotometric Assay for Protein Precipitants such as Tannins” *Journal of Chemical Ecology*, volume 11 (11), p. 1535-1544

[41] H. P. S. Makkar, K. Becker (1996) “Effect of pH, Temperature, and Time on Inactivation of Tannins and Possible Implications in Detannification Studies” *Journal of Agricultural and Food Chemistry*, volume 44 (5), p. 1291-1295

[42] S. J. Cork, A. K. Krockenberger (1991) “Methods and Pitfalls of Extracting Condensed Tannins and Other Phenolics from Plants: Insights from Investigations on *Eucalyptus* Leaves” *Journal of Chemical Ecology*, volume 17 (1), p. 123-134

[43] M.S. Tswett (1905) “On a New Category of Adsorption Phenomena and on its Application to Biochemical Analysis” *Proceedings of the Warsaw Society of Naturalists*, vol. 14 (6), p. 20-39

[44] L. R. Snyder, J. J. Kirkland, J. K. Glajch (1997) “Practical HPLC Method Development (John Wiley & Sons, New York, 2nd ed.)” ISBN: 978-0-471-00703-6, p. 180

[45] J. J. Van Deemter, F. J. Zuiderweg, A. Klinkenberg (1956) “Longitudinal Diffusion and Resistance to Mass Transfer as Causes of Non Ideality in Chromatography“ *Chemical Engineering Science*, volume 3, p. 271-289

[46] G. H. Lathe, C. R. Ruthven (1955) “The Separation of Substances on the Basis of Their Molecular Weights, Using Columns of Starch and Water” *The Biochemical Journal*, volume 62 (4), p. 665-674

[47] R. M. B. O. Duarte, A. C. Duarte (2011) “Optimizing Size-Exclusion Chromatographic Conditions Using a Composite Objective Function and Chemometric Tools: Application to Natural Organic Matter Profiling” *Analytica Chimica Acta*, volume 688 (1), p. 90-98

[48] I. I. Rabi, J. R. Zacharias, S. Millman, P. Kusch (1938) “A New Method of Measuring Nuclear Magnetic Moment” *The Physical Review*, volume 53 (4), p. 318

[49] W. P. Aue, E. Bartholdi, R. R. Ernst (1976) “Two-dimensional Spectroscopy. Application to Nuclear Magnetic Resonance” *Journal of Chemical Physics*, volume 64, p. 2229-2246

[50] E. Östervåla (2006) “Instructions 56-1190-96 AC Sephadex G-25 medium” *GE Healthcare*, retrieved 2015-04-28

[51] S. K. Sze, W. Wang, W. Meng, R. Yuan, T. Guo, Y. Zhu, J. P. Tam (2009) “Elucidating the Structure of Cyclotides by Partial Acid Hydrolysis and LC-MS/MS Analysis” *Analytical Chemitry*, volume 81, p. 1079-1088

[52] M. T. Neves-Petersen, Z. Gryczynski, J. Lakowicz, P. Fojan, S. Pedersen, E. Petersen, S. B. Petersen (2002) “High Probability of Disrupting a Disulphide Bridge Mediated by an Endogenous Excited Tryptophan Residue” *Protein Science*, volume 11 (3), p. 588-600

[53] K. J. Rosengren, N. L. Daly, P. J. Harvey, D. J. Craik (2013) “The Self-Association of the Cyclotide Kalata B2 is Guided by Hydrophobic Interactions” *Peptide Science*, volume 100 (5), p. 453-460

Appendix

The tables found in this section contains raw data from the extraction assay (table 9), protein standard (table 10), UV detection assay (table 11-14), size exclusion and molar attenuation chromatograms after separation (table 15-18).

Tables are presented chronologically in page 69-79.

Due to the big size of the table 15-18, they were split up and captioned as a continuation of the previous table.

Table 9: Estimated lyophilized dryweight in mg per 50 mL sample for extraction assay.

	Method 1			Method 2			Method 3			Method 4			
Homogenizing (minutes)	MilliQ			50% MeOH			MilliQ			50% MeOH			Time (hours)
5	0.7	0.4	0.6	0.9	0.7	0.9	0.36	0.24	0.36	0.3	0.75	0.6	0.5
10	1.1	1.2	1.1	1.35	1.2	1.2	0.24	0.24	0.36	0.4	0.1	0.3	
15	2.2	1.6	1.9	1.2	1.2	1.52	0.36	0.24	0.48	0.25	0.15	0.15	
5	1.3	1	1.4	0.6	0.5	0.5	0.98	0.7	0.98	0.9	0.75	0.15	1
10	1.3	0.8	0.8	1.08	1.08	1.2	0.28	0.42	0.7	0.45	0.6	1.05	
15	0.9	1.4	1.2	1.92	1.6	1.76	0.72	0.24	0.48	0.24	0.36	0.48	
5	0.1	0.3	0.2	1.6	1.4	1.4	0.48	0.36	0.6	0.15	0.45	0.15	2
10	1.4	1.4	1.1	1.1	1.1	1.1	1.05	1.35	1.65	1.05	1.35	0.9	
15	0.3	0.3	0.4	1.5	0.6	1.1	0.9	0.75	0.9	1.95	1.8	0.9	
5	1	1	1.4	0.8	0.7	0.9	0.75	1.35	1.2	0.75	0.45	0.6	3
10	1.1	1.7	1.2	1.7	2.2	2.4	1.35	2.4	0.75	0.3	0.45	0.45	
15	1.2	1.3	1.3	2.32	2.32	2.32	1.35	1.2	1.05	0.9	0.75	0.9	
	10k	12k	14k	10k	12k	14k	10k	12k	14k	10k	12k	14k	
	Centrifugation												

Table 10: UV detection of purified Kalata B1 at 280nm, 285nm and 410nm.

Standard for UV-detection of Kalata					
A_{280}	0.185	0.415	0.638	0.858	1.068
A_{285}	0.185	0.408	0.629	0.843	1.047
A_{410}	0.033	0.032	0.032	0.032	0.035
	0.2	0.4	0.6	0.8	1
	Concentration of kalata (mg/mL)				

Table 11: Absorbance at 280nm, 285nm, 360nm, 450nm and 550nm for decoction in MilliQ water post extraction treatment.

UV-detection of method 1 (diluted ¼)							
Maceration time (mins.)	Time (hrs.)	Centrifugation (xg)	A_{280}[a]	A_{285}[a]	A_{360}[a]	A_{450}[a]	A_{550}[a]
5	0.5	10k	1.241	1.285	0.614	0.072	0.062
5	0.5	12k	1.190	1.230	0.656	0.082	0.067
5	0.5	14k	1.175	1.215	0.714	0.095	0.072
10	0.5	10k	0.833	0.862	0.452	0.060	0.062
10	0.5	12k	0.870	0.898	0.466	0.064	0.063
10	0.5	14k	0.838	0.867	0.457	0.062	0.063
15	0.5	10k	1.002	0.989	0.476	0.055	0.059
15	0.5	12k	0.871	0.860	0.428	0.049	0.056
15	0.5	14k	1.038	1.025	0.496	0.062	0.062
5	1	10k	0.999	1.040	0.489	0.041	0.051
5	1	12k	1.185	1.230	0.565	0.051	0.056
5	1	14k	1.165	1.210	0.561	0.057	0.061
10	1	10k	0.716	0.738	0.396	0.043	0.051
10	1	12k	0.865	0.884	0.492	0.070	0.065
10	1	14k	0.832	0.856	0.459	0.055	0.059
15	1	10k	0.984	1.019	0.528	0.064	0.062
15	1	12k	0.985	1.019	0.526	0.067	0.064
15	1	14k	1.154	1.191	0.548	0.055	0.057
5	2	10k	0.789	0.814	0.439	0.063	0.062
5	2	12k	0.931	0.947	0.487	0.075	0.068
5	2	14k	0.895	0.909	0.482	0.075	0.067
10	2	10k	0.947	0.981	0.476	0.056	0.058
10	2	12k	1.006	1.048	0.489	0.060	0.061
10	2	14k	1.027	1.058	0.492	0.055	0.058
15	2	10k	0.700	0.700	0.414	0.060	0.062
15	2	12k	0.711	0.740	0.369	0.036	0.052
15	2	14k	0.697	0.728	0.371	0.034	0.052
5	3	10k	1.075	1.071	0.475	0.058	0.057
5	3	12k	1.002	0.997	0.450	0.054	0.055
5	3	14k	1.145	1.138	0.503	0.061	0.058
10	3	10k	0.901	0.911	0.456	0.057	0.059
10	3	12k	0.877	0.886	0.448	0.062	0.063
10	3	14k	0.793	0.798	0.400	0.049	0.055
15	3	10k	0.939	0.969	0.452	0.041	0.052
15	3	12k	0.947	0.981	0.466	0.043	0.054
15	3	14k	0.898	0.923	0.431	0.044	0.054
[a] Absorbance varies with ±0.0005 upon measurement.							

Table 12: Absorbance at 280nm, 285nm, 360nm, 450nm and 550nm for infusion in 50% MeOH post extraction treatment.

UV-detection of method 2 (diluted ¼)							
Maceration time (mins.)	Time (hrs.)	Centrifugation (xg)	A_{280}[a]	A_{285}[a]	A_{360}[a]	A_{450}[a]	A_{550}[a]
5	0.5	10k	0.997	1.028	0.615	0.046	0.058
5	0.5	12k	1.053	1.090	0.656	0.058	0.066
5	0.5	14k	1.026	1.058	0.630	0.046	0.056
10	0.5	10k	0.778	0.822	0.416	0.025	0.046
10	0.5	12k	0.759	0.802	0.409	0.025	0.045
10	0.5	14k	0.884	0.929	0.481	0.025	0.045
15	0.5	10k	1.176	1.249	0.639	0.045	0.054
15	0.5	12k	1.028	1.094	0.570	0.036	0.048
15	0.5	14k	1.138	1.211	0.655	0.054	0.061
5	1	10k	0.823	0.867	0.462	0.028	0.046
5	1	12k	0.958	1.007	0.565	0.046	0.060
5	1	14k	0.897	0.942	0.528	0.047	0.063
10	1	10k	0.775	0.813	0.422	0.024	0.044
10	1	12k	0.639	0.680	0.386	0.035	0.056
10	1	14k	0.767	0.828	0.454	0.065	0.057
15	1	10k	0.596	0.635	0.362	0.019	0.041
15	1	12k	0.911	0.953	0.502	0.035	0.052
15	1	14k	0.904	0.947	0.500	0.030	0.047
5	2	10k	1.218	1.316	0.673	0.039	0.052
5	2	12k	1.530	1.659	0.855	0.058	0.065
5	2	14k	1.333	1.440	0.758	0.046	0.056
10	2	10k	1.029	1.080	0.536	0.044	0.055
10	2	12k	1.247	1.311	0.631	0.046	0.055
10	2	14k	1.097	1.153	0.565	0.037	0.049
15	2	10k	1.822	2.007	0.947	0.049	0.052
15	2	12k	1.358	1.428	0.778	0.061	0.063
15	2	14k	1.802	1.980	0.928	0.051	0.055
5	3	10k	1.210	1.274	0.677	0.050	0.057
5	3	12k	1.030	1.112	0.572	0.028	0.045
5	3	14k	1.097	1.188	0.623	0.029	0.045
10	3	10k	1.543	1.596	0.780	0.068	0.064
10	3	12k	1.619	1.675	0.799	0.062	0.054
10	3	14k	1.572	1.621	0.767	0.065	0.060
15[b]	3	10k	0.486	0.535	0.272	0.015	0.041
15[b]	3	12k	0.498	0.547	0.275	0.012	0.038
15[b]	3	14k	0.429	0.472	0.246	0.013	0.039

[a] Absorbance varies with ±0.001 upon measurement.
[b] Samples have been diluted twice.

Table 13: Absorbance at 280nm, 285nm, 360nm, 450nm and 550nm for percolation in MilliQ water post extraction treatment.

UV-detection of method 3 (diluted ½)							
Maceration time (mins.)	Time (hrs.)	Centrifugation (xg)	A_{280}[a]	A_{285}[a]	A_{360}	A_{450}	A_{550}
5	0.5	10k	0.477	0.473	0.249	0.073	0.075
5	0.5	12k	0.467	0.464	0.247	0.069	0.072
5	0.5	14k	0.447	0.448	0.236	0.060	0.067
10	0.5	10k	0.700	0.694	0.356	0.097	0.083
10	0.5	12k	0.810	0.797	0.400	0.126	0.102
10	0.5	14k	0.774	0.767	0.386	0.107	0.088
15	0.5	10k	0.727	0.717	0.373	0.102	0.085
15	0.5	12k	0.835	0.821	0.426	0.134	0.104
15	0.5	14k	0.772	0.757	0.395	0.111	0.090
5	1	10k	0.945	0.937	0.451	0.106	0.081
5	1	12k	1.083	1.076	0.526	0.138	0.101
5	1	14k	0.698	0.712	0.368	0.086	0.079
10	1	10k	0.710	0.716	0.375	0.095	0.085
10	1	12k	0.831	0.836	0.436	0.124	0.101
10	1	14k	0.769	0.776	0.407	0.102	0.088
15	1	10k	0.803	0.813	0.414	0.121	0.100
15	1	12k	0.768	0.776	0.396	0.107	0.091
15	1	14k	1.065	1.058	0.564	0.204	0.159
5	2	10k	0.907	0.887	0.446	0.135	0.101
5	2	12k	0.934	0.913	0.455	0.125	0.092
5	2	14k	0.886	0.867	0.425	0.136	0.104
10	2	10k	1.151	1.113	0.539	0.158	0.111
10	2	12k	1.046	1.018	0.495	0.137	0.097
10	2	14k	1.449	1.476	0.676	0.153	0.105
15	2	10k	1.118	1.155	0.508	0.114	0.088
15	2	12k	1.230	1.277	0.580	0.150	0.115
15	2	14k	1.158	1.208	0.553	0.122	0.094
5	3	10k	0.955	0.942	0.446	0.112	0.084
5	3	12k	0.967	0.951	0.458	0.117	0.087
5	3	14k	1.088	1.068	0.512	0.148	0.109
10	3	10k	0.887	0.877	0.446	0.106	0.083
10	3	12k	0.927	0.917	0.476	0.115	0.090
10	3	14k	1.034	1.038	0.526	0.126	0.095
15	3	10k	1.108	1.107	0.526	0.155	0.114
15	3	12k	1.080	1.075	0.500	0.137	0.104
15	3	14k	1.028	1.018	0.488	0.152	0.116
[a]Absorbance varies with ±0.0005 upon measurement.							

Table 14: Absorbance at 280nm, 285nm, 360nm, 450nm and 550nm for percolation in 50% MeOH post extraction treatment.

UV-detection of method 4 (diluted ½)							
Macerationtime (mins.)	Time (hrs.)	Centrifugation (xg)	A_{280}[a]	A_{285}[a]	A_{360}[a]	A_{450}[a]	A_{550}[a]
5	0.5	10k	0.849	0.874	0.554	0.030	0.055
5	0.5	12k	0.722	0.748	0.427	0.028	0.054
5	0.5	14k	0.827	0.856	0.475	0.036	0.062
10	0.5	10k	1.331	1.360	0.617	0.070	0.066
10	0.5	12k	1.338	1.369	0.599	0.063	0.060
10	0.5	14k	1.574	1.624	0.760	0.093	0.074
15	0.5	10k	1.699	1.650	0.687	0.156	0.087
15	0.5	12k	1.765	1.716	0.692	0.155	0.089
15	0.5	14k	1.557	1.499	0.616	0.147	0.095
5	1	10k	1.113	1.143	0.574	0.063	0.065
5	1	12k	1.342	1.444	0.743	0.050	0.065
5	1	14k	1.347	1.450	0.750	0.040	0.056
10	1	10k	1.745	1.826	0.867	0.080	0.065
10	1	12k	1.570	1.637	0.806	0.080	0.068
10	1	14k	1.681	1.755	0.853	0.081	0.067
15	1	10k	1.230	1.327	0.673	0.038	0.056
15	1	12k	1.184	1.220	0.616	0.072	0.065
15	1	14k	1.250	1.290	0.646	0.074	0.065
5	2	10k	0.702	0.724	0.402	0.042	0.058
5	2	12k	0.827	0.850	0.465	0.047	0.059
5	2	14k	1.114	1.091	0.561	0.074	0.069
10	2	10k	0.985	0.969	0.516	0.131	0.103
10	2	12k	1.288	1.308	0.657	0.079	0.066
10	2	14k	1.275	1.295	0.654	0.078	0.066
15	2	10k	0.996	0.979	0.490	0.067	0.066
15	2	12k	1.069	1.048	0.523	0.069	0.067
15	2	14k	0.752	0.774	0.435	0.045	0.059
5	3	10k	1.035	1.108	0.580	0.039	0.061
5	3	12k	0.784	0.809	0.416	0.045	0.062
5	3	14k	0.825	0.857	0.431	0.044	0.057
10	3	10k	0.693	0.728	0.413	0.027	0.055
10	3	12k	0.644	0.677	0.396	0.027	0.055
10	3	14k	0.593	0.626	0.334	0.035	0.057
15	3	10k	0.635	0.657	0.341	0.041	0.058
15	3	12k	1.157	1.247	0.660	0.037	0.058
15	3	14k	0.965	1.047	0.553	0.035	0.056
[a]Absorbance varies with ±0.001 upon measurement.							

Table 15: Raw absorbance, dryweight, concentration, molarity and molar attenuation coefficient data for SEC run 1.

Fraction	Fraction volume	Weight eppendorf tubes (g)	Weight eppendorf tubes w/sample (g)	Dry weight (mg)	Dilutionfactor	Dilution
1	1	0.9428	0.9428	0	1	1
2	1	0.9509	0.951	0.1	1	1
3	1	0.997	0.997	0	1	1
4	1	0.9394	0.9394	0	1	1
5	1	0.9751	0.9754	0.3	1	1
6	1	0.9383	0.939	0.7	1	1
7	1	0.9486	0.9486	0	1	1
8	1	0.9551	0.9557	0.6	1	1
9	1	0.9397	0.9402	0.5	1	1
10	1	0.9845	0.9856	1.1	1	1
11	1	0.9457	0.9459	0.2	1	1
12	1	0.9377	0.9381	0.4	1	1
13	1	0.9516	0.9521	0.5	1	1
14	1	0.9554	0.9556	0.2	1	1
15	1	0.9557	0.9557	0	1	1
16	1	0.9513	0.9512	0	1	1
17	1	0.9467	0.947	0.3	1	1
18	1	0.9301	0.9298	0	1	1
19	1	0.951	0.9511	0.1	1	1
20	1	0.9376	0.9377	0.1	1	1
21	1	0.9747	0.975	0.3	1	1
22	1	0.9503	0.9506	0.3	1	1

Table 15 cont.: Absorbance, dryweight, concentration, molarity and molar attenuation coefficient data for SEC run 1.

A280	A285	Conc. (mg/mL)	Molarity (mol/L)	e280	Purity280
0.187	0.192	0.197182	6.61E-05	2828.399	0.859219
0.213	0.221	0.220818	7.4E-05	2876.807	0.873925
0.239	0.256	0.244455	8.2E-05	2915.853	0.885787
0.26	0.279	0.263545	8.84E-05	2942.278	0.893814
0.277	0.301	0.279	9.35E-05	2961.021	0.899508
0.285	0.307	0.286273	9.6E-05	2969.141	0.901974
0.267	0.288	0.269909	9.05E-05	2950.256	0.896237
0.25	0.266	0.254455	8.53E-05	2930.189	0.890142
0.213	0.222	0.220818	7.4E-05	2876.807	0.873925
0.185	0.185	0.195364	6.55E-05	2824.19	0.857941
0.179	0.174	0.189909	6.37E-05	2811.08	0.853958
0.168	0.162	0.179909	6.03E-05	2784.98	0.846029
0.185	0.175	0.195364	6.55E-05	2824.19	0.857941
0.18	0.169	0.190818	6.4E-05	2813.317	0.854638
0.165	0.156	0.177182	5.94E-05	2777.35	0.843712
0.153	0.145	0.166273	5.58E-05	2744.33	0.833681
0.138	0.13	0.152636	5.12E-05	2696.416	0.819125
0.119	0.112	0.135364	4.54E-05	2621.868	0.796479
0.111	0.106	0.128091	4.29E-05	2584.464	0.785116
0.101	0.097	0.119	3.99E-05	2531.281	0.76896
0.075	0.072	0.095364	3.2E-05	2345.548	0.712538
0.064	0.061	0.085364	2.86E-05	2236.006	0.67926

Table 16: Absorbance, dilution factor, dryweight, concentration, molarity and molar attenuation coefficient data for SEC run 3.

Fraction	Fraction volume	Weight eppendorf tubes (g)	Weight eppendorf tubes w/sample (g)	Dry weight (mg)	Dilutionfactor	Dilution
1	1	1.0226	1.0291	6.5	4	4
2	0.9	0.9555	0.9607	5.2	4	3.6
3	1	0.95	0.9569	6.9	8	8
4	0.9	0.9448	0.9507	5.9	8	7.2
5	1	0.9495	0.9555	6	4	4
6	0.85	0.9785	0.984	5.5	4	3.4
7	1	0.9761	0.9818	5.7	4	4
8	0.95	0.9292	0.9351	5.9	4	3.8
9	0.85	0.9423	0.9477	5.4	4	3.4
10	0.95	0.9857	0.9916	5.9	4	3.8

11	0.8	0.9949	1.0002	5.3	4	3.2
12	1	0.9556	0.9616	6	4	4
13	0.9	0.949	0.955	6	4	3.6
14	1	0.9479	0.9537	5.8	4	4
15	1	0.9482	0.9541	5.9	4	4
16	1	0.9573	0.963	5.7	4	4
17	0.9	0.9752	0.9814	6.2	4	3.6
18	0.9	0.979	0.9834	4.4	2	1.8
19	1	0.9371	0.9424	5.3	2	2
20	0.9	0.9502	0.9541	3.9	1	0.9
21	0.9	0.938	0.9416	3.6	1	0.9
22	1	0.9905	0.9947	4.2	1	1
23	0.9	0.9317	0.936	4.3	1	0.9
24	0.85	0.9432	0.9466	3.4	1	0.85
25	0.8	0.964	0.9672	3.2	1	0.8
26	0.8	0.938	0.941	3	1	0.8
27	0.8	0.9506	0.9532	2.6	1	0.8
28	0.75	0.9499	0.9532	3.3	1	0.75
29	0.7	0.9408	0.9435	2.7	1	0.7
30	0.6	0.9814	0.983	1.6	1	0.6
31	1	0.9404	0.9436	3.2	1	1
32	1	0.9402	0.9433	3.1	1	1
33	1	0.9919	0.9942	2.3	1	1
34	1.2	0.9554	0.9582	2.8	1	1.2
35	1.2	0.9569	0.9598	2.9	1	1.2
36	1.3	0.9486	0.9518	3.2	1	1.3
37	1.15	0.9374	0.9397	2.3	1	1.15
38	1	0.9569	0.9589	2	1	1
39	1	0.9504	0.9524	2	1	1
40	0.95	0.9505	0.956	5.5	1	0.95
41	1	0.946	0.948	2	1	1
42	0.95	0.9384	0.9398	1.4	1	0.95
43	1	0.964	0.9653	1.3	1	1
44	1	0.9496	0.9507	1.1	1	1
45	1	0.9558	0.9567	0.9	1	1
46	0.9	0.9403	0.9414	1.1	1	0.9
47	0.5	0.9848	0.9849	0.1	1	0.5
48	1	0.9576	0.9585	0.9	1	1
49	1	0.9811	0.9819	0.8	1	1
50	1	0.979	0.9796	0.6	1	1
51	1	0.9406	0.9432	2.6	1	1
52	0.9	0.9414	0.9415	0.1	1	0.9
53	1	0.9909	0.9911	0.2	1	1
54	1.1	0.9441	0.9442	0.1	1	1.1
55	1	0.9397	0.941	1.3	1	1
56	1	0.9434	0.9434	0	1	1
57	1	0.9548	0.9548	0	1	1

Table 16 cont.: Absorbance, dilution factor, dryweight, concentration, molarity and molar attenuation coefficient data for SEC run 3.

A280	A285	A410	Conc. (mg/mL)	Molarity (mol/L)	e280	Purity280
0.996	0.948	0.049	0.932636	0.000313	3185.025	0.967556
2.6748	2.5092	0.172	2.458818	0.000824	3244.373	0.985585
3.736	3.496	0.055	3.423545	0.001148	3254.593	0.98869
4.176	3.888	0.067	3.823545	0.001282	3257.318	0.989518
3.64	3.4	0.113	3.336273	0.001119	3253.911	0.988483
2.652	2.4752	0.061	2.438091	0.000817	3244.065	0.985492
3.592	3.34	0.11	3.292636	0.001104	3253.557	0.988375
3.3326	3.1084	0.096	3.056818	0.001025	3251.468	0.987741
2.7642	2.5874	0.086	2.540091	0.000852	3245.533	0.985938
3.0286	2.8386	0.076	2.780455	0.000932	3248.568	0.98686
2.5184	2.3744	0.087	2.316636	0.000777	3242.147	0.984909
3.352	3.172	0.091	3.074455	0.001031	3251.635	0.987791
2.538	2.4012	0.075	2.334455	0.000783	3242.441	0.984998
2.66	2.52	0.06	2.445364	0.00082	3244.174	0.985525
2.668	2.528	0.071	2.452636	0.000822	3244.282	0.985557
2.304	2.192	0.052	2.121727	0.000711	3238.611	0.983835
1.4364	1.3644	0	1.333	0.000447	3213.743	0.97628
1.125	1.0566	0.065	1.049909	0.000352	3195.705	0.970801
1.128	1.038	0	1.052636	0.000353	3195.925	0.970868
0.8622	0.801	0.12	0.811	0.000272	3170.685	0.9632
0.6948	0.6417	0.1	0.658818	0.000221	3145.286	0.955484
0.745	0.688	0.103	0.704455	0.000236	3154.054	0.958148
0.5409	0.4968	0.046	0.518909	0.000174	3108.791	0.944398
0.4505	0.4131	0.081	0.436727	0.000146	3076.454	0.934574
0.3472	0.3184	0.069	0.342818	0.000115	3020.52	0.917583
0.2928	0.2664	0.061	0.293364	9.84E-05	2976.67	0.904262
0.2488	0.2256	0.046	0.253364	8.5E-05	2928.68	0.889683
0.192	0.17025	0	0.201727	6.76E-05	2838.589	0.862315
0.1974	0.1799	0.055	0.206636	6.93E-05	2849.091	0.865505
0.1524	0.1398	0.055	0.165727	5.56E-05	2742.565	0.833144
0.353	0.318	0.036	0.348091	0.000117	3024.46	0.91878
0.341	0.306	0.025	0.337182	0.000113	3016.172	0.916262
0.436	0.397	0.12	0.423545	0.000142	3070.099	0.932644
0.6432	0.5832	0.135	0.611909	0.000205	3134.91	0.952332
0.6804	0.6144	0.14	0.645727	0.000217	3142.542	0.954651
0.7436	0.6682	0.114	0.703182	0.000236	3153.825	0.958078
0.60145	0.5359	0.142	0.573955	0.000192	3125.273	0.949405
0.4	0.355	0.103	0.390818	0.000131	3052.468	0.927288
0.353	0.309	0.042	0.348091	0.000117	3024.46	0.91878
0.33155	0.285	0.033	0.328591	0.00011	3009.258	0.914161
0.417	0.371	0.111	0.406273	0.000136	3061.148	0.929924
0.39995	0.35435	0.093	0.390773	0.000131	3052.441	0.92728
0.414	0.368	0.096	0.403545	0.000135	3059.664	0.929474
0.413	0.364	0.095	0.402636	0.000135	3059.165	0.929322
0.372	0.331	0.085	0.365364	0.000123	3036.571	0.922459

0.2574	0.2205	0.005	0.261182	8.76E-05	2939.216	0.892884
0.087	0.078	0.036	0.106273	3.56E-05	2441.537	0.741697
0.279	0.249	0.065	0.280818	9.42E-05	2963.09	0.900136
0.238	0.21	0.003	0.243545	8.17E-05	2914.492	0.885373
0.272	0.246	0.066	0.274455	9.2E-05	2955.727	0.8979
0.205	0.185	0	0.213545	7.16E-05	2863.053	0.869747
0.1566	0.1395	0	0.169545	5.68E-05	2754.682	0.836825
0.194	0.176	0.105	0.203545	6.82E-05	2842.538	0.863514
0.2068	0.1859	0.143	0.215182	7.22E-05	2866.229	0.870711
0.088	0.078	0.038	0.107182	3.59E-05	2448.654	0.743859
0.108	0.095	0.105	0.125364	4.2E-05	2569.319	0.780515
0.095	0.088	0.07	0.113545	3.81E-05	2495.283	0.758024

Table 17: Absorbance, dilution factor, dryweight, concentration, molarity and molar attenuation coefficient data for SEC run 4.

Fraction	Fraction volume	Weight eppendorf tubes (g)	Weight eppendorf tubes w/sample (g)	Dry weight (mg)	Dilutionfactor	Dilution
1	1	0.9752	0.9772	2	1	1
2	1	0.9307	0.9329	2.2	1	1
3	1	0.9757	0.9774	1.7	1	1
4	1	0.9939	0.9951	1.2	2	2
5	1	0.9502	0.9512	1	4	4
6	1	0.9844	0.985	0.6	4	4
7	1	0.9554	0.9563	0.9	4	4
8	1	0.9902	0.9906	0.4	2	2
9	1	0.9614	0.9618	0.4	1	1
10	1	0.9932	0.993	0	1	1
11	1	0.9972	0.997	0	1	1
12	1	0.9939	0.9946	0.7	1	1
13	1	0.9831	0.9836	0.5	1	1
14	1	0.9435	0.9436	0.1	1	1
15	1	0.9416	0.9415	0	1	1
16	1	0.9864	0.9862	0	1	1

Table 17 cont.: Absorbance, dilution factor, dryweight, concentration, molarity and molar attenuation coefficient data for SEC run 4.

A280	A285	A410	Conc. (mg/mL)	Molarity (mol/L)	e280	Purity280
0.655	0.636	0.079	0.622636	0.000209	3137.42	0.953095
0.82	0.786	0.088	0.772636	0.000259	3165.225	0.961541
0.895	0.863	0.085	0.840818	0.000282	3174.584	0.964385
1.024	1.048	0.019	0.958091	0.000321	3187.566	0.968328
1.892	1.972	0.037	1.747182	0.000586	3229.601	0.981098
2.568	2.668	0.065	2.361727	0.000792	3242.882	0.985132
1.756	1.8	0.039	1.623545	0.000544	3225.715	0.979917
1.172	1.188	0.073	1.092636	0.000366	3199.027	0.97181
0.72	0.735	0.122	0.681727	0.000229	3149.834	0.956866
0.492	0.497	0.071	0.474455	0.000159	3092.69	0.939506
0.333	0.329	0.058	0.329909	0.000111	3010.342	0.914491
0.258	0.256	0.03	0.261727	8.78E-05	2939.927	0.8931
0.215	0.208	0.035	0.222636	7.47E-05	2880.105	0.874927
0.136	0.132	0.004	0.150818	5.06E-05	2689.373	0.816986
0.106	0.103	0	0.123545	4.14E-05	2558.851	0.777335
0.085	0.085	0	0.104455	3.5E-05	2426.931	0.73726

Table 18: Absorbance, dilution factor, concentration, molarity and molar attenuation coefficient data for SEC run 5.

Fraction	Dilution factor	Dilution	A280	A285	A410	Conc. (mg/mL)	Molarity (mol/L)	e280	Purity280
1	1	1	0.536	0.461	0.054	0.514455	0.000176	3038.56	0.972339
2	1	1	1.624	1.435	0.328	1.503545	0.000516	3150.065	1.008021
3	1	1	0.793	0.697	0.099	0.748091	0.000257	3091.497	0.989279
4	1	1	0.64	0.556	0.049	0.609	0.000209	3064.875	0.98076
5	1	1	0.653	0.557	0.029	0.620818	0.000213	3067.601	0.981632
6	1	1	0.732	0.617	0.021	0.692636	0.000237	3082.165	0.986293
7	1	1	0.768	0.644	0.018	0.725364	0.000249	3087.845	0.98811
8	1	1	0.738	0.625	0.02	0.698091	0.000239	3083.149	0.986608
9	1	1	0.798	0.702	0.036	0.752636	0.000258	3092.201	0.989504
10	1	1	1.225	1.115	0.108	1.140818	0.000391	3131.625	1.00212
11	1	1	0.727	0.656	0.087	0.688091	0.000236	3081.333	0.986027
12	1	1	0.408	0.359	0.036	0.398091	0.000136	2989.014	0.956485
13	1	1	0.273	0.234	0.013	0.275364	9.44E-05	2891.386	0.925244
14	1	1	0.202	0.171	0.001	0.210818	7.23E-05	2794.431	0.894218
15	1	1	0.15	0.129	0	0.163545	5.61E-05	2674.871	0.855959
16	1	1	0.118	0.102	0	0.134455	4.61E-05	2559.509	0.819043
17	1	1	0.093	0.084	0	0.111727	3.83E-05	2427.581	0.776826
18	1	1	0.078	0.071	0	0.098091	3.36E-05	2319.081	0.742106
19	1	1	0.06	0.058	0	0.081727	2.8E-05	2141.087	0.685148
20	1	1	0.057	0.055	0	0.079	2.71E-05	2104.252	0.673361

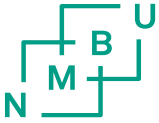

Norwegian University
of Life Sciences

Postboks 5003
NO-1432 Ås, Norway
+47 67 23 00 00
www.nmbu.no